Volatility in financial markets: long memory, asymmetry, forecasting

Aleksandr Pereverzin

School of Economics
University of East Anglia
Norwich, UK

A thesis submitted for the degree of
Doctor of Philosophy

August 2020

Abstract

In this thesis, we investigate several aspects of asset price volatility dynamics in financial markets.

In Chapter 1, we focus on the long memory property of financial volatility and study whether the long memory in the volatility is true (genuine) or spurious. We address the problem of a correct identification of a memory structure of financial volatility by considering it in the context of temporal aggregation. Firstly, we generalize the up-to-date theoretical knowledge about temporal aggregation in long memory processes to show that the long memory property of ARFIMA series is invariant to temporal aggregation. Secondly, we conduct a Monte Carlo simulation experiment and provide a regression analysis of the experiment results in order to validate the established theoretical implications for the semiparametric GPH method of ARFIMA estimation. Finally, we analyze empirically the long memory property of volatility of the GBP/USD foreign exchange rate returns at various time scales. We focus on different established volatility proxies (such as absolute returns, squared returns and realized volatility) and use the semiparametric ARFIMA estimation methods to investigate the long memory dynamics of the volatility at various levels of temporal aggregation. Based on the theoretical implications, we formally test the hypothesis of equivalence of the estimated long memory parameters at different time scales. We have found evidence that volatility of the returns is a true long memory process as it is characterized by the same fractional differencing parameter across the observed time scales. The evidence is particularly strong in case of realized volatility.

In Chapter 2, we investigate the connection between the phenomenon of volatility asymmetry and the asymmetry of investor attention to good and bad market news. As an advanced and direct measure of investor attention, we utilize the Search Volume Index (SVI) provided by the Google Trends service. We use a long span of daily data for a range of international stock market indexes and employ a methodological framework of SVAR and ARDL models to study the direction and timing of the asymmetric effects.

Our findings indicate that both volatility and investor attention are similarly asymmetric in their response to market news represented by index return: a negative return has a stronger impact on both volatility and investor attention than a positive return of the same absolute magnitude. We provide new evidence of positive relationship between volatility and investor attention and demonstrate that the magnitude of the impact of investor attention on volatility is stronger during periods of negative returns. We show that, in the established theoretical framework, retail investor attention can contribute to volatility asymmetry and create temporary asymmetric volatility fluctuations but is unlikely to be responsible for permanent shifts in market volatility.

In Chapter 3, we introduce a new realized volatility forecasting technique based on the component structure of the volatility dynamics. Time series of financial volatility is well known for having a complex structure including several heterogeneous patterns: linear and nonlinear, long-run and short-run, etc. We propose a new two-component model of realized volatility that is based on combination of econometric and machine learning approaches. In our model, the ARFIMA framework is used to capture the linear component of realized volatility while the artificial neural network is used to model the corresponding nonlinear part. The model exploits both the strength of ARFIMA in linear modeling and the high nonlinear modeling capability of artificial neural networks. We also develop a modification of the cyclical volatility model where artificial neural networks are used to model both trend and cyclical components of realized volatility. We apply the proposed hybrid approaches to produce out-of-sample forecasts of realized volatility of the GBP/USD and the EUR/GBP exchange rates returns. The proposed models provide an improvement in out-of-sample forecasting accuracy over the competing approaches.

Contents

List of Tables

List of Figures

Introduction

The importance of volatility in the area of financial economics should never be underestimated. Volatility as a phenomenon as well as a concept has been central to financial markets and academic research in recent decades. Loosely speaking, volatility is defined as a measure of asset price variability over some period of time. Arguably, it is the most common measure of financial risk involved in investments in traded securities. When volatility is interpreted as risk or uncertainty, it becomes an essential input to financial investment decisions and portfolio design. For example, in the seminal work of Markowitz (1952) on portfolio theory, a rational investor aims to maximize his profit, measured as the expected portfolio return, and minimize his risk, measured as the portfolio's variance of return (i.e., volatility).

Volatility plays a crucial role in the pricing of derivative securities, such as options and futures contracts. The market of financial derivatives is gigantic, the trading volume of the market is often estimated as trillions of dollars. In the well-known option pricing framework of Black and Scholes (1973), the most important variable is the volatility of the underlying asset between the settlement and expiry of the option. Moreover, in recent years new derivative contracts have been introduced. These new contracts are written on volatility itself, which means that volatility now serves as the underlying asset. Currently, the futures and options written on the CBOE Volatility Index (VIX) are among the most actively traded derivative contracts at the Chicago Board Options Exchange (CBOE).

During periods of financial and economic turmoil, market volatility attracts particularly close attention from financial professionals. The financial crisis of 2007-2008 has demonstrated that extreme financial market volatility is costly not only for financial industry but also affects the economy as a whole. In particular, high market volatility negatively influences aggregate investment behaviour which significantly limits the possibilities for companies to attract external financing. Recently, in March 2020, the COVID-19 pandemic contributed to extreme price fluctuations for various groups of assets which caused panic among traders and massive outflow of investors from financial markets. These cases clearly demonstrate the important link between market uncertainty and collective behaviour of investors.

Volatility is closely tracked by retail investors and institutional investors like investment funds, pension funds and policy makers. For central banks, market estimates of volatility often serve as a barometer for the vulnerability of financial markets and the economy as a whole. In particular, the Federal Reserve of the United States and the Bank of England usually take into account the volatility of different securities and commodities in developing and establishing monetary policy. Since introduction of the first Basel Accords, volatility has become an important variable for determining capital requirements for many financial institutions around the world, such as banks and trading houses.

The indisputable importance of volatility in the practice of financial and economic risk management explains the fact that the concept of volatility has been at the center of academic research in both finance and econometrics in recent decades. The research efforts of economists globally are aimed at explaining the various empirical features of volatility as well as enhancing the ability to model and forecast it. The link between volatility and economic fundamentals is another active research area. The dominant paradigm in financial market research, the Efficient Market Hypothesis (EMH) of Fama (1970), claims that the volatility of stock prices should reflect changes in the true investment value. However, as pointed out by Shiller (1981), historical volatility of security prices is too high to be justified just by changes in market fundamentals. The rich evidence of other empirical characteristics of financial volatility, such as volatility clustering, is another direct violation of the EMH.

Every new study on volatility often establishes a lot of new questions while attempting to answer the already existing ones. Hence, financial volatility can still be considered an active research topic. This thesis contributes to the literature by investigating several relevant aspects of volatility in financial markets. First, we focus on the long memory property of volatility and study whether the long memory in volatility is true or spurious. Second, we investigate the phenomenon of volatility asymmetry and consider how asymmetry in investor attention can contribute to the asymmetry in volatility. Finally, we analyze the factor structure of volatility, with the particular focus on using the factor decomposition for volatility forecasting techniques.

The structure of the thesis is organized as follows. Every chapter of the thesis is self-contained and can thus be read independently.

In Chapter 1, we consider the long memory feature of financial volatility through the concept of temporal aggregation. Long-range dependence, i.e., the phenomenon of slow hyperbolic decay of the autocorrelation function of a process, is widely documented for volatility of returns of various assets. Nowadays, the research in the area of long-range dependence in volatility focuses on the source and the nature of this long memory property. There is no consensus in the literature whether the long memory in volatility is true and an intrinsic characteristic of the volatility generating process or it is spurious and nothing more than a temporary anomaly that arises at a certain time scale as a result of occasional structural shifts or regime breaks. At the same time, the increased availability of high frequency financial data of good quality provides a chance for academic researchers to investigate the persistence of volatility at different time scales more substantially. We address the problem of correct identification of the memory structure of financial volatility by considering it in the context of temporal aggregation. It is a well known theoretical result that the long memory property of Autoregressive Fractionally Integrated Moving Average (ARFIMA) processes is invariant to temporal aggregation. In the first step, we conduct a Monte Carlo simulation to validate this theoretical result for the particular semiparametric ARFIMA estimation method. In the second step, we analyze empirically the long memory property of volatility of the GBP/USD foreign exchange rate at various time scales. We focus on different established volatility proxies (such as absolute returns, squared returns and realized volatility) and use the semiparametric ARFIMA estimation methods to investigate the long memory dynamics of the volatility at various levels of temporal aggregation. Based on the theoretical implications, we formally test the hypothesis of equivalence of the estimated long memory parameters at different time scales and draw conclusions about the nature of long memory in volatility of the foreign exchange rate returns.

In Chapter 2, we investigate the phenomenon of volatility asymmetry and explore the link between volatility asymmetry and the asymmetry of investor attention to positive and negative returns. Volatility asymmetry describes the relationship between price changes and its volatility and refers to the fact that negative returns have stronger effect on volatility than positive returns of the same absolute magnitude. Generally, positive or negative returns are associated respectively with good or bad market news. In the literature, there is still no clearly recognized explanation of volatility asymmetry, despite longstanding attempts to explain it. The current research in academic literature shows that the most common hypotheses, such as the leverage effect or volatility feedback, are clearly incapable to fully explain volatility asymmetry, and that there are other factor driving the effect. Several promising hypotheses come from the area of behavioral finance, proposing the link between volatility asymmetry and individual aspects of investor behavior, in particular, investor attention. However, empirical investigations of the connection between investor attention and volatility were limited due to the problem of measuring and quantifying the attention, the absence of an adequate proxy. In our study, we use a recently introduced direct measure of investor attention which is based on the number of internet searches and provided by the Google Trends service. For several international stock market indexes, we employ a Structural Vector Autoregressive (SVAR) framework along with impulse response analysis to investigate the short-term and long-term relationship between index return, volatility and investor attention. We use an Autoregressive Distributed Lag (ARDL) model to explore the asymmetric reaction of both investor attention and volatility to positive and negative returns. We graphically illustrate the asymmetric effect with news impact curves. Finally, in the ARDL framework, we explore the impact of investor attention on volatility and suggest how, according to the established theoretical model, asymmetric attention can contribute to volatility asymmetry.

In Chapter 3, we introduce a new realized volatility forecasting technique based on the component structure of the volatility dynamics. Time series of financial volatility is well known for having a complex structure including several heterogeneous patterns. In particular, there is a widely documented evidence that volatility dynamics includes not only linear but also complex nonlinear dependencies. However, standard realized volatility forecasting models (such as ARFIMA) are essentially linear and are not able to effectively capture the nonlinear patterns in the time series of financial volatility. To address this issue, we propose a new two-component volatility model which is based on the combination of econometric and machine learning approaches. In our model, the time series of realized volatility is decomposed into the linear and nonlinear components, then ARFIMA model is used to forecast the linear part and the nonlinear autoregressive artificial neural network (ANN) is used to forecast the nonlinear part of the process. The proposed hybrid ARFIMA-ANN model is intended to capture both phenomena: long memory and nonlinearity in the volatility dynamics. The model exploits both the strength of ARFIMA in linear modeling and the high nonlinear modeling capability of artificial neural networks. We apply the proposed hybrid model to produce out-of-sample forecasts of realized volatility of the GBP/USD and the EUR/GBP exchange rates returns and compare the forecasting accuracy of the ARFIMA-ANN approach with several modifications of the recently introduced cyclical volatility model.

The final section of the thesis provides some concluding remarks, where we summarize the results of the chapters and attempt to identify the emerging themes for future research.

Chapter 1

On the long memory feature through temporal aggregation: an application to financial volatility

1.1 Introduction

The discovery of the long memory phenomenon has had a significant impact on the science of time series analysis and on our understanding of the nature of stochastic processes. Under the concept of long-range dependence, the behavior of a system depends on the state of its parameters in the distant past. Technically speaking, the long memory behavior of a stationary stochastic process is represented by the slow hyperbolic decay rate of the autocorrelation function of the series as a function of the time lag. In the frequency domain, the long memory behavior is characterized by a burst of the power spectral density function of a series near the origin (frequencies very close to zero).

The fundamentals of the long memory framework were developed by H.Hurst and B.Mandelbrot. Hurst introduced a concept of long memory and proposed a special test for the long-range dependence which is known as Hurst's rescaled range test (Hurst, 1951; Hurst, 1957). Mandelbrot was the one who laid the foundation of a long memory concept applied to the subject of mathematical finance. Mandelbrot and Van Ness (1968) proposed the first paradigmatic models of long memory processes - the fractional Gaussian noise (FGN) and the fractional Brownian motion (FBM). Mandelbrot (1971) found the long-range dependence in asset returns and proved the relevance of the rescaled range test to detect long memory in financial and economic time series. Since the early seminal works of Hurst and Mandelbrot, long memory processes are also known as self-similar processes (fractals).

The application of the long memory concept in statistics and quantitative finance significantly increased after introduction of the fractional autoregressive integrated moving average (ARFIMA) model. The model was independently developed by Granger and Joyeux (1980) and Hosking (1981) on the basis of the standard time series modeling ARIMA framework (Box and Jenkins, 1976). In the ARFIMA model, the mathematical trick of fractional differentiation has allowed to capture effectively the special autocorrelation structure of time series with long memory properties. The ARFIMA model has become an important instrument for modeling and forecasting the dynamics of financial and economic time series. The development of the concept of long memory in the context of economics and financial science is of particular importance. Many different financial and economic time series exhibit the properties of a long-range dependence: GDP growth rates, inflation rates, forward premiums, volatility of assets returns, etc. The discovery of the phenomenon of long memory in financial and economic processes provides a new methodological tool for describing the behavior of economic agents and systems.

One of the key features of empirical work with economic or financial time series is that the time series under consideration is often aggregated in time. There are several reasons for this. Sometimes the true data generating process in not observable directly or the time scale of the data generating process is unknown. In some cases, the true data generating process includes "noise" components or periodic behavior that complicates its modeling. Hence, in finance and economics, it is natural to work with temporally aggregated data. In the context of this work, we refer to temporal aggregation when the low frequency variable is the sum of the high frequency variables over several periods.

In the practice of financial econometrics, aggregated data is often used in empirical investigations for time series modeling, including testing for and modeling a long memory dynamics. This fact naturally raises many important questions about the consequences of temporal aggregation in long memory processes. Is the long memory property of a series invariant to the sampling frequency? Is it possible to identify correctly the nature of the true data generating process when observing the series in the temporally aggregated form?

In some cases, the slow hyperbolic decay rate of the autocorrelation function of a process might be just a statistical artifact that does not reflect the true long memory property of the series and that is observable only in a certain period and at a certain time resolution. This artifact can occur, for example, due to structural breaks or regime shifts. In this regard, investigating the process and testing for long memory based on only one particular time scale can lead to misleading conclusions about the nature of the process and, as a consequence, to model misspecification and serious forecasting errors. Following the very essence of self-similar processes, exploring their statistical properties at different time scales is of particular importance. The knowledge about the consequences of temporal aggregation allows more precise identification of the memory properties of a series and the nature of the system that generates the process.

The earliest works which study temporal aggregation in the context of long memory are Granger (1980), Diebold and Rudebusch (1989) and Ding, Granger, and Engle (1993). Granger (1980) explained that aggregation of dynamic equations could lead to the situation when the aggregated series exhibit fundamentally different statistical properties than the original series. Diebold and Rudebusch (1989), using annually and quarterly sampled macroeconomic data, found that the estimated long memory parameter is not the same at different aggregation frequencies. On the other hand, Ding, Granger, and Engle (1993), based on simulation studies, made a conjecture that temporal aggregation does not change the decay rate of the autocorrelation function or the spectral density function and, hence, does not affect the long memory parameter of ARFIMA series.

Chambers (1998) investigates temporal aggregation in discrete time and continuous time long memory processes using the frequency domain analysis. His findings indicate that, in case of temporal aggregation, the decay rate of the spectral density function is not affected by sampling intervals and that temporally aggregated variable retains the same order of fractional differencing as the original series. His empirical analysis of the U.K. macroeconomic data, however, shows the contradictory results as the long memory parameter is affected by aggregation. Chambers (1998) notes that semiparametric methods are superior for the purposes of estimating the true long memory parameter of ARFIMA series than parametric methods. Hwang (2000) follows the steps of Chambers (1998) and finds that in short lags the autocorrelation function of ARFIMA process is affected as an outcome of aggregation, whereas in large lags the autocorrelation function remains unaffected. Because of that, although temporal aggregation does not change the true long memory parameter of the series, the estimated long memory parameter can be biased. Hwang's (2000) results of the simulation analysis are consistent with the proposition of Chambers (1998) that semiparametric methods perform better in estimation the true long memory parameter than parametric techniques.

Baillie, Nijman, and Tschernig (1994) and Tschernig et al. (1995) found that the class of ARFIMA processes is not closed with respect to temporal aggregation and that, as a result of the aggregation, ARFIMA(p, d, q) process turns out to be an ARFIMA(p, d, ∞). Similar results were obtained by Teles, Wei, and Crato (1999) and Man and Tiao (2006).

In finance, volatility of asset returns is well known for exhibiting long memory dynamics. The empirical literature that documents the presence of long memory in the various volatility proxies, such as absolute or squared returns, is extensive. Here we list the most important works. For example, Ding, Granger, and Engle (1993), Ding and Granger (1996) find the presence of substantially high autocorrelation between daily absolute returns of S&P 500 stocks. Lobato and Savin (1998) finds the strong evidence of long memory in squared S&P 500 daily stocks returns. Dacorogna et al. (1993), Bhar (1994), Tschernig et al. (1995), Wang (2004), Dufrénot et al. (2008), Aloy et al. (2011) report the presence of long memory in absolute and squared returns on the foreign exchange market.

Increased availability of high frequency financial data of good quality gave a chance for academic researchers to investigate more deeply the structure of financial returns at high frequencies. In seminal paper, Andersen and Bollerslev (1997a) find long-range dependence in the series of high frequency absolute and squared the Deutschemark and the US dollar exchange rate returns. Andersen and Bollerslev (1997a) document that the degree of fractional integration in the absolute and the squared returns is invariant with respect to temporal aggregation. Dacorogna et al. (1998) and Caporale and Gil-Alana (2013) document long-term dependence in high frequency volatility data on the various exchange rates. Gurgul, Wójtowicz, et al. (2006), Tan, Khan, et al. (2010), Kang, Cheong, and Yoon (2010) find the property of long-range dependence in the volatility of stock market high frequency returns.

Bollerslev and Wright (2000) use semiparametric estimation methods to investigate the property of long memory in high frequency squared, log-squared and absolute foreign exchange returns under temporal aggregation. Bollerslev and Wright (2000) show that different volatility estimators can provide different conclusions about the value of the fractional differencing parameter estimated on various levels of temporal aggregation. Similar results are obtained by Mcmillan and Speight (2008) who show that the property of invariance of long memory parameter with respect to temporal aggregation does not hold if noisy volatility estimators are used to estimate temporal dependencies. Deo and Hurvich (2001) and Arteche (2004) also claim that noisy volatility proxies may induce bias in estimating long memory parameter.

Andersen et al. (2001), Andersen et al. (2003) propose a new volatility estimator based on high frequency returns which is called realized volatility and provide wide evidence of long memory in realized volatility of exchange rate returns. The literature that provides further evidence of long memory in realized measure of returns volatility is massive and includes papers of Barndorff-Nielsen and Shephard (2002), Corsi (2009), Choi, Yu, and Zivot (2010), Raggi and Bordignon (2012), Rossi and De Magistris (2013) as well as more recent works of Wenger, Leschinski, and Sibbertsen (2017), Baillie et al. (2018), etc.

The question of the current research of long-range dependence in volatility is not even the existence of the long memory but rather its strength and source. The debates in the literature about the nature of long memory in volatility of various financial assets returns are active. There is no consensus whether the long memory in volatility is true and an intrinsic characteristic of the volatility generating process or it is spurious and nothing more than a temporary anomaly that arises only at a certain time scale. Andersen and Bollerslev (1997a), on the basis of the empirical analysis of foreign exchange market, propose that long memory characteristics constitute an intrinsic feature of the return generating process and is not caused by occasional structural shifts. On the contrary, Diebold and Inoue (2001) show theoretically and using simulation analysis that structural breaks can cause a strong persistence in the autocorrelation function of a time series and generate spurious long memory. Granger and Hyung (2004) propose that occasional structural breaks can cause spurious long memory in S&P500 absolute stock returns. Choi, Yu, and Zivot (2010) claim that long memory in realized volatility can be explained by the presence of structural breaks. The works of Bollerslev and Wright (2000) and Mcmillan and Speight (2008) show that identification of the true long memory volatility dynamics is highly dependent on the choice of volatility measures. Ohanissian, Russell, and Tsay (2008) find that volatility in exchange rates returns is a true long memory process. Wenger, Leschinski, and Sibbertsen (2017) propose that the volatility of exchange rates is subject to spurious long memory while Baillie, Cecen, and Han (2015) and Baillie et al. (2018) claim that the volatility of exchange rates is consistent with dynamics of self similar processes with true long memory.

The discussion about the nature of long memory in volatility is far from being over. At the same time, the problem of a correct identification of a memory structure of financial volatility is crucial in the context of its predictive modeling. Large forecasting errors due to the use of incorrectly specified volatility time series models may lead to excessive risk of financial losses.

The present work seeks to extend the literature by providing a new evidence of the long memory phenomenon in financial volatility in the context of temporal aggregation. In the first step, we generalize the up to date theoretical knowledge about temporal aggregation in long memory time series. Combining both time and frequency domain analyses, we describe the properties of the autocorrelation, the autocovariance and the spectral density functions of temporally aggregated ARFIMA processes. We demonstrate that a long memory property of ARFIMA series is, in theory, invariant with respect to temporal aggregation. In the next step, we conduct a Monte Carlo simulation experiment in order to validate the theoretical implications about the effect of temporal aggregation on long memory processes. We also contribute to the literature by providing a regression analysis of the numerical experiment results. In line with the studies of Chambers (1998) and Hwang (2000), the simulation experiment results show that the semiparametric ARFIMA estimation methods are able to obtain a correct estimate of the long memory parameter on any level of temporal aggregation. Finally, we use the theoretical implications about temporal aggregation in long memory processes to analyze empirically the long memory property of volatility of the GBP/USD foreign exchange rates returns at various time scales and contribute to the recent discussion (Wenger, Leschinski, and Sibbertsen, 2017; Baillie et al., 2018) about the nature and the source of long memory in financial volatility. We use a long dataset of the high frequency foreign exchange data for the seven years from 2010 to 2016 and concentrate our attention on different established volatility measures (such as absolute returns, squared returns and realized volatility). The rescaled range test of Hurst (1951), the modified rescaled range test of Lo (1991) and the semiparametric methodology of Geweke and Porter-Hudak (1983) are used to investigate and model the long memory dynamics of the exchange rate returns volatility on different levels of temporal aggregation. Based on the empirical results, we discuss the properties of using the stated volatility proxies in modeling long memory in volatility and draw a conclusion about the source of long memory in volatility of the foreign exchange rate returns.

The remainder of the chapter is organized as follows. In Section 1.2, we present the theoretical framework of long memory processes in the context of temporal aggregation. Section 1.3 describes the design of the numerical experiment and the corresponding results. Section 1.4 describes the data utilized in the empirical analysis. Section 1.5 presents the empirical results. In Section 1.6, we provide a summary and suggest potential directions of further research.

1.2 Theoretical framework

1.2.1 Long memory processes

In this section we observe different definitions of long memory processes. Following Parzen (1980), we define the concept of long memory thorough the time domain and the frequency domain time series analysis.

Let us consider $\{y_t; t = 0, 1, 2...\}$ - a discrete time stationary stochastic process. Also, let γ_j denote the autocovariance, ρ_j denote the autocorrelation, $f(\omega)$ denote the spectral density of the process y_t.

Definition 1.2.1 *A stationary process y_t with the autocovariance function γ_j is a long memory process in the covariance sense if*

$$\sum_{j=-\infty}^{\infty} |\gamma_j| = \infty. \tag{1.1}$$

In other words, a long memory process has the autocovariance sequence that is not absolutely summable. It is also possible to define long memory using a speed of convergence of the autocovariance function towards zero (Granger and Joyeux, 1980).

Definition 1.2.2 *A stationary process y_t with the autocovariance function γ_j is a long memory process in the covariance sense with a speed of convergence of order $2d$ if,*

$$\gamma_j = C(d)\, j^{2d-1} \qquad as \;\; j \to \infty \tag{1.2}$$

with $d \in (0, 0.5)$ and $C(d)$ is a constant that depends on d.

In the present context, the parameter d is interpreted as a fractional differencing parameter. Fractional differencing is the essential instrument of modeling the long range behavior of a time series in such models as ARFIMA which detailed description will be given later.

Now we shall present the definition of a long memory in the spectral density sense (Cox et al., 1981).

Definition 1.2.3 *A stationary process y_t with the spectral density function $f(\omega)$ is a long memory process in the spectral density sense with a power law of order $2d$ if $f(\omega)$ is bounded above on $[\delta, \pi]$ for every $\delta > 0$ and if*

$$f(\omega) = c|\omega|^{-2d} \qquad as \;\; \omega \to 0, \tag{1.3}$$

where $\omega \in [-\pi, \pi]$, $d \in (0, 0.5)$ and for some $0 < c < \infty$.

Again, in the stated definition, d represents the fractional differencing parameter.

We shall note that, in general, the definitions of a long memory in the covariance sense and in the spectral density sense are not equivalent. There are processes which have long memory behavior in the covariance sense but not in the spectral density sense, and the opposite case also exists. The non-equivalence of the definitions arises when the fractional differencing parameter d has negative values $-0.5 < d < 0$. However, for the values $0 < d < 0.5$ of the fractional differencing parameter d, the definitions of a long memory through the time domain condition and the frequency domain condition are equivalent. That is why the case $0 < d < 0.5$ is of particular interest in time series analysis in the financial or economic context.

Figure 1.1: Typical autocovariance function of short memory and long memory processes

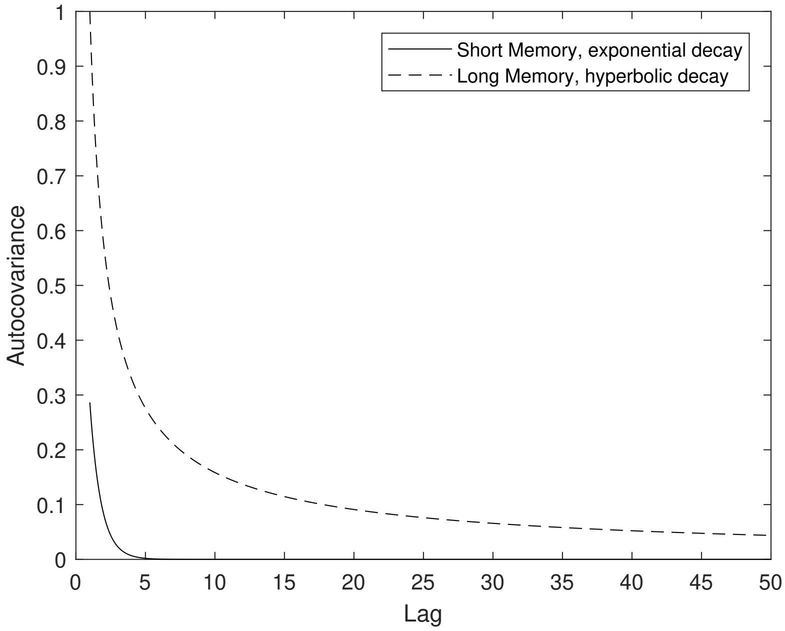

Figure 1.1 shows the graphs of the typical autocovariance functions of short memory and long memory processes. As we can see, the autocovariance function of the short memory process converges quickly to a zero value after few lags, with a decay rate that is exponential. On the other hand, the decay rate of the autocovariance function of the long memory process with increasing number of lags is hyperbolic and it takes many lags for the autocovariance function to reach zero.

1.2.2 ARFIMA model

Autoregressive fractionally integrated moving average (ARFIMA), proposed by Granger and Joyeux (1980) and Hosking (1981), is a widely used approach to model long memory in the dynamics of a time series. ARFIMA model is a generalization of autoregressive integrated moving average (ARIMA) - the popular linear univariate time series model of Box and Jenkins (1976).

Formally, a standard ARIMA(p,d,q) process y_t can be defined as

$$\phi(L)(1-L)^d y_t = \theta(L)\epsilon_t, \tag{1.4}$$

where L is the backshift (lag) operator, $\phi(L) = 1 - \sum_{j=1}^{p}\phi_j L^j$ and $\theta(L) = 1 + \sum_{j=1}^{q}\theta_j L^j$ are autoregressive and moving average polynomials of orders p and q respectively, ϵ_t is a white noise process with variance σ^2 and d is a differencing parameter that is a non-negative integer.

The family of ARIMA processes can be generalized by permitting the degree of differencing to take fractional values. Granger and Joyeux (1980) and Hosking (1981) suggested that non-integer values of the differencing parameter d can be useful and introduced autoregressive fractionally integrated moving average (ARFIMA) model.

An ARFIMA(p,d,q) process is given by:

$$\phi(L)(1-L)^d y_t = \theta(L)\epsilon_t, \tag{1.5}$$

where $-0.5 < d < 0.5$.

The fractional differencing operator $(1-L)^d$ can be represented in the following form using the binomial series expansion:

$$(1-L)^d = \sum_{j=0}^{\infty}\frac{\Gamma(j-d)}{\Gamma(j+1)\Gamma(-d)}L^j, \tag{1.6}$$

where $\Gamma(\cdot)$ is the gamma function.

ARFIMA model offers a parsimonious way to model a long memory - the phenomenon of a slowly decaying autocorrelation function of a time series. The characteristics of an ARFIMA(p,d,q) series depend on the value of the fractional differencing parameter d. For $-0.5 < d < 0.5$ the process is stationary and for $0 < d < 0.5$ the process exhibit long memory properties. In an ARFIMA(p,d,q) model, parameter d describes the long run behavior of the underlying process y_t (it describes the autocorrelation structure of distant observations of the process), whereas autoregressive and moving average polynomials $\phi(L) = 1 - \sum_{j=1}^{p}\phi_j L^j$ and $\theta(L) = 1 + \sum_{j=1}^{q}\theta_j L^j$ describes the behavior of the series in the short run (and, respectively, capture the process's autocorrelation structure for low lags).

Now we present the spectral density, the autocovariance and the autocorrelation functions of an ARFIMA(p, d, q) process (the detailed derivations of the functions can be found in Sowell (1992)).

The spectral density function for an ARFIMA(p, d, q) process is given by:

$$f(\omega) = \frac{\sigma^2}{2\pi}\left|1 - e^{-i\omega}\right|^{-2d}\left|\frac{\theta\left(e^{-i\omega}\right)}{\phi\left(e^{-i\omega}\right)}\right|^2, \tag{1.7}$$

where $\omega \in [-\pi, \pi]$ and $-0.5 < d < 0.5$.

The autocovariance function of an ARFIMA(p, d, q) process is given by:

$$\gamma_j = \sigma^2 \sum_{l=-q}^{q} \sum_{h=1}^{p} \psi(l)\, \zeta_h C(d, p + l - j, \phi_h), \tag{1.8}$$

where

$$\psi(l) = \sum_{k=max(0,l)}^{min(q,q+l)} \theta_k \theta_{k-l} \tag{1.9}$$

$$\zeta_h = \left(\phi_h \prod_{l=1}^{p}(1 - \phi_l \phi_h) \prod_{m \neq h} (\phi_h - \phi_m)\right)^{-1} \tag{1.10}$$

and

$$\begin{aligned} C(d, j, \phi) = {} & \frac{\Gamma(1-2d)\,\Gamma(d+j)}{\Gamma(1-d+j)\,\Gamma(1-d)\,\Gamma(d)} \\ & \times \left[\phi^{2p} F(d+j, 1; 1-d+j; \phi)\right. \\ & \left. + F(d-j, 1; 1-d-j; \phi) - 1\right], \end{aligned} \tag{1.11}$$

where $F(a, b; c; x)$ is the Gaussian hypergeometric function (Gradshteyn and Ryzhik, 2014).

The autocorrelation function of an ARFIMA(p, d, q) process is given by:

$$\rho_j = \frac{\gamma_j}{\gamma_0} = \frac{\sum_{l=-q}^{q} \sum_{h=1}^{p} \psi(l)\, \zeta_h C(d, p + l - j, \phi_h)}{\sum_{l=-q}^{q} \sum_{h=1}^{p} \psi(l)\, \zeta_h C_1(d, p + l - j, \phi_h)}, \tag{1.12}$$

where

$$\begin{aligned} C_1(d, j, \phi) = {} & \frac{\Gamma(1-2d)}{\Gamma(1-d)\,\Gamma(1-d)} \\ & \times \left[\phi^{2p} F(d, 1; 1-d; \phi)\right. \\ & \left. + F(d, 1; 1-d; \phi) - 1\right]. \end{aligned} \tag{1.13}$$

In the absence of autoregressive and moving average parameters (so that $p = 0$ and $q = 0$) we obtain an ARFIMA$(0, d, 0)$ specification that is a special case of an ARFIMA(p, d, q) model. An ARFIMA$(0, d, 0)$ is called a fractional white noise process and its spectral density and autocovariance functions take the following forms:

$$f(\omega) = \frac{\sigma^2}{2\pi}\left|1 - e^{-i\omega}\right|^{-2d} = \frac{\sigma^2}{2\pi}\left(2\sin\frac{\omega}{2}\right)^{-2d}, \tag{1.14}$$

$$\gamma_j = \sigma^2 \frac{\Gamma(1-2d)\,\Gamma(d+j)}{\Gamma(1-d+j)\,\Gamma(1-d)\,\Gamma(d)}, \tag{1.15}$$

where $\omega \in [-\pi, \pi]$, $d \in (0, 0.5)$ and $j \geq 0$.

It is also possible to obtain the autocorrelation function of an ARFIMA$(0, d, 0)$ process:

$$\rho_j = \frac{\gamma_j}{\gamma_0} = \frac{\sigma^2 \frac{\Gamma(1-2d)\Gamma(d+j)}{\Gamma(1-d+j)\Gamma(1-d)\Gamma(d)}}{\sigma^2 \frac{\Gamma(1-2d)\Gamma(d)}{\Gamma(1-d)\Gamma(1-d)\Gamma(d)}} = \frac{\Gamma(1-d)\,\Gamma(j+d)}{\Gamma(d)\,\Gamma(j+1-d)}. \tag{1.16}$$

Now we shall examine the convergence of the spectral density, the autocovariance and the autocorrelation functions of an ARFIMA$(0, d, 0)$ process for extreme values of parameters ω and j.

$$f(\omega) \approx \frac{\sigma^2}{2\pi}\omega^{-2d} \qquad \text{as } \omega \to 0, \tag{1.17}$$

$$\gamma_j \approx \frac{\Gamma(1-2d)\,\sigma^2}{\Gamma(d)\,\Gamma(1-d)} j^{2d-1} \qquad \text{as } j \to \infty, \tag{1.18}$$

$$\rho_j \approx \frac{\Gamma(1-d)}{\Gamma(d)} j^{2d-1} \qquad \text{as } j \to \infty. \tag{1.19}$$

1.2.3 Estimation of an ARFIMA model

The estimation procedure of an ARFIMA model is not trivial and includes several approaches. The approaches can be classified into two groups: semiparametric and parametric methods. In the methodology of the semiparametric methods, it is assumed that the short memory ARMA components of a time series are relatively less important and the focus is only on estimating the fractional differencing parameter d. The parametric methods imply estimating not only the long memory parameter d but also the short run autoregressive and moving average components of an ARFIMA(p, d, q) model. Within the first group of methods, the most popular, usually referred to as the GPH method, was proposed by Geweke and Porter-Hudak (1983). In the latter, the methods proposed by Fox and Taqqu (1986), Haslett and Raftery (1989) and Sowell (1992), which involve the maximum likelihood estimation of the model, are the most popular.

In the context of the present work, we are particularly interested in the semiparametric estimator of Geweke and Porter-Hudak (1983). The GPH method uses a spectral regression estimator to evaluate the d parameter without any specifications of the short memory parameters of the series. The approach makes use of the fact that the low frequency dynamics of a long memory process are parameterized by the fractional differencing parameter d. So, the GPH semiparametric method obtains an estimate of the memory parameter d for a long memory ARFIMA process y_t.

The periodogram for y_t is defined as the squared modulus of the discrete-time Fourier transformation of the process:

$$I_y\left(\omega_s\right) = \frac{1}{2\pi n}\left|\sum_{t=1}^{n} y_t e^{-it\omega_s}\right|^2, \tag{1.20}$$

where $\omega_s = \frac{2\pi s}{n}$ and $s = 1, ..., m; m < n$ and n is a sample size.

The GPH method is based on the regression equation using the periodogram function as an estimate of the spectral density. The estimate of d is obtained from the following regression model:

$$\log\left(I_y\left(\omega_s\right)\right) = c - d\log\left|1 - e^{-i\omega_s}\right|^2 + e_s, \tag{1.21}$$

where c is a constant and e_s is the error term which is asymptotically independent identically distributed (i.i.d.) across harmonic frequencies.

Then, setting $x_s = \log\left|1 - e^{-i\omega_s}\right|$, d can be estimated by applying an ordinary least squares regression to Equation 1.21 which gives:

$$\hat{d} = 0.5\frac{\sum_{s=1}^{m} x_s \log\left(I_y\left(\omega_s\right)\right)}{\sum_{s=1}^{m} x_s^2}. \tag{1.22}$$

The choice of m, the number of Fourier frequencies included in the regression, is essential to the estimate of the parameter d. The regression slope estimate is an estimate of the slope of the spectral density function of the series in the vicinity of the zero frequency. If m is small, then the slope is estimated from a small sample, and if a large m is chosen, then the medium and high frequency components of the spectrum will also be included in the regression which could contaminate the estimate. Often, by default, the value of $m = n^{0.5}$ is chosen.

1.2.4 Temporal aggregation

In economics, the ways in which variables aggregate could take three different forms: 1) aggregation of a stock variable through time or systematic sampling, 2) aggregation of a flow variable or temporal aggregation, 3) cross-sectional aggregation or contemporaneous. In the context of the present work, we are particularly interested in temporal aggregation.

Assume that a process is observed at a lower frequency than it is generated at. We denote η as a sampling interval or level of aggregation. Hence, if the dynamics of the true underlying discrete time process y_t^D take place at every $1/\eta$ period, then the behavior of the observed process y_t takes place at every unit moment of time. As we can see, the level of aggregation η is the number of times the dynamics of the true underlying process y_t^D take place between observations. Under the assumption that the true process is observed at a lower frequency, η is an integer strictly greater than 1. In case $\eta = 1$, the observed process takes place at the same frequency as the true one and both time series are equivalent.

If the true underlying process y_t^D is temporally aggregated then its values are aggregated between sampling intervals. The formal definition is given as follows: a discrete-time temporally aggregated process y_t^{DA}, whose true process y_t^D has $1/\eta$ dynamic periods, consists of $\left\{ y_t^{DA} = \sum_{k=0}^{\eta-1} y_{t-(k/\eta)}^D \,; t = 1, 2, 3... \right\}$.

The procedure of temporal aggregation with the value of $\eta = 5$ is demonstrated in the Figure 1.2. The temporally aggregated process y_t^{DA} is generated by summing every 5 values of the true underlying process y_t^D.

Figure 1.2: Temporal aggregation

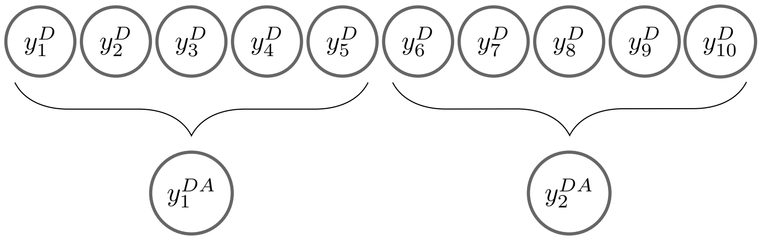

We shall also give a financial time series example. If the true process is the returns series that is generated every business day, then temporal aggregation in intervals of 5 days allows to obtain the weekly returns series. The example can be illustrated formally. Assume that P_t is a price process where $t = 1, 2, 3...$ represent business weeks. The daily continuously compounded rate of return is given by:

$$r_t^D = \ln\left(\frac{P_t}{P_{t-1/5}}\right). \tag{1.23}$$

Then, the weekly continuously compounded rate of return is given by:

$$r_t^{DA} = \ln\left(\frac{P_t}{P_{t-1}}\right). \tag{1.24}$$

The equation above can be expanded as:

$$r_t^{DA} = \ln\left[\left(\frac{P_t}{P_{t-1/5}}\right)\left(\frac{P_{t-1/5}}{P_{t-2/5}}\right)\left(\frac{P_{t-2/5}}{P_{t-3/5}}\right)\left(\frac{P_{t-3/5}}{P_{t-4/5}}\right)\left(\frac{P_{t-4/5}}{P_{t-1}}\right)\right], \tag{1.25}$$

and so

$$\begin{aligned} r_t^{DA} &= \ln\left(\frac{P_t}{P_{t-1/5}}\right) + \ln\left(\frac{P_{t-1/5}}{P_{t-2/5}}\right) + \ln\left(\frac{P_{t-2/5}}{P_{t-3/5}}\right) + \ln\left(\frac{P_{t-3/5}}{P_{t-4/5}}\right) + \ln\left(\frac{P_{t-4/5}}{P_{t-1}}\right) \\ &= r_t^D + r_{t-1/5}^D + r_{t-2/5}^D + r_{t-3/5}^D + r_{t-4/5}^D. \end{aligned} \tag{1.26}$$

Hence, the weekly returns series is a temporally aggregated daily returns series with the level of aggregation of $\eta = 5$.

1.2.5 Temporal aggregation in ARFIMA processes

In this section we investigate the effect of temporal aggregation on long memory processes following ARFIMA model. Firstly, we present the spectral density, the autocovariance and the autocorrelation functions of the aggregated ARFIMA$(0, d, 0)$ processes and compare them with those of not aggregated series in order to investigate the effect of aggregation on a system's response to innovation (we borrow from Chambers, 1998 and Hwang, 2000). Then we observe the order structure of the temporally aggregated ARFIMA$(0, d, 0)$ processes.

Following the notations we introduced earlier, if the true process y_t^D has $1/\eta$ dynamic periods, its ARFIMA$(0, d, 0)$ specification is given by:

$$\left(1 - L^{1/\eta}\right)^d y_t^D = \epsilon_t, \qquad t = 1, 1 + 1/\eta, 1 + 2/\eta, 1 + 3/\eta, ..., \tag{1.27}$$

where ϵ_t is a white noise process with variance σ^2.

Theorem 1.2.1 (Temporally aggregated ARFIMA(0,d,0) process) *If we sum a discrete true ARFIMA$(0,d,0)$ process y_t^D up to $(\eta-1)/\eta$ lags, we obtain a discrete temporally aggregated ARFIMA$(0,d,0)$ process y_t^{DA}:*

$$
\begin{aligned}
y_t^{DA} &= \sum_{j=0}^{\eta-1} y_{t-(j/\eta)}^{D} \\
&= \left(1+L^{1/\eta}+L^{2/\eta}+,...,+L^{(\eta-1)/\eta}\right)\left(1-L^{1/\eta}\right)^{-d}\epsilon_t \\
&= (1-L)\left(1-L^{1/\eta}\right)^{-d-1}\epsilon_t \\
&= \sum_{j=0}^{\eta-1}\sum_{k=0}^{\infty}\frac{\Gamma(k+d)}{\Gamma(d)\Gamma(k+1)}\epsilon_{t-(k/\eta)-(j/\eta)}, \qquad t=1,2,3,....
\end{aligned}
\tag{1.28}
$$

The spectral density $f^{DA}(\omega)$, the autocovariance γ_j^{DA} and the autocorrelation ρ_j^{DA} functions are given by: [1]

$$
\begin{aligned}
f^{DA}(\omega) &= \frac{\sigma^2}{2\pi}\left(2\sin\frac{\omega}{2\eta}\right)^{-2(d+1)}\left(2\sin\frac{\omega}{2}\right)^{2} \\
&\approx \frac{\sigma^2}{2\pi}\eta^{2d+2}\omega^{-2d} \quad \textit{as } \omega\to 0,
\end{aligned}
\tag{1.29}
$$

$$
\begin{aligned}
\gamma_j^{DA} =& \frac{\sigma^2\Gamma(1-2d)}{2(1+2d)\Gamma(1+d)\Gamma(1-d)}\times\left[\frac{\Gamma(1+j\eta+d+\eta)}{\Gamma(j\eta-d+\eta)}\right. \\
&\left.+\frac{\Gamma(1+j\eta+d-\eta)}{\Gamma(j\eta-d-\eta)}-2\frac{\Gamma(1+j\eta+d)}{\Gamma(j\eta-d)}\right] \\
\approx& \frac{\sigma^2\Gamma(1-2d)}{2(1+2d)\Gamma(1+d)\Gamma(1-d)} \\
&\times\eta^{1+2d}\left[(j+1)^{1+2d}+(j-1)^{1+2d}-2j^{1+2d}\right] \quad \textit{for large } \eta \\
\approx& \frac{\sigma^2\Gamma(1-2d)}{\Gamma(d)\Gamma(1-d)}\eta^{1+2d}j^{2d-1} \qquad \textit{as } j\to\infty,
\end{aligned}
\tag{1.30}
$$

[1] The expression for the spectral density $f^{DA}(\omega)$ in Theorem 1.2.1 does not account for the aliasing effect. See Section 1.7.1 (Appendix) for the expression for the $f^{DA}(\omega)$ that accounts for the aliasing effect provided by Souza (2005) and subsequent discussion.

$$\rho_j^{DA} = \frac{\frac{\Gamma(1+j\eta+d+\eta)}{\Gamma(j\eta-d+\eta)} + \frac{\Gamma(1+j\eta+d-\eta)}{\Gamma(j\eta-d-\eta)} - 2\frac{\Gamma(1+j\eta+d)}{\Gamma(j\eta-d)}}{2\frac{\Gamma(1+d+\eta)}{\Gamma(-d+\eta)} - 2\frac{\Gamma(1+d)}{\Gamma(-d)}}$$
$$\approx \frac{\eta^{1+2d}\left[(j+1)^{1+2d} + (j-1)^{1+2d} - 2j^{1+2d}\right]}{2\eta^{1+2d} - 2\frac{\Gamma(1+d)}{\Gamma(-d)}} \quad \textit{for large } \eta \tag{1.31}$$
$$\approx \frac{\eta^{1+2d}d\,(1+2d)}{\eta^{1+2d} - \frac{\Gamma(1+d)}{\Gamma(-d)}} j^{2d-1} \qquad \textit{as } j \to \infty,$$

where σ^2 is a variance of a white noise process ϵ_t, ω is a frequency, d is a fractional differencing parameter, j is a lag, η is a sampling interval and $\omega \in [-\pi, \pi]$, $d \in (0, 0.5)$, $j \geq 0$, $\eta \geq 1$.

The proof of the stated theorem can be found in Chambers (1998) or Hwang (2000).

Now we shall compare the properties of the spectral density, the autocovariance and the autocorrelation functions of temporally aggregated process with those of the true process. To do that, we compare Equations 1.17 - 1.19 with Equations 1.29 - 1.31 of Theorem 1.2.1. First of all, as we can see, the decay rate of the spectral density function of the temporally aggregated ARFIMA$(0, d, 0)$ process at low frequencies, $-2d$, is the same as that of the true ARFIMA$(0, d, 0)$ process. The decay rate of the autocovariance and the autocorrelation functions of temporally aggregated ARFIMA$(0, d, 0)$ series for large lags, j^{2d-1}, is also the same as the decay rate of those functions for the true disaggregated series.

However, the value of the autocovariance and the autocorrelation functions of temporally aggregated ARFIMA$(0, d, 0)$ process is always larger than the value of those functions of the true ARFIMA$(0, d, 0)$ process for $0 < d < 0.5$. To see why:

$$\frac{\gamma_j^{DA}}{\gamma_j^{D}} = \frac{\frac{\sigma^2\Gamma(1-2d)}{\Gamma(d)\Gamma(1-d)}\eta^{1+2d}j^{2d-1}}{\sigma^2\frac{\Gamma(1-2d)}{\Gamma(d)\Gamma(1-d)}j^{2d-1}} = \eta^{1+2d} > 1, \tag{1.32}$$

as η^{1+2d} is always larger than 1 for positive integer $\eta > 1$ and $0 < d < 0.5$.

In case of the autocorrelation function:

$$\frac{\rho_j^{DA}}{\rho_j^{D}} = \frac{\frac{\eta^{1+2d}d(1+2d)}{\eta^{1+2d}-\frac{\Gamma(1+d)}{\Gamma(-d)}}j^{2d-1}}{\frac{\Gamma(1-d)}{\Gamma(d)}j^{2d-1}} = \frac{\frac{\eta^{1+2d}d(1+2d)}{\eta^{1+2d}-\frac{\Gamma(1+d)}{\Gamma(-d)}}}{\frac{\Gamma(1-d)}{\Gamma(d)}} > 1, \tag{1.33}$$

as the denominator is always smaller than the numerator for for positive integer $\eta > 1$ and $0 < d < 0.5$. Figure 1.3 illustrates this implication and shows the graphs of the autocorrelation function of temporally aggregated ARFIMA$(0, d, 0)$ process for the sampling intervals of $\eta = 1, 2, 5, 10, 20$, the value of $d = 0.2$ and for the lag values of $1 \leq j \leq 10$. Moreover, as mentioned by Hwang (2000), the major changes in the levels of the autocorrelation function of temporally aggregated ARFIMA$(0, d, 0)$ processes occur at short lags.

Figure 1.3: Autocorrelation function of the temporally aggregated ARFIMA process for different sampling intervals ($d = 0.2$)

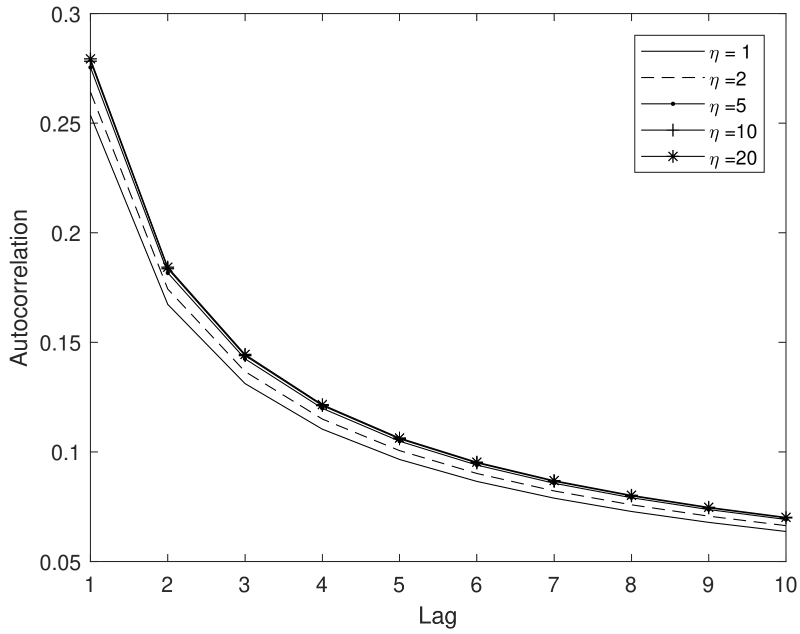

Now we observe the order structure of the temporally aggregated ARFIMA processes. We follow Baillie, Nijman, and Tschernig (1994), Tschernig et al. (1995) and Man and Tiao (2006) in our explanations. Recall that if the true process y_t^D has $1/\eta$ dynamic periods, its ARFIMA$(0, d, 0)$ specification is given by:

$$\left(1 - L^{1/\eta}\right)^d y_t^D = \epsilon_t, \qquad t = 1, 1 + 1/\eta, 1 + 2/\eta, 1 + 3/\eta, ..., \tag{1.34}$$

the discrete temporally aggregated ARFIMA$(0, d, 0)$ process y_t^{DA} is then given by:

$$
\begin{aligned}
y_t^{DA} &= \sum_{j=0}^{\eta-1} y_{t-(j/\eta)}^{D} = \\
&= y_t^D + y_{t-(1/\eta)}^D + ... + y_{t-((\eta-1)/\eta)}^D \\
&= \left(1 + L^{1/\eta} + L^{2/\eta}+, ..., +L^{(\eta-1)/\eta}\right) y_t^D \\
&= \frac{(1-L)}{(1-L^{1/\eta})} y_t^D, \qquad t = 1, 2, 3....
\end{aligned} \tag{1.35}
$$

Then, according to Baillie, Nijman, and Tschernig (1994), Tschernig et al. (1995) and Man and Tiao (2006), to preserve the long memory characteristics for the aggregates, it is possible to write:

$$
\left(1 - L^{1/\eta}\right)^d \frac{(1-L)}{(1-L^{1/\eta})} \frac{(1-L)^d}{(1-L^{1/\eta})^d} y_t^D = \frac{(1-L)^{d+1}}{(1-L^{1/\eta})^{d+1}} \epsilon_t. \tag{1.36}
$$

As Tschernig et al. (1995) and Man and Tiao (2006) claim, from the above we can notice that the moving average process ϵ_t is of infinite order if $d \neq 0$ because the power series expansion of $\left(1 + L^{1/\eta} + L^{2/\eta}+, ..., +L^{(\eta-1)/\eta}\right)^d$ is infinite for any noninteger d (in other words, for noninteger d, the RHS of Equation 1.36 consists of non-terminating terms in L and hence does not have a finite moving average structure in the aggregate time scale). Hence, it is possible to generalize and conclude that any ARFIMA(p, d, q) process is not closed with respect to temporal aggregation since its aggregated form does not admit a finite moving average structure. In other words, as a result of temporal aggregation, ARFIMA(p, d, q) process turns out to be an ARFIMA(p, d, ∞).

Overall, as the decay rate of the spectral density function at low frequencies and the decay rate of the autocorrelation function at large lags are not affected by temporal aggregation, the long memory property of an ARFIMA process is invariant with respect to temporal aggregation. In other words, the long memory parameter d of an ARFIMA series is irrelevant to temporal aggregation and remains unchanged as a result of the latter. However, the autocorrelation function at short lags is affected by temporal aggregation which implies that the short run components of an ARFIMA process change as a result of the aggregation.

The findings of Chambers (1998) and Hwang (2000) indicate that, as the short run components of an ARFIMA series are affected by temporal aggregation, the fully parametric maximum likelihood estimates of the parameter d in temporally aggregated ARFIMA processes, if the changes in the short run specification of the model are not considered, are biased and incorrect. However, as Chambers (1998) and Hwang (2000) also show, the correct estimate of the true long memory parameter d in temporally aggregated ARFIMA processes can be obtained by the semiparametric method of Geweke and Porter-Hudak (1983). Recall that the GPH method concentrates solely on the low frequency properties of the spectral density function which are not affected by temporal aggregation. In the next section, we perform a numerical experiment to validate the stated implications about estimating the true long memory parameter in temporally aggregated ARFIMA series by the semiparametric GPH approach.

1.3 Simulation studies

In this section, we conduct Monte Carlo simulation analysis to investigate the effect of temporal aggregation on the ARFIMA$(0, d, 0)$ processes. The main goal of the simulation analysis is to validate the theoretical implications about estimating the true long memory parameter of ARFIMA processes at various levels of temporal aggregation by the semiparametric approach of Geweke and Porter-Hudak (1983). Recall that ARFIMA$(0, d, 0)$ model is given by:

$$(1 - L)^d y_t = \epsilon_t, \tag{1.37}$$

where ϵ_t is a white noise process.

The numerical experiment design consists of simulating 50 replications with series of 100000 observations from ARFIMA$(0, d, 0)$ model with the values of the long memory parameter $d = 0.2$, $d = 0.3$ and $d = 0.4$. The three different values of the d parameter are chosen in order to obtain the robust conclusion, that does not depend on the particular value of d, about the behavior of the memory parameter on different frequencies. The simulated ARFIMA$(0, d, 0)$ series is then temporally aggregated at different levels $\eta = 2, 5, 10, 20$ and 50 (recall that we denote η as a level of aggregation). The sample sizes of the aggregated data within each replication are: 50000, 20000, 10000, 5000 and 2000 observations for the aggregation levels $\eta = 2, 5, 10, 20$ and 50 respectively.

Theoretical findings in the previous section imply that the true long memory parameter d in temporally aggregated ARFIMA processes can be correctly estimated by the semiparametric methodology of Geweke and Porter-Hudak (1983) as the decay rate of the spectral density function at low frequencies is not affected by temporal aggregation. Hence, we estimate the long memory parameter d in the ARFIMA$(0, d, 0)$ model by applying the semiparametric GPH approach. The number of frequencies used in the GPH regression is chosen to be $N^{0.5}$, where N is a sample size. The mean and the standard deviation of the parameter d estimates over the 50 replications are reported. For the temporally aggregated ARFIMA$(0, d, 0)$ process, the estimation results using the GPH method are reported in Table 1.1.

As we can see in Table 1.1, for the disaggregated series, the mean of the estimated d parameters over the 50 replications is very close to the true value of the long memory parameter. As for the temporally aggregated series, we can see that the mean value of the d parameter estimates is relatively stable for all sampling intervals and all values of the true d. However, the standard deviation of the d parameter estimates increases significantly as the η increases (for example, in case of the series with $d = 0.3$, the standard deviation of the d estimates for the level of aggregation $\eta = 50$ is 3 times larger than the standard deviation of the d estimates for the disaggregated series). Such increase in the standard deviation of the d parameter estimates can be explained by decrease in the sample size as the η increases. Indeed, the sample size for the aggregation level $\eta = 50$ is 50 times smaller than the sample size for the disaggregated series, which impacts the regression estimate of the fractional integration parameter.

Table 1.1: Semiparametric estimation of Geweke and Porter-Hudak (1983) of temporally aggregated ARFIMA$(0, d, 0)$ series

d	$\eta = 1$	$\eta = 2$	$\eta = 5$	$\eta = 10$	$\eta = 20$	$\eta = 50$
0.2	0.208 (0.041)	0.210 (0.050)	0.218 (0.060)	0.218 (0.077)	0.207 (0.088)	0.204 (0.114)
0.3	0.304 (0.030)	0.301 (0.037)	0.297 (0.053)	0.303 (0.057)	0.295 (0.066)	0.295 (0.090)
0.4	0.409 (0.034)	0.413 (0.038)	0.411 (0.051)	0.418 (0.069)	0.425 (0.070)	0.426 (0.078)
Obs.	100000	50000	20000	10000	5000	2000

This table presents the average value and standard deviation (in parenthesis) of estimated long memory parameter d over the 50 replications and the corresponding sample sizes of the aggregated data in each replication.

On the next step, we contribute to the previous studies (such as Hwang, 2000) by also providing a regression analysis of the simulation experiment results. The aim is to formally test the hypothesis of statistical equivalence of the means of the estimated long memory parameters d across all the observed levels of aggregation against the alternative hypothesis that the means of the d estimates are statistically different across the aggregation levels. Formally, we test the null hypothesis

$$H_0 : \mu_1 = \mu_2 = \mu_5 = \mu_{10} = \mu_{20} = \mu_{50}$$

against the alternative

$$H_1 : \mu_1 \neq \mu_2 \neq \mu_5 \neq \mu_{10} \neq \mu_{20} \neq \mu_{50},$$

where μ_1, μ_2, μ_5, μ_{10}, μ_{20}, μ_{50} are the means of the estimated long memory parameters d across the aggregation levels $\eta = 1, 2, 5, 10, 20, 50$.

Firstly, we run a simple OLS linear regression where we regress the estimated parameter d on the categorical variable which represents the particular aggregation level. Let i denote the i^{th} of $I = 300$ estimates of d in the sample. The regression equation can be formally written as:

$$d_i = \gamma + \eta_{2i}\beta_2 + \eta_{5i}\beta_3 + \eta_{10i}\beta_4 + \eta_{20i}\beta_5 + \eta_{50i}\beta_6 + u_i, \tag{1.38}$$

where d_i is the estimated value of the long memory parameter; γ is a constant; η_{2i}, η_{5i}, η_{10i}, η_{20i}, η_{50i} are dummy variables representing the level of aggregation $\eta = 2, 5, 10, 20, 50$ respectively and correspondingly taking value one or zero; u_i is the error term and $i = 1, ..., 300$.

Secondly, we also run the same linear regression as stated above but with standard errors clustered by the replication number to account for the positive correlation between the d estimates at different aggregation levels within each replication. Let r denote the r^{th} of $R = 50$ clusters corresponding to 50 replications. Then, the regression equation is given by:

$$d_{jr} = \gamma + \eta_{2jr}\beta_2 + \eta_{5jr}\beta_3 + \eta_{10jr}\beta_4 + \eta_{20jr}\beta_5 + \eta_{50jr}\beta_6 + u_{jr}, \tag{1.39}$$

where d_{jr} is the estimated value of the long memory parameter; γ is a constant; η_{2jr}, η_{5jr}, η_{10jr}, η_{20jr}, η_{50jr} are dummy variables representing the level of aggregation $\eta = 2, 5, 10, 20, 50$ respectively and correspondingly taking value one or zero; u_{jr} is the error term; $j = 1, ..., 6$ and $r = 1, ..., 50$.

In the stated regression models, the F-test of joint significance of the regression coefficients is also a test of our null hypothesis of statistical equivalence of the means of the estimated long memory parameters d across the levels of aggregation. The F-statistics with the corresponding p-values for the simple OLS regression and for the OLS regression with clustered standard errors applied to the experiment results with the estimates of d obtained by the GPH method are shown in Table 1.2.

Table 1.2: Regression analysis of the GPH estimation of temporally aggregated ARFIMA$(0, d, 0)$ series

d	F-stat(simple)	p-value(simple)	F-stat(clustered)	p-value(clustered)
0.2	0.32	0.9023	1.13	0.3558
0.3	0.63	0.6772	1.82	0.1265
0.4	0.78	0.5662	1.23	0.3107

This table presents the F-statistics with the corresponding p-values for the simple OLS and the clustered OLS linear regressions applied to the experiment results with the simulated data.

As we can see in Table 1.2 for the GPH estimation of the temporally aggregated series, the null hypothesis of statistical equivalence of the means of the estimated long memory parameters d across the levels of aggregation is not rejected for the experiments with the true $d = 0.2$, $d = 0.3$ and $d = 0.4$ in both simple and clustered regression models.

Overall, the results of our Monte Carlo simulation experiment with the ARFIMA$(0, d, 0)$ series coincide with the results obtained by Chambers (1998) and Hwang (2000) for much smaller sample sizes. The result is consistent with the theoretical implications that temporal aggregation does not affect the long memory properties of the series and that the semiparametric estimation procedure of Geweke and Porter-Hudak (1983) is able to obtain a correct estimate of the true d parameter on any level of temporal aggregation. We proceed with the empirical analysis of financial volatility on the foreign exchange market.

1.4 Data

1.4.1 Preparation and volatility measures

The empirical analysis in the present work focuses on the long-term dependence in the volatility of returns on the foreign exchange market on different levels of temporal aggregation.

The raw dataset consists of the high frequency tick-by-tick spot exchange rates quotation data with fractional pip spreads in millisecond resolution for the pound sterling and the US dollar (GBP/USD) currency pair over a sample period from January 4, 2010 to December 30, 2016. The dataset consists of approximately 900 million observations of tick-by-tick quotations over the full sample period of seven years. We perform automated filtering to avoid data errors which raw intraday high frequency data is subject to. A data error is simply defined as a price quotation that does not reflect the real situation on the market. Such errors include, for example, price quotation that is significantly different from the two neighboring ticks, decimal error, missing bid or ask value, incorrect time stamp, etc.

From the raw tick-by-tick quotation data that is irregularly spaced we construct a natural evenly spaced grid of prices following methodology that was proposed by Dacorogna et al. (1993) and Wasserfallen and Zimmermann (1985). Let N be a number of raw tick prices, $p_{t(j)}, j = 0, ..., N$, observed during a trading day. Then, $t(0), ..., t(N)$ are moments of time at which tick prices $p_{t(j)}$ are observed. We refer to a tick price $p_{t(j)}$ as a mid-quote at time $t(j)$:

$$p_{t(j)} = \frac{p(bid)_{t(j)} + p(ask)_{t(j)}}{2}$$

We denote τ as any arbitrary point in the time interval $[t(0), t(N))$. Then, the artificial continuous time process is

$$p(\tau) = p_{t(j)}, \tau \in [t(j), t(j+1))$$

So, when any price grid point $p(\tau)$ falls between two adjacent randomly spaced ticks $p_{t(j)}$ and $p_{t(j+1)}$, we choose price $p(\tau)$ to be equal to $p_{t(j)}$. This is the idea of the previous-tick method to construct an equidistant grid of prices from raw non-equidistant tick-by-tick data. The artificial continuous time price process allows to construct evenly spaced intraday and non-intraday returns for any frequency, using the definition of returns as the first difference of logarithmic prices and temporal aggregation technique. In order to avoid complicating the inference by the slower trading activity on weekends and holiday periods, we exclude from the data sample all the price quotations from Saturday 00:00:00 GMT to Sunday 23:59:59 GMT and some other inactive days.

In the present work, we analyze volatility of the GBP/USD exchange rate returns sampled at the following time scales: 30 minutes, 1 hour, 2 hours, 3 hours, 4 hours, 1 day. The choice of the analyzed time scales is motivated by the previous literature (such as Mcmillan and Speight, 2008) and computational resources required to estimate long memory models for the stated time series. For volatility measures, we use absolute and squared returns which are widely used in the literature as the most common proxies of the conditional variability of financial returns (see, e.g, Andersen and Bollerslev, 1997a; Bollerslev and Wright, 2000; etc). We also use the realized measure of returns volatility proposed by Andersen et al. (2001). The returns volatility measures used the study are discussed below.

Assume that the logarithmic price $p(t)$ of a liquid asset follows the standard continuous time process

$$\mathrm{d}p(t) = \mu(t)\ \mathrm{d}t + \sigma(t)\ \mathrm{d}W(t), \tag{1.40}$$

where $W(t)$ is a standard Brownian motion, $\mu(t)$ is an instantaneous conditional mean and $\sigma(t)$ is an instantaneous conditional volatility of the process which is assumed to follow a long memory dynamics with the fractional parameter d $(0 < d < 0.5)$.[2]

The integrated volatility associated with day t, for this diffusion process, is the integral of the instantaneous volatility over the one day interval $(t - 1d; t)$, where a full trading day is represented by the time interval $1d$,

$$\sigma_t^{(d)} = \left(\int_{t-1d}^{t} \sigma^2(\omega)\mathrm{d}\omega \right)^{1/2}. \tag{1.41}$$

As demonstrated by Rossi and De Magistris (2014), the integrated volatility is also a long memory process and characterized by the same order of fractional differencing d as the instantaneous volatility.

As firstly proposed by Merton (1980) and then by Andersen et al. (2001), the sum of intraday squared returns can be used to approximate the integrated volatility $\sigma_t^{(d)}$ to an arbitrary precision. The nonparametric estimator

[2]For example, the instantaneous volatility can follow the fractional Ornstein-Uhlenbeck process of Comte and Renault (1998):

$$\mathrm{d}\ln\sigma^2(t) = -k\ln\sigma^2(t)\mathrm{d}t + \gamma\mathrm{d}W_d(t),$$

where $k > 0$ is the drift parameter, $\gamma > 0$ and $W_d(t)$ is the fractional Brownian motion.

of the integrated (actual) volatility based on the sum of intraday squared returns is called realized volatility. Following Andersen et al. (2001) and Corsi (2009), the realized volatility over a time interval of one day can be defined as

$$RV_t^{(d)} = \sqrt{\sum_{j=0}^{M-1} r_{t-j\Delta}^2}, \tag{1.42}$$

where $\Delta = \frac{1d}{M}$ ($1d$ indicates one trading day; M indicates the number of intraday periods) and $r_{t-j\Delta} = p(t-j\Delta) - p(t-(j+1)\Delta)$ defines continuously compounded Δ-frequency returns, that is, intraday returns sampled at time interval Δ (the subscript t indexes the day, while j indexes the time within the day t).

In other words, realized volatility over a time interval of one day is the square root of the sum of squared high frequency intraday returns. In the similar manner to daily return, realized volatility can be constructed for any arbitrary return time scale. Under certain assumptions, realized volatility is an unbiased volatility estimator and, as the sampling frequency Δ increases, the realized volatility provides a consistent nonparametric measure of the integrated volatility of returns over the fixed time interval (see Andersen et al. (2003) and Corsi (2009) for details). Rossi and De Magistris (2014) also show that realized volatility has the same long memory dynamics as the integrated volatility and the instantaneous volatility with the equal value of the differencing parameter d. Moreover, in absence of market microstructure noise, the spectral density of realized volatility converges to that of the integrated volatility as the sampling frequency Δ increases.

However, in practice, realized measure of returns volatility suffers from the market microstructure noise bias if sampling frequency Δ of squared returns is too high (Andersen et al., 2001). For the foreign exchange market, for the purpose of constructing realized volatility, it is generally accepted in the literature that returns sampled at 5 minutes frequency provide an optimal trade off between the precision of volatility estimator and bias induced by the market microstructure noise (see, e.g., Barndorff-Nielsen and Shephard, 2002; Andersen et al., 2003; etc). Hence, in the present work, we use 5 minutes returns to construct realized volatility measures for the 30 minutes, 1 hour, 2 hours, 3 hours, 4 hours and daily returns.

For the purpose of comparison, we also apply the more traditional volatility proxies than realized volatility, such as absolute and squared returns. It is important to mention the differences between realized volatility and absolute or squared returns as volatility measures. Absolute and squared returns are considered as proxies for the latent conditional volatility and are typically contaminated by substantial measurement error which dwarfs the variation in the actual volatility process. On the contrary, realized volatility, as an estimate of the integrated volatility, can be treated as observable variable rather than latent. Moreover, under general conditions, realized volatility is approximately free of measurement error (see Andersen et al., 2001; Hansen, Huang, and Shek, 2012).

1.4.2 Descriptive statistics and intraday periodicity

Now we present the summary of the descriptive statistics of the GBP/USD exchange rate returns series for all the observed time resolutions (30 minutes, 1 hour, 2 hours, 3 hours, 4 hours, 1 day) and for the 5 minutes returns used to calculate realized volatility. Table 1.3 reports the descriptive statistics for the returns for different frequencies: number of observations, mean, standard deviation, skewness, kurtosis and the Ljung-Box (Ljung and Box, 1978) portmanteau tests statistics for up to 100-order and up to 1000-order serial correlation.

Table 1.3: Descriptive statistics

Frequency	Obs.	Mean	Std Dev	Skewness	Kurtosis	$Q(100)$	$Q(1000)$
5 min	518370	-5.15e-07	0.0003667	-6.479783	961.5511	4754.9118***	6839.0358***
30 min	86395	-3.10e-06	0.0008268	-1.444307	78.07625	351.8650***	1767.0417***
1 hour	43197	-6.18e-06	0.0011752	-3.091013	166.1308	256.0069***	1416.6112***
2 hours	21598	-0.0000123	0.0016712	-3.640864	149.6781	241.8622***	1338.1674***
3 hours	14399	-0.0000185	0.0020211	-3.063773	107.0523	199.8560***	1171.1478***
4 hours	10799	-0.0000245	0.0023634	-3.589248	127.8814	197.734***	1158.4292***
1 day	1799	-0.0001481	0.0055295	-1.00379	13.22705	93.0122	754.7189

The table reports descriptive statistics for the time series of the GBP/USD returns for different frequencies: number of observations, mean, standard deviation, skewness, kurtosis and the Ljung-Box portmanteau test Q-statistics for up to 100-lags and 1000-lags serial correlation. The sample period is from January 4, 2010 to December 30, 2016. ***, ** and * indicate statistical significance at the 1%, 5% and 10% levels respectively.

As we can see, the mean of the returns is approximately zero for all the observed time resolutions. The standard deviation of the returns increases as the frequency of observation becomes lower. It is easy to notice that the standard deviation does not increase in proportion to the square root of the sampling frequency, $\sqrt{\eta}$, indicating the presence of serial correlation in the returns distribution. For all the observed frequencies, the returns are skewed and display large kurtosis indicating that the returns distribution is "fat tailed" and cannot be considered as normal. However, as the level of aggregation increases, the returns distribution becomes less skewed and leptokurtic and looks more and more like a normal distribution. The standard Ljung-Box portmanteau test indicates the presence of serial correlation in the returns for up to 100 lags and for up to 1000 lags for all the frequencies except 1 day. In general, the described properties of the GBP/USD exchange rate returns distribution are consistent with the stylized facts of financial assets returns distribution documented in the literature (see, e.g., Cont, 2001; Christoffersen, 2012).

In order to explore the intraday periodicity in the GBP/USD returns series, we consider the mean properties, the autocorrelation and the spectral density structure of the returns processes. Figure 1.4 shows the plots of the mean return and the mean absolute return for each of the 48 intraday 30-min intervals. Clearly, the mean return for each 30-min intraday interval is concentrated around zero and does not demonstrate any kind of periodic pattern over the trading day cycle. However, if we observe the mean absolute return for each 30-min intraday interval, it is possible to notice a kind of "M-shape" intraday pattern associated with a cyclical behavior of the absolute returns during a trading day. Such a form of intraday seasonality can be explained by the properties of the functioning of the foreign exchange market. As the market is open 24 hours, the observed periodic cycles of high and low mean absolute returns are caused by the functioning of various exchanges around the world, the peak of business activity of which falls at different hours of Greenwich Mean Time (GMT). For example, the trading session in London (where the majority of all transactions with the British pound takes place) opens at 8:00 GMT and closes at 17:00 GMT. The intraday period from 8:00 GMT to 17:00 GMT corresponds to the period between the 16th and the 34th 30-min intervals during a day. The graph of the mean absolute returns between the 16th and the 34th 30-min intervals has a "U-shape" pattern indicating relatively high absolute returns during the first and the last hours of a trading session in London and relatively low absolute returns in the midday.

Figure 1.5 shows the correlograms of GBP/USD 30-min returns, squared returns and absolute returns. The maximum number of lags under consideration is 480 that corresponds to 10 trading days. As we can see, the autocorrelation function of the returns is concentrated around zero and does not exhibit any kind of periodic behavior. The periodic behavior of the autocorrelation function of the squared returns is not clearly observable because the autocorrelations at high lags are relatively small. However, the autocorrelation function of the absolute returns has a clear cyclical dynamics demonstrating the "U-shape" patterns with peaks at every 48 interval that corresponds to the periodicity in the limits of 1 day. We should note that the pronounced "U-shape" pattern in the dynamics of the autocorrelation function of the absolute intraday returns of financial assets is a well known phenomena and widely documented in the literature (see, e.g., Andersen and

Bollerslev, 1997b; McMillan and Speight, 2004; Baillie, Cecen, and Han, 2015).

We supplement the preceding investigation of the intraday periodicity in the data with the analysis of the returns processes in the frequency domain. Figure 1.6 shows the periodograms of GBP/USD 30-min returns, squared returns and absolute returns.[3] The goal of the analysis is to identify the important frequencies (and, consequently, periods) in the observed series. If a certain frequency is important in explaining the variation of a series, the periodogram of the series at this frequency will exhibit a clear dominant spike. So, the periodogram of the returns does not exhibit any dominant spikes indicating the absence of a cyclical behavior in the series of the returns. However, both the periodogram of the squared returns and the periodogram of the absolute returns reveal two dominant spikes. The first dominant spike occurs at the origin of the function indicating the potential presence of the long memory dynamics in the series of the absolute and squared returns. The second dominant spike corresponds to a frequency of 0.02083333. The period for this frequency value is equal to $1/0.02083333 = 48$. This indicates that the series of the absolute and squared returns contain a periodic component with a period of 48 30-min intervals, in other words, the series contain daily periodic component. Notice that the frequency domain analysis allows to precisely investigate the cyclical behavior of the series even if the periodicity is not directly observable in the time domain (as is the case with the autocorrelation function of the squared returns).

Although we report here the detailed analysis of the intraday periodicity of only 30-min returns data, the same seasonal dynamics is present in the intraday data for all the observed time scales (such as 30 minutes, 1 hour, 2 hours, 3 hours, 4 hours).

As we can see, the periodic component strongly affects the autocorrelation functions of the intraday absolute and squared returns. This fact significantly complicates the investigation of the long memory in the series because the observed periodicity makes it impossible to clearly identify the decay rate of the autocorrelation function of the processes. Also, the standard long memory time series models (such as ARFIMA) are not designed to capture such periodic patterns in the process dynamics. Thus, ignoring the periodic behavior in the series will result in a distortion in the long memory parameter estimates.

[3]We use the Fast Fourier Transform (FFT) approach to obtain the spectral density function of the processes and construct the periodograms. The FFT algorithm is implemented in most of statistical packages and allows to rapidly compute the Discrete Fourier Transform (DFT) of a sequence. The detailed description of the algorithm can be found in Cooley and Tukey (1965).

There are several approaches which allow to model and remove the strong intraday periodicity in the high frequency financial data. After some preliminary analysis, we chose the approach suggested by Andersen and Bollerslev (1997b) that involves standardizing the series by its mean absolute value for each particular intraday time interval. The stated approach proved its superiority and simplicity in removing intraday periodicities in comparison with other methods.[4]. The periodicity adjusted returns are given by:

$$r_{\tau,n} = R_{\tau,n}/|\overline{R}|_n, \tag{1.43}$$

where $|\overline{R}|_n = T^{-1}\sum_\tau |R_{\tau,n}|$ and $R_{\tau,n}$ is a raw return over the intraday interval n on a certain day τ, T is the total number of trading days in the sample.

Hence, we use the stated approach to standardize the intraday returns for all the observed time resolutions in order to remove the strong intraday periodicity. Figure 1.7 shows the correlogram of the periodicity adjusted GBP/USD 30-min returns as well as squared and absolute periodicity adjusted 30-min returns. As we can see, the autocorrelation function of the periodicity adjusted returns is concentrated around zero and its shape has not changed significantly after the standardizing procedure. However, if we observe the correlograms of the squared and absolute periodicity adjusted returns, we can notice that they do not exhibit any kind of periodic behavior indicating that the used approach is effective in removing the intraday periodicity in the data. Moreover, the slow hyperbolic decay rate of the autocorrelation function is now clearly observable for the absolute adjusted returns.

Let us now observe the properties of the adjusted returns in the frequency domain. Figure 1.8 shows the periodograms of the periodicity adjusted GBP/USD 30-min returns, squared returns and absolute returns. Clearly, the periodograms of the squared and absolute adjusted returns have the only dominant peak at the origin that indicates not only the absence of any intraday periodic dynamics in the series but also the presence of the long-range dependence in the series of the squared and absolute periodicity adjusted returns. This fact provides an additional evidence that the approach of standardizing the series by its mean absolute value for each particular intraday time interval is an effective tool in removing the intraday periodicity in the high frequency financial data. The pronounced approach was also successful in removing the intraday periodicity in returns for all other time resolutions under consideration (although here we only present the results of removing

[4] For a comparative analysis of the various methods of removing the intraday periodicity in the high frequency financial data, including the Flexible Fourier Form approach of Andersen and Bollerslev (1997a), see McMillan and Speight (2004)

the intraday periodicity for 30 min returns series).

Also, to prevent realized volatility of the analyzed intraday returns (such as 30 minutes, 1 hour, 2 hours, 3 hours, 4 hours returns) from suffering from intraday periodicity, we use periodicity adjusted 5 minutes returns to calculate realized volatility for the intraday returns under consideration. As for an example, the correlogram and periodogram of the realized volatility of the 30 min returns constructed from raw 5 min returns exhibit clear periodic pattern (see Figure 1.9). On the contrary, constructing realized volatility of the 30 min returns from the periodicity adjusted 5 min returns makes it possible to significantly reduce periodic pattern in the series dynamics and explore long memory behaviour (see Figure 1.10).

Figure 1.4: GBP/USD Mean return for each 30-min intraday interval

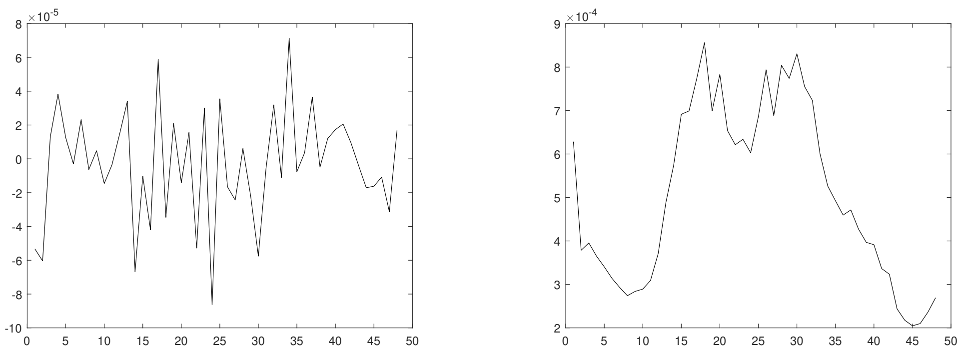

(a) Returns (b) Absolute returns

Figure 1.5: GBP/USD Correlogram of 30-min returns

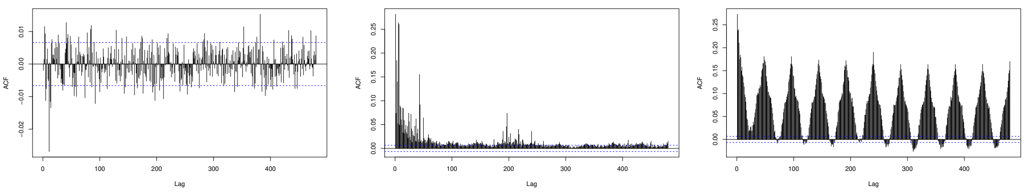

(a) Returns (b) Squared returns (c) Absolute returns

Figure 1.6: GBP/USD Periodogram of 30-min returns

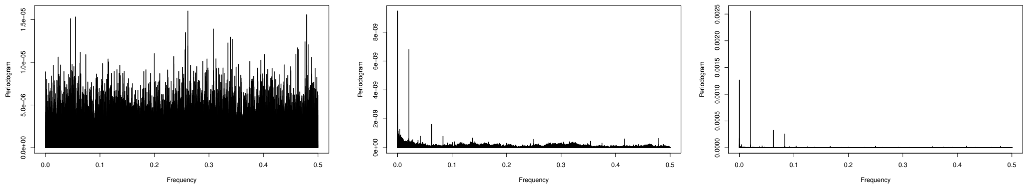

(a) Returns (b) Squared returns (c) Absolute returns

Figure 1.7: GBP/USD Correlogram of 30-min periodicity adjusted returns

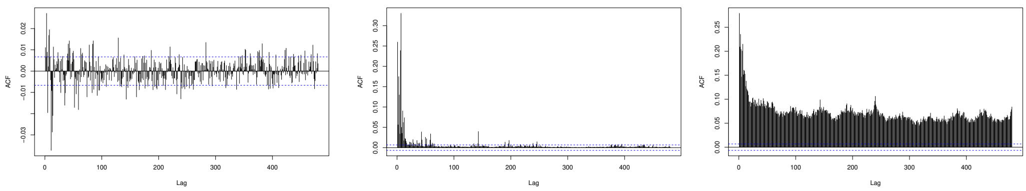

(a) Returns (b) Squared returns (c) Absolute returns

Figure 1.8: GBP/USD Periodogram of 30-min periodicity adjusted returns

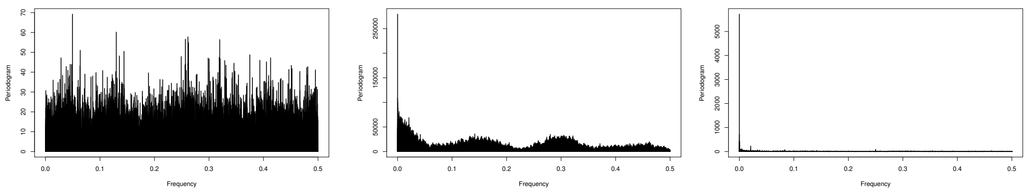

(a) Returns (b) Squared returns (c) Absolute returns

Figure 1.9: GBP/USD Correlogram and periodogram of realized volatility of 30-min returns constructed from raw 5-min returns

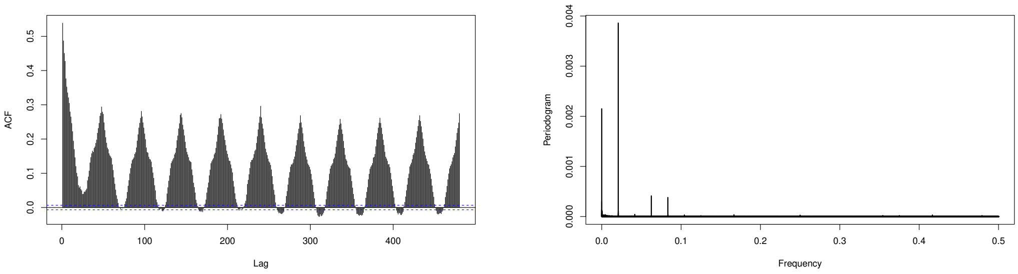

(a) Correlogram (b) Periodogram

Figure 1.10: GBP/USD Correlogram and periodogram of realized volatility of 30-min returns constructed from periodicity adjusted 5-min returns

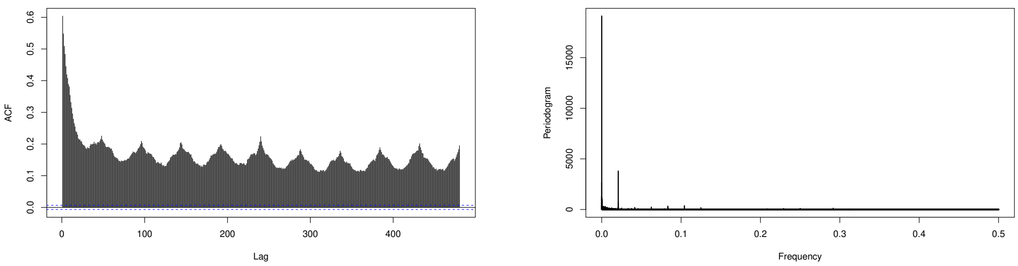

(a) Correlogram (b) Periodogram

1.5 Empirical results

In this section, we investigate the long-range dependence in volatility of 30 minutes, 1 hour, 2 hours, 3 hours, 4 hours and 1 day returns. The volatility is measured by absolute returns, squared returns and realized volatility as stated in the previous section.[5] Firstly, we implement the rescaled range test of Hurst (1951) and the modified rescaled range test of Lo (1991) to test for the long-range dependence in the series of absolute returns, squared returns and realized volatility.[6] Then, we also use the semiparametric regression methodology of Geweke and Porter-Hudak (1983) to model the long memory dynamics of the stated series of volatility proxies at all the analyzed time scales and to estimate the fractional differencing parameter d.

Table 1.4: The summary of Hurst (1951) rescaled range test statistic for the series of absolute returns, squared returns and realized volatility

30 min	1 hour	2 hours	3 hours	4 hours	1 day
Absolute					
27.00	18.60	12.40	11.40	9.43	4.88
Squared					
4.51	2.62	1.94	2.54	1.92	2.61
Realized Vol					
42.30	32.50	24.60	20.80	18.70	8.39
Number of obs.					
86395	43197	21598	14399	10799	1799

This table presents the rescaled range test statistic for each observed sampling frequency for the series of absolute returns, squared returns and realized volatility. The null hypothesis of the test is the process is not long-range dependent. The critical values are as follows: 90%: $[0.861, 1.747]$, 95%: $[0.809, 1.862]$, 99%: $[0.721, 2.098]$.

Table 1.4 presents the results of the rescaled range test of Hurst (1951) applied to the series of absolute returns, squared returns and realized volatility at different time scales. As we can see, for the series of absolute returns and realized volatility, the null hypothesis of no long-range dependence is rejected at the 99% confidence level for all the time scales. For the series of squared returns, the null hypothesis of no long-range dependence is rejected

[5]Recall that we use absolute and squared periodicity adjusted returns to measure the volatility of intraday returns at time scales: 30 minutes, 1 hour, 2 hours, 3 hours, 4 hours. We also use periodicity adjusted 5-min returns to construct realized volatility of the intraday returns. In order to avoid the frequent mentioning of the same notations, hereafter in this section the periodicity adjusted intraday returns will be referred to as simply "returns".

[6]The description of the rescaled range test of Hurst (1951) and the modified rescaled range test of Lo (1991) is provided in Section 1.7.2 (Appendix).

Table 1.5: The summary of Lo (1991) modified rescaled range test statistic for the series of absolute returns, squared returns and realized volatility

330 min	1 hour	2 hours	3 hours	4 hours	1 day
Absolute					
15.30	10.90	7.63	7.44	6.17	3.30
Squared					
2.83	1.91	1.48	1.90	1.52	1.89
Realized Vol					
17.40	13.50	10.70	9.34	8.47	4.00
Number of obs.					
86395	43197	21598	14399	10799	1799

This table presents the rescaled range test statistic for each observed sampling frequency for the series of absolute returns, squared returns and realized volatility. The null hypothesis of the test is the process is not long-range dependent. The critical values are as follows: 90%: $[0.861, 1.747]$, 95%: $[0.809, 1.862]$, 99%: $[0.721, 2.098]$.

at the 99% level for the time scales of 30 min, 1 hour, 3 hours and 1 day; for the time scales of 2 hours and 4 hours, the null hypothesis is rejected at the 95% level.

In the next step, we also implement the modified rescaled range test of Lo (1991) to test for long memory in the series of returns. The results of the test are reported in Table 1.5. According to the test results, the null hypothesis of no long-range dependence is rejected at the 99% confidence level for the series of absolute returns and realized volatility at all observed time scales. For the series of squared returns, the null hypothesis is rejected at the 99% level for the frequency of 30 min and at the 95% level for the frequencies of 1 hour, 3 hours and 1 day. However, for the frequencies of 2 hours and 4 hours, the null hypothesis of no long-range dependence is not rejected.

Table 1.6 presents the results of the long memory parameter d estimates in the series of absolute returns, squared returns and realized volatility using the semiparametric GPH approach. The number of frequencies used in the GPH regression is chosen to be $N^{0.5}$, where N is a sample size. For the absolute returns, the d parameter estimates vary from the value of 0.237 for the frequency of 2 hours to 0.355 for the frequency of 30 min. For the squared returns, the d estimates vary from 0.040 for the frequency of 2 hours to 0.185 for the frequency of 1 day. For realized volatility, the d estimates vary from 0.357 for the frequency of 30 min to 0.444 for the frequency of 4 hours. For the series of absolute returns and realized volatility, the standard error of the d estimates tends to increase as the level of aggregation increases. The standard error of the d estimates for the series of squared returns does not exhibit a consistent pattern. The GPH estimates of the long memory parameter d

Table 1.6: Semiparametric regression analysis of Geweke and Porter-Hudak (1983) for the series of absolute returns, squared returns and realized volatility

30 min	1 hour	2 hours	3 hours	4 hours	1 day
Absolute					
0.355*	0.320*	0.237*	0.316*	0.296*	0.299*
(0.034)	(0.040)	(0.041)	(0.060)	(0.062)	(0.103)
Squared					
0.078*	0.070*	0.040*	0.102*	0.066*	0.185*
(0.014)	(0.011)	(0.010)	(0.020)	(0.015)	(0.063)
Realized Vol					
0.357*	0.381*	0.389*	0.394*	0.444*	0.364*
(0.037)	(0.047)	(0.056)	(0.062)	(0.070)	(0.115)
Number of obs.					
86395	43197	21598	14399	10799	1799

This table presents the estimated value and the standard error (in parenthesis) of the long memory parameter d for each observed sampling frequency for the series of absolute returns, squared returns and realized volatility. * indicate statistical significance at the 5% level.

across all the observed time scales for the series of absolute returns, squared returns and realized volatility are statistically significant at 5% level. This clearly indicates that the volatility of the returns at various time scales follow the long memory dynamics and corresponds with a resounding evidence reported in the literature (see, e.g, Ding, Granger, and Engle, 1993; Andersen and Bollerslev, 1997a; Bollerslev and Wright, 2000; Mcmillan and Speight, 2008; Rodrigues, Demetrescu, and Rubia, 2018).

As the notion of volatility as a true long memory process implies that the degree of fractional integration in volatility is invariant with respect to temporal aggregation, now we observe the consistency of the GPH estimates of the long memory parameter d across the analyzed time scales for the series of absolute returns, squared returns and realized volatility. We contribute to the literature by proposing a Z-test to formally test the null hypothesis of statistical equivalence of the estimates of the d parameter at the time scale i and at the time scale j ($H_0 : d_i = d_j$, where i, j denotes the observed time scales of 30 min, 1 hour, 2 hours, 3 hours, 4 hours, 1 day and $i \neq j$) against the alternative hypothesis of a difference between the two estimates of d ($H_1 : d_i \neq d_j$). The test statistic is calculated as:

$$Z = \frac{d_i - d_j}{\sqrt{se_i^2 + se_j^2 - 2\rho_{ij} se_i se_j}}, \tag{1.44}$$

where d_i, d_j are the estimates and se_i, se_j are the standard errors of the estimates of the long memory parameter d at the time scales i and j respectively and ρ_{ij} is the correlation between the estimates d_i and d_j.

The simulation experiment conducted in Section 1.3 provides the intuition about the linear dependence between the estimates of the d parameter at various time scales. In general, the correlation between the estimates of d is not constant and depends on the difference in aggregation levels. For example, the correlation between the estimates of d at the levels of aggregation 1 and 2 is usually very high, while the corresponding correlation between the estimates of d at the levels of aggregation 1 and 50 is usually very low. In general, the correlation coefficient lies in the approximate range from 0.10 to 0.90, being relatively high for close aggregation levels and relatively low for distant ones. Thus, as the correlation between the estimates of d is not constant and varies in different conditions, in our framework of the Z-test, for robustness, we estimate the two values of the test statistics: the lower bound, assuming zero dependence between the d estimates ($\rho = 0$), and the upper bound, assuming a very high linear dependence ($\rho = 0.90$).

In our framework, there are 15 pairwise comparisons of the d estimates at various aggregation levels, so the p-values of the test should be adjusted for multiple comparisons to control the family-wise error rate. To adjust the p-values, we use the simple approach of Bonferroni (1936) as well as the methods of Holm (1979), Hochberg (1988) and Hommel (1988) which are known to be more powerful than Bonferroni correction and more robust in case of positively associated hypothesis tests.[7]

For the test of the statistical equivalence of the GPH estimates of the long memory parameter d at various time scales, Tables 1.7 and 1.8 show the Z-statistics with the corresponding raw (unadjusted) p-values and the p-values adjusted for multiple comparisons. Table 1.7 presents the results based on the lower bound of the Z-statistics, while Table 1.8 presents the results based on the upper bound of the Z-statistics.

For the lower bound of the test statistics, the results in Table 1.7 indicate that, after controlling for multiple comparisons, for the series of absolute returns, squared returns and realized volatility, there is no evidence of a statistical difference between the d estimates across any of the time scales at the 5% significance level. The test result indicates that the long memory in volatility of the returns is characterized by the same fractional differencing parameter across all the time scales. In the most conservative setting and the corresponding upper bound of the test statistics, the results in Table 1.8 indicate no evidence of the difference between the d estimates across the analyzed time scales for the series of realized volatility. However, for

[7]The description of the different applied p-value adjustment methods is provided in Section 1.7.3 (Appendix).

the series of absolute and squared returns, the null hypothesis of statistical equivalence of the d estimates is rejected in several pairwise tests.

As we can see, for the series of realized volatility, the null hypothesis of statistical equivalence of the GPH estimates of the d parameter across various time scales cannot be rejected in case of both lower and upper bounds of the test statistics. This observation shows that the evidence in favor of the hypothesis of equivalence of the long memory parameters is stronger for the series of realized volatility than for the absolute and squared returns. This might indicate that relatively less noisy volatility proxies (such as realized volatility) more fully represent the long memory property of the unobserved true volatility than relatively more noisy volatility measures (such as absolute or squared returns). This is in line with the empirical evidence in the literature that different volatility measures can provide different conclusions about the persistence in volatility (see, e.g., Bollerslev and Wright, 2000; Deo and Hurvich, 2001; Arteche, 2004; Mcmillan and Speight, 2008; etc).

Overall, as a result of applying various tests for the long-range dependence as well as the semiparametric estimation techniques of the ARFIMA model to the GBP/USD exchange rates data, we document the presence of the long memory dynamics in the volatility component of the exchange rates returns at different time scales. Moreover, using the semiparametric GPH method applied to the series of realized volatility, we found a strong evidence that the persistence in the volatility does not change with respect to temporal aggregation. This result lends broad support to the proposition that volatility of financial returns is a true long memory process and is consistent with the notion of returns as self-similar (or fractal) processes (see, e.g., Bollerslev and Wright, 2000; Ohanissian, Russell, and Tsay, 2008; Mcmillan and Speight, 2008; Baillie, Cecen, and Han, 2015). Our findings indicate that the properties of financial volatility as a true long memory process are more clearly reflected if less noisy and more precise proxies (such as realized volatility) are used for volatility modeling and estimation.

Interestingly, the GPH estimates of the d parameter for the series of absolute returns for the frequencies of 30 min and 4 hours reported in the present work (0.355 and 0.296 respectively) are strikingly consistent with the GPH d estimates reported by Mcmillan and Speight (2008) for the series of 30-min and 4-hours absolute GBP/USD exchange rates returns for the period from 1 January 1996 to 31 December 1996 (0.360 and 0.300 respectively). This result indicates stability of the long memory in the volatility of the exchange rate returns across long periods of time and provides another argument in favor of the proposition of Andersen and Bollerslev (1997a) that long memory is an intrinsic feature of the returns generating process and is not caused by occasional structural shifts.

Table 1.7: Z-test of the statistical equivalence of the GPH estimates of the d parameter at various time scales for the series of absolute returns, squared returns and realized volatility (lower bound, $\rho = 0$)

Test	Z-stat	Raw p-value	Bonferroni	Holm	Hochberg	Hommel
Absolute						
30min-1h	0.6667	0.5050	0.9999	0.9999	0.9801	0.9801
30min-2h	2.2154	0.0267	0.4005	0.4005	0.4005	0.4005
30min-3h	0.5655	0.5717	0.9999	0.9999	0.9801	0.9801
30min-4h	0.8344	0.4041	0.9999	0.9999	0.9801	0.9801
30min-1day	0.5163	0.6057	0.9999	0.9999	0.9801	0.9801
1h-2h	1.4490	0.1473	0.9999	0.9999	0.9801	0.9801
1h-3h	0.0555	0.9558	0.9999	0.9999	0.9801	0.9801
1h-4h	0.3253	0.7450	0.9999	0.9999	0.9801	0.9801
1h-1day	0.1901	0.8493	0.9999	0.9999	0.9801	0.9801
2h-3h	1.0871	0.2770	0.9999	0.9999	0.9801	0.9801
2h-4h	0.7938	0.4273	0.9999	0.9999	0.9801	0.9801
2h-1day	0.5593	0.5760	0.9999	0.9999	0.9801	0.9801
3h-4h	0.2318	0.8167	0.9999	0.9999	0.9801	0.9801
3h-1day	0.1426	0.8866	0.9999	0.9999	0.9801	0.9801
4h-1day	0.0250	0.9801	0.9999	0.9999	0.9801	0.9801
Squared						
30min-1h	0.4493	0.6532	0.9999	0.9999	0.8297	0.8297
30min-2h	2.2087	0.0272	0.4080	0.3536	0.3536	0.2950
30min-3h	0.9831	0.3256	0.9999	0.9999	0.8297	0.8297
30min-4h	0.5848	0.5587	0.9999	0.9999	0.8297	0.8297
30min-1day	1.6580	0.0973	0.9999	0.8757	0.8297	0.5838
1h-2h	2.0180	0.0436	0.6540	0.5232	0.5232	0.3620
1h-3h	1.4019	0.1609	0.9999	0.9999	0.8297	0.8045
1h-4h	0.2150	0.8297	0.9999	0.9999	0.8297	0.8297
1h-1day	1.7982	0.0721	0.9999	0.7271	0.7210	0.4881
2h-3h	2.7727	0.0056	0.0840	0.0840	0.0840	0.0840
2h-4h	1.4422	0.1492	0.9999	0.9999	0.8297	0.7460
2h-1day	2.2731	0.0230	0.3450	0.3220	0.3220	0.2758
3h-4h	1.4400	0.1499	0.9999	0.9999	0.8297	0.7495
3h-1day	1.2557	0.2092	0.9999	0.9999	0.8297	0.8297
4h-1day	1.8375	0.0661	0.9915	0.7221	0.7210	0.4627
Realized Vol						
30min-1h	0.4012	0.6883	0.9999	0.9999	0.9538	0.9538
30min-2h	0.4768	0.6335	0.9999	0.9999	0.9538	0.9538
30min-3h	0.5125	0.6083	0.9999	0.9999	0.9538	0.9538
30min-4h	1.0988	0.2719	0.9999	0.9999	0.9538	0.9538
30min-1day	0.0579	0.9538	0.9999	0.9999	0.9538	0.9538
1h-2h	0.1094	0.9129	0.9999	0.9999	0.9538	0.9538
1h-3h	0.1671	0.8673	0.9999	0.9999	0.9538	0.9538
1h-4h	0.7472	0.4549	0.9999	0.9999	0.9538	0.9538
1h-1day	0.1368	0.8912	0.9999	0.9999	0.9538	0.9538
2h-3h	0.0598	0.9523	0.9999	0.9999	0.9538	0.9538
2h-4h	0.6135	0.5395	0.9999	0.9999	0.9538	0.9538
2h-1day	0.1954	0.8450	0.9999	0.9999	0.9538	0.9538
3h-4h	0.5347	0.5929	0.9999	0.9999	0.9538	0.9538
3h-1day	0.2296	0.8184	0.9999	0.9999	0.9538	0.9538
4h-1day	0.5942	0.5524	0.9999	0.9999	0.9538	0.9538

This table presents the Z-statistics (lower bound, $\rho = 0$) with the corresponding raw (unadjusted) p-values and the p-values adjusted for multiple comparisons by the methods of Bonferroni (1936), Holm (1979), Hochberg (1988) and Hommel (1988) respectively.

Table 1.8: Z-test of the statistical equivalence of the GPH estimates of the d parameter at various time scales for the series of absolute returns, squared returns and realized volatility (upper bound, $\rho = 0.90$)

Test	Z-stat	Raw p-value	Bonferroni	Holm	Hochberg	Hommel
Absolute						
30min-1h	1.9943	0.0461	0.6915	0.5532	0.5532	0.4912
30min-2h	6.5174	0.0000	0.0000	0.0000	0.0000	0.0000
30min-3h	1.1845	0.2362	0.9999	0.9999	0.9560	0.9560
30min-4h	1.6992	0.0893	0.9999	0.8930	0.8930	0.8037
30min-1day	0.7578	0.4486	0.9999	0.9999	0.9560	0.9560
1h-2h	4.5759	0.0000	0.0000	0.0000	0.0000	0.0000
1h-3h	0.1348	0.8927	0.9999	0.9999	0.9560	0.9560
1h-4h	0.7667	0.4433	0.9999	0.9999	0.9560	0.9560
1h-1day	0.3033	0.7616	0.9999	0.9999	0.9560	0.9560
2h-3h	2.7049	0.0068	0.1020	0.0884	0.0884	0.0884
2h-4h	1.9148	0.0555	0.8325	0.6105	0.6105	0.5550
2h-1day	0.9055	0.3652	0.9999	0.9999	0.9560	0.9560
3h-4h	0.7313	0.4646	0.9999	0.9999	0.9560	0.9560
3h-1day	0.3061	0.7596	0.9999	0.9999	0.9560	0.9560
4h-1day	0.0552	0.9560	0.9999	0.9999	0.9560	0.9560
Squared						
30min-1h	1.2681	0.2048	0.9999	0.4096	0.4096	0.4096
30min-2h	5.7287	0.0000	0.0000	0.0000	0.0000	0.0000
30min-3h	2.5022	0.0123	0.1845	0.0984	0.0984	0.0819
30min-4h	1.8300	0.0673	0.9999	0.2692	0.2106	0.2019
30min-1day	2.1076	0.0351	0.5265	0.1860	0.1755	0.1404
1h-2h	6.2554	0.0000	0.0000	0.0000	0.0000	0.0000
1h-3h	2.8622	0.0042	0.0630	0.0420	0.0420	0.0378
1h-4h	0.5714	0.5677	0.9999	0.5677	0.5677	0.5677
1h-1day	2.1569	0.0310	0.4650	0.1860	0.1755	0.1240
2h-3h	5.2400	0.0000	0.0000	0.0000	0.0000	0.0000
2h-4h	3.5058	0.0004	0.0060	0.0044	0.0044	0.0044
2h-1day	2.6765	0.0074	0.1110	0.0667	0.0667	0.0592
3h-4h	3.9047	0.0001	0.0014	0.0011	0.0011	0.0011
3h-1day	1.8108	0.0702	0.9999	0.2692	0.2106	0.2106
4h-1day	2.3833	0.0172	0.2580	0.1204	0.1204	0.1032
Realized Vol						
30min-1h	1.1341	0.2567	0.9999	0.9999	0.9330	0.9330
30min-2h	1.1492	0.2505	0.9999	0.9999	0.9330	0.9330
30min-3h	1.1239	0.2611	0.9999	0.9999	0.9330	0.9330
30min-4h	2.1703	0.0300	0.4500	0.4500	0.4500	0.4200
30min-1day	0.0841	0.9330	0.9999	0.9999	0.9330	0.9330
1h-2h	0.3246	0.7455	0.9999	0.9999	0.9330	0.9330
1h-3h	0.4574	0.6474	0.9999	0.9999	0.9330	0.9330
1h-4h	1.8286	0.0675	0.9999	0.9450	0.9330	0.7180
1h-1day	0.2251	0.8219	0.9999	0.9999	0.9330	0.9330
2h-3h	0.1850	0.8532	0.9999	0.9999	0.9330	0.9330
2h-4h	1.7569	0.0789	0.9999	0.9999	0.9330	0.7890
2h-1day	0.3620	0.7173	0.9999	0.9999	0.9330	0.9330
3h-4h	1.6378	0.1015	0.9999	0.9999	0.9330	0.9135
3h-1day	0.4610	0.6448	0.9999	0.9999	0.9330	0.9330
4h-1day	1.3269	0.1845	0.9999	0.9999	0.9330	0.9330

This table presents the Z-statistics (upper bound, $\rho = 0.90$) with the corresponding raw (unadjusted) p-values and the p-values adjusted for multiple comparisons by the methods of Bonferroni (1936), Holm (1979), Hochberg (1988) and Hommel (1988) respectively.

1.6 Conclusion

In this study, we investigated a phenomenon of the long-range dependence in volatility of the foreign exchange returns in the light of the theory of temporal aggregation in discrete time long memory processes.

In the first step, we generalized the up-to-date theoretical knowledge about temporal aggregation in the context of long memory time series. We provided several definitions of long memory processes and described an ARFIMA framework of modeling the long-range dependence. We defined the procedure of temporal aggregation and explained its relevance to the construction of financial time series. Combining both time and frequency analyses, we observed the autocovariance, the autocorrelation and the spectral density functions of temporally aggregated ARFIMA processes in order to evaluate the effect of the aggregation on the long memory property of the series. The theoretical results imply the irrelevance of the long memory parameter to temporal aggregation. However, the short run components of ARFIMA processes change as a result of the aggregation.

In the second step, we conducted a Monte Carlo simulation experiment and provided a regression analysis of the experiment results in order to validate the theoretical implications about the consequences of temporal aggregation in the ARFIMA processes and estimating the true long memory parameter at various levels of the aggregation. The results of the simulation experiment are broadly consistent with the implications of the theory and the results reported in the literature: temporal aggregation does not affect the long memory property of ARFIMA processes and the semiparametric GPH approach provides consistent estimates of the fractional differencing parameter at different levels of temporal aggregation.

Finally, in the empirical part of the work, we provided a recent evidence of the long memory in volatility of exchange rates returns on various levels of temporal aggregation. We analyzed the GBP/USD foreign exchange returns series over a period of 7 years sampled at various intraday and daily frequencies. After controlling for intraday periodicity, we implemented the rescaled range test of Hurst (1951), the modified rescaled range test of Lo (1991) and the semiparametric estimation approach of Geweke and Porter-Hudak (1983) to explore and model the long memory dynamics in volatility of the temporally aggregated returns measured by absolute returns, squared returns and realized volatility.

To formally investigate the consistency of the GPH estimates of the long memory parameter across different time scales, we developed the Z-test with the size adjustments for multiple hypothesis testing. We found evidence that volatility of the returns is characterized by the same fractional differencing parameter across the observed time scales. The evidence is particularly strong in case of realized volatility, consistent with the notion of realized volatility as more advanced and less noisy volatility proxy.

Our findings indicate that volatility of financial returns is a true long memory process. In other words, long memory is an intrinsic property of financial volatility and is not caused by occasional structural shifts or regime breaks. It is possible to propose that the returns volatility series contains an identical amount of information about the past events at every aggregation frequency and is predictable up to many periods ahead. Long memory framework seems to be an appropriate instrument for modeling and forecasting returns volatility and should work equally well irrespective of a time scale of volatility measuring and modeling.

The study presented in this chapter can be extended in many ways. For example, an interesting line of further investigations would be to observe the consequences of temporal aggregation in the long memory FIGARCH models.

1.7 Appendix

1.7.1 Temporal aggregation in light of the aliasing effect

As stated in Souza (2005), the expression for the spectral density function of the temporally aggregated ARFIMA processes derived in Chambers (1998) and Hwang (2000) does not account for the aliasing effect over frequencies. The aliasing effect occurs since temporal aggregation includes at some part the act of skip-sampling or systematic sampling. The intuitive explanation, according to Souza (2005), is the following. When the aggregation frequency is lower than that of the true process by a factor η, a component with frequency λ in the original process will have (nominal) frequency $\omega = \eta\lambda$ in the newly sampled series, possibly falling outside $(-\pi, \pi]$. In other words, the frequency interval $(-\pi, \pi]$ for ω in the spectrum of the aggregated process is equivalent to the interval $(-\pi/\eta, \pi/\eta]$ for λ in the original series. Hence, some frequencies of the original process cannot be directly observed in the aggregated process and, so, will not appear in its spectral density. The components with these unobservable frequencies will have an apparent (lower) frequency in the aggregated process, different from the "true" frequency.

Souza (2005) proposed the expression for the spectral density function of the temporally aggregated ARFIMA processes that accounts for the aliasing effect. So, assume that the underlying variable y_t^D has the following Wold representation:

$$\left(1 - L^{1/\eta}\right)^d y_t^D = \sum_{h=0}^{\infty} \rho_h \epsilon_{t-h/\eta}, \tag{1.45}$$

where $\rho_0 = 1, \sum_{h=0}^{\infty} |\rho_h| < \infty$, ϵ_t is a white noise process with variance σ^2, η is a positive integer and $-0.5 < d < 0.5$. Then, the formula for the spectral density function of the aggregated process y_t^{DA} that accounts for the aliasing effect is given by:

$$f^{DA}(\omega) = \sigma^2 \sum_{j=0}^{\eta-1} \left[\left|1 - e^{-i(\omega+j2\pi)/\eta}\right|^{-2d} \left|\rho(e^{-i(\omega+j2\pi)/\eta})\right|^2 F_\eta((\omega + j2\pi)/\eta) \right], \tag{1.46}$$

where the function F_η is the Fejer kernel (see Priestley (1981) for details).

However, as Souza (2005) notes, the presence of aliasing effect does not change the implication of Chambers (1998) that the order of integration remains constant after temporal aggregation (aggregation of flow-type variables). The implication that the order of integration should be the same when estimated from different temporal aggregation levels is also true.

1.7.2 The Classical and the Modified Rescaled Range (R/S) test

The semiparametric modified rescaled range (R/S) test were developed by Lo (1991) on the basis of the original R/S test proposed by Hurst (1951). The test is the range of the partial sums of deviations of a time series from its mean, then rescaled by its standard deviation. For example, for a sample of n values $y_1, ..., y_n$, the test statistic is given by:

$$Q_n = \frac{1}{S_n}\left[\max_{1\leq k\leq n}\sum_{i=1}^{k}(y_i - \bar{y}_n) - \min_{1\leq k\leq n}\sum_{i=1}^{k}(y_i - \bar{y}_n)\right], \quad (1.47)$$

where S_n is the maximum likelihood estimator of the standard deviation of y. The term $\max_{1\leq k\leq n}\sum_{i=1}^{k}(y_i - \bar{y}_n)$ is the maximum of the partial sums of the first k deviations from the mean, which is non-negative. Another term $\min_{1\leq k\leq n}\sum_{i=1}^{k}(y_i - \bar{y}_n)$ is the minimum of the partial sums of the first k deviations from the mean, which is non-positive. So, the difference of the two quantities will be such that $Q_n > 0$. Lo (1991) claims that the original R/S statistic is excessively sensitive to short-term dependence. In particular, he shows that an AR(1) process with large sample size can seriously bias the R/S statistic. To account for the short-term effect, Lo (1991) modified the test by applying a "Newey-West" correction to derive a consistent estimate of the long-range variance of the time series. In the modified version of the test S is replaced by $\hat{S}$:

$$\hat{S} = \sqrt{S^2 + 2\sum_{j=1}^{r}\left(1 - \frac{j}{r+1}\right)\gamma_j}, \quad (1.48)$$

where γ_j is the sample autocovariance at lag j and r is the maximum lag over which short-term autocorrelation might be important. By default, the null hypothesis of the test is that the observed variable is not long-range dependent.

1.7.3 Multiple comparisons p-value adjustment methods

In case of multiple hypotheses testing problem, to control for the family-wise error rate, the p-values of the tests should be adjusted. In the present study, we use the methods of Bonferroni (1936), Holm (1979), Hochberg (1988) and Hommel (1988) to adjust the p-values. The description of the methods is given below.

Suppose, m is the number of null hypotheses to be tested, $H_{01}, ..., H_{0m}$. The corresponding raw p-values are $p_1, ..., p_m$. Denote the ordered raw p-values as $p_{(1)} \leq ... \leq p_{(m)}$.

The Bonferroni (1936) adjusted p-value, p_i^{Bonf}, for test i, $i = 1, ..., m$, is given by: $p_i^{Bonf} = mp_i$. If the adjusted p-value exceeds 1, it is set to 1.

The Holm (1979) adjusted p-values, $p_{(i)}^{Holm}$, are given by:

$$p_{(i)}^{Holm} = \begin{cases} mp_{(1)}, & \text{for } i\text{=1} \\ max(p_{(i-1)}^{Holm}, (m-i+1)p_{(i)} & \text{for } i\text{=2,...,m} \end{cases}$$

The Hochberg (1988) adjusted p-values, $p_{(i)}^{Hoch}$, are given by:

$$p_{(i)}^{Hoch} = \begin{cases} p_{(m)}, & \text{for } i\text{=m} \\ min(p_{(i+1)}^{Hoch}, (m-i+1)p_{(i)} & \text{for } i\text{=m-1,...,1} \end{cases}$$

The Hommel (1988) p-value adjustment method is based on the Simes (1986) procedure. The Simes (1986) p-value for a joint test of any set of N hypotheses with p-values $p_{(1)} \leq ... \leq p_{(N)}$ is $min((N/1)p_{(1)}, ..., (N/N)p_{(N)})$. The Hommel (1988) adjusted p-values for test i is the maximum of all such Simes (1986) p-values, taken over all joint tests that include i as one of their components.

The adjusted p-values from the Hommel (1988) method are always equal or smaller to the adjusted p-values from the Hochberg (1988) procedure. The Hochberg (1988) adjusted p-values are always equal or smaller to the p-values from the Holm (1979) procedure. And in its turn, the Holm (1979) adjusted p-values are always equal or smaller to the Bonferroni (1936) adjusted p-values.

Chapter 2

Can asymmetric attention explain volatility asymmetry? Evidence from international equity markets

2.1 Introduction

In finance, volatility measures the degree of variation of a trading price of a certain asset over time. Because of its indisputable importance for risk management and derivative pricing, the concept of volatility has always attracted significant attention from academic researchers and financial market professionals. The dynamics of financial volatility are characterized by several widely documented empirical phenomena which are also called "stylized facts". Some of the most well-known stylized facts about volatility are long-range dependence, clustering, nonlinear dynamics, etc. Another interesting empirical feature of financial volatility is "volatility asymmetry". Volatility asymmetry commonly refers to a negative relationship between returns and volatility, with this relation being more pronounced for negative returns. In other words, volatility asymmetry describes the relationship between price changes and its volatility and refers to the fact that negative returns have stronger effect on volatility than positive returns of the same magnitude. Following Engle and Ng (1993), who identify positive or negative returns with good or bad market news respectively, volatility asymmetry implies a stronger reaction of volatility to the arrival of bad news from the market than to the arrival of good news. The volatility asymmetry effect has been found in various markets such as currencies (see, e.g., Laopodis, 1998; McKenzie, 2002; Wang and Yang, 2009), commodities (see, e.g, Baur, 2012; Ji and Fan, 2012; Chkili, Hammoudeh, and Nguyen, 2014), stocks (see, e.g., Ebens et al., 1999; Bollerslev and Zhou, 2006; Dennis, Mayhew, and Stivers, 2006) and is especially apparent during market crashes when a large decrease in market prices is followed by a large increase in price volatility.

Despite longstanding attempts to explain volatility asymmetry, there is still no clearly recognized explanation of this phenomenon. Black (1976) and Christie (1982) are the first studies which document asymmetric volatility and explain it with the so-called "leverage effect". Under the leverage effect, a decrease in the stock price of a firm reduces the equity value and increases financial leverage which increases the riskiness of the stock and subsequently increases its volatility. However, later studies demonstrate that the level of financial leverage is not able to completely explain asymmetric volatility dynamics (Schwert, 1989; Bekaert and Wu, 2000; Figlewski and Wang, 2000; Aydemir, Gallmeyer, and Hollifield, 2007; Talpsepp and Rieger, 2010). Moreover, Hens and Steude (2009) and Hasanhodzic and Lo (2011) show that volatility asymmetry cannot be justified by financial leverage as there is a wide range of stocks with zero leverage still exhibiting asymmetric volatility.

In the works of Pindyck (1984), Engle, Lilien, and Robins (1987), French, Schwert, and Stambaugh (1987) and Campbell and Hentschel (1992), the time-varying risk premium theory is used to explain the phenomenon of volatility asymmetry. According to the theory, return changes are caused by shocks in conditional volatility (the effect that is frequently called "volatility feedback"): an increase in volatility leads to an increase in the required return on equity that, in its turn, leads to a decline in stock prices. This explanation finds support in the studies of Bansal and Yaron (2004) and Drechsler and Yaron (2010). On the other hand, Bekaert and Wu (2000), Li et al. (2005) and Bae, Kim, and Nelson (2007) claim that the time-varying risk premium theory is also incapable of fully explaining volatility asymmetry, and that there are other factors driving the asymmetric effect.

The weakness of the leverage effect and volatility feedback hypotheses is that they are intended to explain asymmetric volatility only for equity markets and only on a firm level. However, as stated above, volatility asymmetry is not only an equity markets phenomenon. Moreover, as demonstrated by Tauchen, Zhang, and Liu (1996), Andersen et al. (2001) and Dzieliński, Rieger, and Talpsepp (2018), the asymmetric volatility effect is generally more prominent for aggregate market indexes than for individual stocks.

The behavioral finance literature also proposes several explanations of the asymmetric volatility effect. Sentana and Wadhwani (1992) connect volatility asymmetry with positive feedback trading activities of noisy and uninformed traders. In the model of McQueen and Vorkink (2004), investors have different sensitivities to positive and negative return shocks, being more sensitive to negative ones. In the case of a negative shock, investor behaviour leads to rising volatility which exacerbates price declines and results in asymmetry. Avramov, Chordia, and Goyal (2006) claim that herding in selling activity of uninformed investors drives the effect of asymmetric volatility. Shefrin (2008) and Hens and Steude (2009) explain asymmetric volatility by individual behavioural preferences and biased expectations of retail investors. The latter findings are supported by Talpsepp and Rieger (2010), who show that a higher level of volatility asymmetry is associated with more efficient and developed markets, the markets where the share of individual investors is large.

There is also a growing number of works which study the relationship between volatility dynamics and individual aspects of investor behaviour, in particular, investor attention. As stated by Huberman and Regev (2001), prices react to new information only when investors pay attention to it. Grossman and Stiglitz (1980), Radner and Stiglitz (1984), Merton (1987) and Sims (2003) provide the basic theoretical insights into the role of investor attention for security prices, market equilibrium and market efficiency. However, empirical investigations of the connection between investor attention and volatility face the problem of measuring and quantifying attention. Using indirect proxies for attention, such as news announcements, unusual trading volume and extreme returns, Barber and Odean (2007) demonstrate that attention-grabbing stocks are often associated with higher price volatility. DellaVigna and Pollet (2009) show that earnings announcements can significantly affect stock returns and volatility. Using the number of analysts following a given firm as a proxy for investor attention, Dzieliński, Rieger, and Talpsepp (2018) claim that asymmetry in investor attention to good and bad news can drive volatility asymmetry and that firms with a higher level of attention also exhibit higher volatility asymmetry.

A number of recent studies introduced a new measure of investor attention which is based on internet searches. This approach exploits the revolutionary role of the internet in disseminating information in the financial industry and a growing intention among investors to use the internet for informational and trading services (see, e.g., Barber and Odean, 2001; Antweiler and Frank, 2004; Rubin and Rubin, 2010; etc.). Da, Engelberg, and Gao (2011) propose the number of Google search queries as a measure of investor attention. In particular, they utilize the Search Volume Index (SVI) provided by the Google Trends service, which allows tracking of the popularity of different search terms over time. For a large sample of Russell 3000 stocks, they track the number of search queries for the keywords which represent stock ticker symbols. The authors claim that the Search Volume Index is a direct measure of investor attention because if a certain investor searches for a stock in Google, he is undoubtedly paying attention to it. Also, as Da, Engelberg, and Gao (2011) show, the SVI mostly captures the attention of less-sophisticated retail investors rather than professional ones. Professional security traders are less likely to use Google to search for a stock because professional trading platforms have the necessary news coverage services already implemented in the system. Da, Engelberg, and Gao (2011) provide evidence that changes in the Search Volume Index can be useful in explaining temporary stock price fluctuations.

Dzielinski (2012) uses Google search frequency data to measure economic uncertainty and investor attention and shows that it has a significant relationship with aggregate stock returns and volatility. Vlastakis and Markellos (2012) demonstrate that informational demand (investor attention) measured by the Google Search Volume Index is significantly positively related to historical and implied measures of volatility and to trading volume. They also claim that investor attention increases significantly during periods of higher absolute market returns. Vozlyublennaia (2014) analyzes the relationship between several security indexes and investor attention as measured by the SVI. Her findings indicate the existence of significant relationship between investor attention and index return and volatility. Moreover, according to Vozlyublennaia (2014), increased investor attention improves market efficiency. Andrei and Hasler (2014) provide a theoretical framework of the role of investor attention in determining asset prices. In their model, fluctuations in investor attention are governed by changes in the state of the economy that can be represented by stock market return. In its turn, investor attention drives stock volatility: higher attention leads to higher market volatility. They validate the theoretical predictions using Google search data as a proxy of investor attention. Baur and Dimpfl (2016) investigate investor attention on the gold market and find a significant relationship between gold price changes and Google search queries for gold. They also document that investor attention is predominantly higher in periods of negative gold returns. A number of studies show that the Search Volume Index can be used to significantly improve volatility and returns forecasts in various models (see, e.g., Joseph, Wintoki, and Zhang, 2011; Hamid and Heiden, 2015; Bijl et al., 2016; Dimpfl and Jank, 2016; Chronopoulos, Papadimitriou, and Vlastakis, 2018; etc.).

The present study contributes to the growing literature on the relationship between investor attention and market volatility, in particular, investigating the connection between the well-known volatility asymmetry phenomenon and the asymmetry of investor attention to good and bad news. Following the argument of Tauchen, Zhang, and Liu (1996), Andersen et al. (2001) and Dzieliński, Rieger, and Talpsepp (2018) that asymmetric volatility is more profound for market indexes than for individual stocks, and the proposition of Peng and Xiong (2006) and Vozlyublennaia (2014) that individual investors are more likely to confine their attention to broad asset categories (indexes) rather than individual securities, we concentrate our analysis on the main international stock market indexes: FTSE100, CAC40, DAX, Dow Jones Industrial Average (DJIA), NIKKEI225, S&P500 and Shanghai Composite (SSE). For each index, we study the relationship between return, realized volatility and investor attention to the index measured by the Google SVI. Unlike most of the previous studies which predominantly work with weekly or monthly data (such as Da, Engelberg, and Gao, 2011; Vlastakis and Markellos, 2012; Vozlyublennaia, 2014; Baur and Dimpfl, 2016; etc.), we investigate the stated relationship at a daily time scale over the long period from January 2, 2004 to February 28, 2019. Also, in contrast to previous works, instead of using a particular term as a search keyword (such as an index name or ticker symbol), we utilize the SVI for a topic (which includes all search terms related to a particular stock market index). We propose that this approach provides a more precise measure of investor attention using the internet search frequency data.

In the first step, we use a Structural Vector Autoregressive (SVAR) model and impulse response analysis to explore the short-term and long-term relationship between the analyzed variables. We demonstrate that the effect of returns on realized volatility is generally persistent and long lasting while the effects of returns on investor attention and of investor attention on volatility are only temporary. Using the Granger Causality framework, we identify statistical causality from return to both volatility and investor attention and we identify bidirectional causality between attention and volatility. In the next step, we study the contemporaneous and dynamic asymmetric effect of returns on realized volatility and investor attention in the multivariate Autoregressive Distributed Lag (ARDL) framework. We provide evidence that realized volatility and investor attention exhibit the same kind of asymmetry, having a stronger reaction to negative returns than to positive ones. We graphically illustrate the asymmetric effect of returns on both volatility and attention with news impact curves. In line with the studies of Vlastakis and Markellos (2012), Vozlyublennaia (2014) and Andrei and Hasler (2014), we provide new evidence of a positive relationship between investor attention and volatility. Moreover, we show that the impact of investor attention on volatility is stronger during periods of negative returns. We propose several reasons of the discovered asymmetry in investor attention to good and bad news and suggest how, in the established theoretical framework, asymmetric attention can lead to volatility asymmetry.

The remainder of the chapter is organized as follows. In Section 2.2, we describe the data and econometric models utilized in the study. Section 2.3 presents the empirical results. In Section 2.4, we provide a summary and suggest potential directions of further research.

2.2 Data and methodology

2.2.1 Data

In this chapter, we investigate the relationship between return, volatility and investor attention measured by the internet search frequency for international stock market indexes. Firstly, we describe the characteristics and the sources of the financial data which we use, then we describe the features of the investor attention data employed in the study.

The financial data includes daily returns and realized volatility for the main international stock market indexes, such as the FTSE100, CAC40, DAX, Dow Jones Industrial Average (DJIA), NIKKEI225, S&P500 and Shanghai Composite (SSE). The data is obtained from the Realized Library of the Oxford-Man Institute of Quantitative Finance and covers the period from January 2, 2004 to February 28, 2019. The sample size is determined by the data availability for all our variables of interest. The time series of returns is constructed as a first difference of the daily close-to-close logarithmic index prices. We use realized volatility as a proxy for the true index volatility which is not observable directly. Following Andersen et al. (2001) and Corsi (2009), the realized volatility over a time interval of one day can be defined as

$$RV_t^{(d)} = \sqrt{\sum_{j=0}^{M-1} r^2_{t-j\Delta}}, \tag{2.1}$$

where $\Delta = \frac{1d}{M}$ ($1d$ indicates one trading day; M indicates the number of intraday periods) and $r_{t-j\Delta} = p(t-j\Delta) - p(t-(j+1)\Delta)$ defines continuously compounded Δ-frequency returns, that is, intraday returns sampled at time interval Δ (the subscript t indexes the day, while j indexes the time within the day t).

In other words, realized volatility over a time interval of one day is the square root of the sum of squared high frequency intraday returns. Under certain assumptions, realized volatility is an unbiased estimator of the true integrated volatility. In our dataset, the realized volatility estimator is based on the index intraday logarithmic returns sampled at 5 minutes frequency. Also, in order to avoid complicating the inference by the slower trading activity on weekends and holiday periods, we exclude from the data sample all observations for weekends and some other inactive days.

Following Da, Engelberg, and Gao (2011), Vlastakis and Markellos (2012), Vozlyublennaia (2014), Andrei and Hasler (2014), etc., investor attention in the present study is measured by the Google Search Volume Index (SVI) obtained from the Google Trends service (http://www.google.com/trends). Currently, Google is the most popular search engine in the world.[1] In the form of the SVI, Google reports web searches for a certain keyword as a percentage of the total number of the searches for all keywords over time. The SVI time series is represented as an index, so that the observation with the largest number of searches over a given time span takes the value of 100.

In contrast to the previous works which use a particular term as a search keyword to obtain the SVI, we use the advanced functionality of Google Trends and utilize the SVI not for a particular keyword but for a topic. Topic is a group of terms which are related to the same concept. For example, in case of the FTSE100 Index, the topic "FTSE100: Market Index" includes search terms such as "ftse", "ftse 100", "ftse price", "ftse index", etc. We claim that using the SVI for a topic allows us to consider more ways for investors to search for an index in Google, so it allows us to more fully and precisely measure the actual interest of investors. Moreover, this method reduces the unrelated noise in the search data. In this manner, the SVI is obtained for each stock market index under consideration.

The SVI data is at a daily frequency and covers the period from January 2, 2004 to February 28, 2019. By default, Google Trends provides data from January 2004 onwards at a monthly frequency. The data at a daily frequency is available for periods up to a quarter. However, the time series at a daily frequency, constructed from several consecutive downloads of quarterly periods, would be inconsistent since every quarter has its own specific scale from 0 to 100. Hence, to obtain the consistent time series of daily data for the full sample period from January 2004 to February 2019, we rescale the raw inconsistent time series at a daily frequency, constructed from consecutive downloads of monthly periods, using the corresponding data at a monthly frequency for the full sample period.[2] Analyzing the data at a daily scale more effectively reveals the relationship between investor attention and financial variables, as this relationship is much less pronounced at lower time frequencies (Vozlyublennaia, 2014). By analogy with the financial data, the SVI observations for weekends and inactive days are excluded from the sam-

[1] According to StatCounter GlobalStats, Google's share of worldwide internet searches in August 2019 was 92.37% (September 19, 2019; https://gs.statcounter.com/search-engine-market-share).

[2] As a robustness check, we also construct a consistent daily SVI time series using the methodology proposed by Chronopoulos, Papadimitriou, and Vlastakis (2018). Both methods provide qualitatively similar results and the correlation between the daily time series obtained by using the two methods is very high (on average, about 0.9 across different indexes). Applying the SVI time series constructed by the method of Chronopoulos, Papadimitriou, and Vlastakis (2018) in further econometric analysis also does not alter the conclusions. These results are available from the author upon request.

ple.

Tables 2.1, 2.2 and 2.3 report the descriptive statistics for the time series of returns, realized volatility and the SVI of the analyzed stock market indexes. Each table shows the mean, standard deviation, minimum, maximum, skewness, kurtosis and the Ljung-Box (Ljung and Box, 1978) portmanteau test Q-statistics for up to 20-lags serial correlation. As we can see from the tables, the series of returns, realized volatility and SVI are non-normal and predominantly autocorrelated. Following Da, Engelberg, and Gao (2011), Vlastakis and Markellos (2012) and Vozlyublennaia (2014), in further econometric analysis, the series of realized volatility and SVI are converted into natural logarithms. The stationarity of the variables under consideration is assessed using the Augmented Dickey-Fuller test (Dickey and Fuller, 1979). The results of the test, which are available from the author upon request, suggest that there is no evidence of unit root dynamics in the time series of returns, realized volatility and SVI (both levels and logarithmic transformation).

Figure 2.1 shows the graphs of the returns, realized volatility and SVI for one of the analyzed stock market indexes, in particular, FTSE100 Index. As we can see, the SVI variable co-moves quite strongly with the realized volatility. The volatility and investor attention spike abruptly on October 10, 2008 when global stock markets crashed as a result of the financial crisis and on June 24, 2016 when the final results of the United Kingdom European Union membership referendum were announced.

Table 2.1: Descriptive statistics for daily returns

	FTSE100	CAC40	DAX	DJIA	NIKKEI225	S&P500	SSE
Obs	3820	3857	3841	3799	3704	3802	3583
Mean	0.0001	0.0001	0.0003	0.0002	0.0002	0.0002	0.0002
Std Dev	0.0108	0.0130	0.0131	0.0107	0.0148	0.0114	0.0165
Min	-0.0893	-0.0852	-0.0779	-0.0861	-0.1211	-0.0969	-0.0921
Max	0.0948	0.1044	0.1203	0.1053	0.1323	0.1064	0.0900
Skewness	-0.1395	-0.0953	0.0268	-0.1256	-0.5218	-0.3269	-0.5097
Kurtosis	11.5691	9.5256	10.7328	13.6237	11.1066	14.3621	7.2506
$Q(20)$	50.70*	59.11*	49.85*	117.21*	18.53	125.18*	64.91*

The table reports descriptive statistics for the time series of daily returns for the analyzed stock market indexes: the mean, standard deviation, minimum, maximum, skewness, kurtosis and the Ljung-Box portmanteau test Q-statistics for up to 20-lags serial correlation. The sample period is from January 2, 2004 to February 28, 2019. * indicates statistical significance at the 1% level.

Table 2.2: Descriptive statistics for daily realized volatility

	FTSE100	CAC40	DAX	DJIA	NIKKEI225	S&P500	SSE
Obs	3821	3858	3842	3800	3705	3803	3584
Mean	0.0087	0.0092	0.0095	0.0080	0.0083	0.0079	0.0118
Std Dev	0.0058	0.0054	0.0056	0.0061	0.0049	0.0061	0.0072
Min	0.0012	0.0021	0.0020	0.0014	0.0020	0.0011	0.0025
Max	0.1030	0.0716	0.0767	0.0929	0.0568	0.0880	0.0654
Skewness	4.0877	3.1261	3.4107	4.0215	3.3810	3.6306	2.1785
Kurtosis	37.8622	21.9409	24.9055	31.3855	22.0992	24.9460	10.3118
$Q(20)$	26261.08*	30393.67*	30237.55*	29418.54*	20622.14*	32994.28*	25792.96*

The table reports descriptive statistics for the time series of daily realized volatility for the analyzed stock market indexes: the mean, standard deviation, minimum, maximum, skewness, kurtosis and the Ljung-Box portmanteau test Q-statistics for up to 20-lags serial correlation. The sample period is from January 2, 2004 to February 28, 2019. * indicates statistical significance at the 1% level.

Table 2.3: Descriptive statistics for daily SVI

	FTSE100	CAC40	DAX	DJIA	NIKKEI225	S&P500	SSE
Obs	3821	3858	3842	3800	3705	3803	3584
Mean	19.6811	12.8101	24.5779	14.4255	22.1685	25.4981	16.8282
Std Dev	9.5563	6.8336	11.2325	10.4733	15.9828	10.1847	17.8839
Min	4	0.9	2.16	1.65	1.12	5.89	0.42
Max	100	100	100	100	100	100	100
Skewness	1.6669	2.4059	0.0268	4.0215	1.3248	-0.3269	1.5342
Kurtosis	7.1763	19.7346	10.7328	31.3855	4.2734	14.3621	4.5558
$Q(20)$	41586.48*	40404.43*	45837.25*	50693.02*	55239.92*	41742.00*	56542.53*

The table reports descriptive statistics for the time series of daily Search Volume Index (SVI) for the analyzed stock market indexes: the mean, standard deviation, minimum, maximum, skewness, kurtosis and the Ljung-Box portmanteau test Q-statistics for up to 20-lags serial correlation. The sample period is from January 2, 2004 to February 28, 2019. * indicates statistical significance at the 1% level.

Figure 2.1: The time series of daily FTSE100 returns, realized volatility and SVI

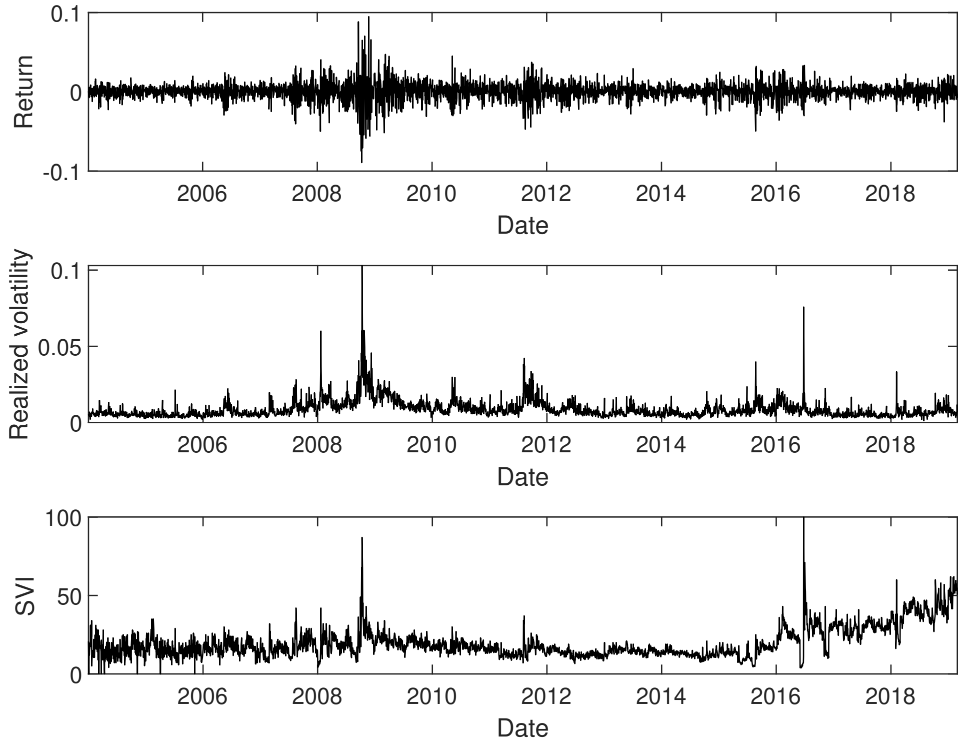

2.2.2 Methodology

In this section, we establish the econometric framework for our analysis. In the first step, we employ a Structural Vector Autoregression (SVAR) model (Sims, 1980) and impulse response analysis to study the short-term and long-term relationships between return, realized volatility and investor attention for each of the stock market indexes under consideration. The Granger Causality test is used to investigate statistical causality between the variables. In the next step, we employ a set of Autoregressive Distributed Lag (ARDL) models to analyze the contemporaneous and dynamic asymmetric effect of index returns on volatility and investor attention.

Initially, the relationship between returns, realized volatility and investor attention are analyzed in the SVAR model which can be written in the following form:

$$A(I_K - A_1 L - A_2 L^2 - ... - A_p L^p)Y_t = A\epsilon_t = Be_t, \tag{2.2}$$

where L is the lag operator, $Y_t = (y_{1t}, ..., y_{Kt})'$ is a $K \times 1$ random vector, A, B and $A_1, ..., A_p$ are $K \times K$ matrices of parameters, ϵ_t is a $K \times 1$ vector of innovations with $\epsilon_t \sim N(0, \Sigma)$ and $E[\epsilon_t \epsilon_s'] = 0_K$ for all $s \neq t$, and e_t is a $K \times 1$ vector of orthogonalized disturbances, that is, $e_t \sim N(0, I_K)$ and $E[e_t e_s'] = 0_K$ for all $s \neq t$. In our case, the vector Y_t takes the following form: $Y_t = (R_t, SVI_t, RV_t)'$, where R_t is the return, SVI_t is the investor attention and RV_t is the realized volatility.

The stated transformation of the innovations allows to analyze the dynamics of the system in terms of a change to an element of e_t. To identify the structural shocks, we follow the Cholesky identification scheme and impose restrictions on A and B matrices: matrix A is assumed to be a lower triangular matrix with ones on the diagonal, while matrix B is assumed to be a diagonal matrix. Formally, the Cholesky restrictions on the constraint matrices are given by:

$$A = \begin{bmatrix} 1 & 0 & 0 \\ \cdot & 1 & 0 \\ \cdot & \cdot & 1 \end{bmatrix} \qquad B = \begin{bmatrix} \cdot & 0 & 0 \\ 0 & \cdot & 0 \\ 0 & 0 & \cdot \end{bmatrix}$$

The identification scheme employed assumes a recursive contemporaneous ordering among the variables in the vector Y_t. This means that any variable in the vector Y_t does not depend contemporaneously on the variables ordered after. With these structural restrictions, index return (R_t) is ordered first and followed by investor attention (SVI_t) and realized volatility (RV_t). In other words, we assume that return is not contemporaneously affected by investor attention or volatility, investor attention is affected contemporaneously by index return but not volatility, volatility is contemporaneously affected by both index return and investor attention. This way of identifying the structural shocks is based on the theoretical foundations of the mutual dynamics of market return, volatility and investor attention provided by Andrei and Hasler (2014) and empirical evidence provided by Dzielinski (2012) and Vlastakis and Markellos (2012).

The SVAR model is estimated using the maximum likelihood estimation procedure. The optimal number of lags in the SVAR model of $p = 4$ is determined according to the Akaike Information Criterion (AIC) and the Bayesian Information Criterion (BIC). The impulse response functions are constructed based on the employed structural shock identification scheme and the estimated SVAR coefficients. The reduced-form VAR is used for the Granger Causality tests. According to Granger (1969), a variable x is said to Granger-cause a variable y if, given the past values of y, past values of x are useful for predicting y. Granger causality test is performed by regressing y on its own lagged values and on lagged values of x and doing the Wald test of the null hypothesis that the estimated coefficients on the lagged values of x are jointly zero.

In the next step, we use the Autoregressive Distributed Lag (ARDL) framework to investigate asymmetric relationships between the variables under consideration. In the ARDL model, the dependent variable is regressed on its own past values as well as on the current and past values of the independent variable. As noted by Pesaran and Shin (1998), the ARDL is a flexible approach, which is able to resolve possible issues of endogeneity/simultaneity through the appropriate modification of the lag structure of the model. In Model 1 (Equations 2.3 and 2.4), we investigate the contemporaneous and dynamic asymmetric relationships between return and realized volatility as well as between return and investor attention. In order to explore the asymmetric effect of return, we introduce an interaction term to allow for different impacts from both current and past negative and positive returns on volatility and investor attention. Formally, for realized volatility and return, the model specification is given by

$$RV_t = \gamma + \sum_{n=1}^{4} \alpha_n RV_{t-n} + \sum_{n=0}^{4} \beta_n R_{t-n} + \sum_{n=0}^{4} \delta_n R_{t-n} \times I\left(R_{t-n} < 0\right) + \epsilon_t, \quad (2.3)$$

where RV_t is the realized volatility, R_t is the return, γ is a constant, ϵ_t is the error term and I is an indicator which takes value one if $R_{t-n} < 0$ and zero otherwise. The coefficient β_n measures the impact of current or lagged returns on current realized volatility if $R_{t-n} \geq 0$, while $(\beta_n + \delta_n)$ measures the impact of current or lagged return on current realized volatility if $R_{t-n} < 0$.

The relationship between investor attention and return is analyzed in the same regression specification, where realized volatility (RV) is replaced with investor attention (SVI). Formally,

$$SVI_t = \gamma + \sum_{n=1}^{4} \alpha_n SVI_{t-n} + \sum_{n=0}^{4} \beta_n R_{t-n} + \sum_{n=0}^{4} \delta_n R_{t-n} \times I\left(R_{t-n} < 0\right) + \epsilon_t. \quad (2.4)$$

In the final step, in Model 2 (Equation 2.5), we employ another ARDL model to investigate the impact of both return and investor attention on realized volatility. Moreover, in this model, we also explore if the sign of current and past return can determine the magnitude of the impact of investor attention on volatility at present. Hence, we introduce an interaction term which allows the impact of current attention on volatility to be dependent on the sign of current and past return. Formally, the model can be represented as

$$
\begin{aligned}
RV_t = & \gamma + \sum_{n=1}^{4} \alpha_n RV_{t-n} + \sum_{n=0}^{4} \beta_n R_{t-n} + \\
& \sum_{n=0}^{4} \lambda_n SVI_{t-n} + \sum_{n=0}^{4} \delta_n SVI_t \times I\left(R_{t-n} < 0\right) + \epsilon_t,
\end{aligned}
\tag{2.5}
$$

where RV_t is the realized volatility, R_t is the return, SVI is the investor attention, γ is a constant, ϵ_t is the error term and I is an indicator which takes value one if $R_{t-n} < 0$ and zero otherwise. Coefficient λ_0 measures the impact of current investor attention on current realized volatility if $R_{t-n} \geq 0$, while $(\lambda_0 + \delta_n)$ measures the impact of current investor attention on current realized volatility if $R_{t-n} < 0$.

The ARDL model is estimated using the OLS method. The optimal number of lags in the ARDL models of $p = 4$ is determined according to the Akaike Information Criterion (AIC) and the Bayesian Information Criterion (BIC).

2.3 Empirical results

In this section, we present the empirical results for the analysis of the relationships between return, realized volatility and investor attention for international stock market indexes.

We begin with the analysis of the contemporaneous correlation. For each of the stock market indexes, Table 2.4 reports the correlation coefficients between return and realized volatility, realized volatility and investor attention as well as return and investor attention. As we can see for every index, the correlation between realized volatility and return is negative and statistically significant at the 5% level which is consistent with the massive empirical literature on volatility asymmetry. In line with the studies of Andrei and Hasler (2014), Dimpfl and Jank (2016), etc., realized volatility is predominantly significantly positively correlated with investor attention. For return and investor attention, the correlation is negative but mostly statistically insignificant.

Table 2.4: Correlation analysis

	FTSE100	CAC40	DAX	DJIA	NIKKEI225	S&P500	SSE
R-RV	-0.0897*	-0.1648*	-0.1736*	-0.1033*	-0.1634*	-0.1169*	-0.1016*
RV-SVI	0.1232*	0.3395*	0.0797*	0.2248*	0.0682*	-0.0344*	0.5764*
R-SVI	-0.0039	-0.0067	-0.0252	-0.0160	-0.0446*	-0.0237	-0.0451*

The table reports the correlation coefficients between the analyzed variables for each of the stock market indexes. *RV-SVI* indicates the correlation between realized volatility and investor attention, *R-SVI* indicates the correlation between return and investor attention, *R-RV* indicates the correlation between return and realized volatility. * indicates statistical significance at the 5% level.

In the next step, we investigate statistical causality between the analyzed variables. Table 2.5 presents the results of the Granger Causality test based on the estimated three-dimensional SVAR model with return, investor attention and realized volatility.[3] As we can see, the null hypothesis that investor attention and realized volatility does not Granger-cause index return either individually or jointly generally cannot be rejected. Hence, in contrast to the results of Joseph, Wintoki, and Zhang (2011) and Bijl et al. (2016), we do not find evidence that past investor attention can be used to predict market return. On the other hand, there is a strong evidence of statistical causality from return to both investor attention and realized volatility. The revealed causality from return to investor attention is consistent with the previous

[3]The results of the estimated SVAR and the reduced-form VAR models are presented in Section 2.5.1 (Appendix).

findings in the literature (see, e.g., Vozlyublennaia, 2014). For NIKKEI225, S&P500 and SSE indexes, there is a strong evidence of bidirectional causality between realized volatility and investor attention. This result is in line with the findings of Hamid and Heiden (2015) and Dimpfl and Jank (2016) and confirms the conjecture of Vozlyublennaia (2014), who, although not finding evidence of a causal relationship between volatility and investor attention at a monthly time scale, proposes that such a relationship is more likely to be revealed over a shorter time range, such as daily. There is also strong evidence for all the indexes that return and realized volatility jointly Granger-cause investor attention and that return and investor attention jointly Granger-cause realized volatility.

Table 2.5: The Granger Causality test results

	FTSE100	CAC40	DAX	DJIA	NIKKEI225	S&P500	SSE
$SVI \not\Rightarrow R$	0.224	0.479	0.203	0.055	0.233	0.475	0.762
$RV \not\Rightarrow R$	0.634	0.623	0.822	0.084	0.717	0.062	0.326
$ALL \not\Rightarrow R$	0.387	0.673	0.458	0.021	0.518	0.118	0.599
$R \not\Rightarrow SVI$	0.000	0.000	0.007	0.000	0.000	0.000	0.006
$RV \not\Rightarrow SVI$	0.001	0.003	0.198	0.001	0.003	0.002	0.000
$ALL \not\Rightarrow SVI$	0.000	0.000	0.000	0.000	0.000	0.000	0.000
$R \not\Rightarrow RV$	0.000	0.000	0.000	0.000	0.000	0.000	0.000
$SVI \not\Rightarrow RV$	0.228	0.124	0.131	0.419	0.001	0.000	0.000
$ALL \not\Rightarrow RV$	0.000	0.000	0.000	0.000	0.000	0.000	0.000

The table reports the p-values for Granger Causality test based on the estimated three-dimensional SVAR model with return (R), investor attention (SVI) and realized volatility (RV). $\not\Rightarrow$ refers to the null hypothesis that the left-hand side variable does not Granger-cause the right-hand side variable; e.g., $SVI \not\Rightarrow R$ refers to the null hypothesis: SVI does not Granger-cause R. ALL refers to all two left-hand side variables in a panel jointly.

Now we move to impulse response analysis to investigate the short-run and long-run relationship between return, realized volatility and investor attention. The impulse response functions are determined by the estimated SVAR model and the structural shocks identification scheme described in Section 2.2.2. Impulse response functions provide a useful way to explore the endogenous propagation of structural shocks within an analyzed system. One can interpret the responses as deviations from the long-run steady-state value that exists before the system is perturbed by the shock.

In our analysis, we focus on three types of impulse response functions: the response of realized volatility to a return shock, the response of investor attention to a return shock and the response of realized volatility to an investor attention shock. For each of the considered stock market indexes, Figures 2.2-2.4 display the graphs of the mentioned impulse response functions respectively. The grey areas on the graphs represent the 95% confidence interval for responses. As we can see, the positive return shock decreases both volatility and investor attention. The impact of a return shock on market volatility is persistent and long lasting; generally it does not completely vanish even after 50 days. In contrast, the response of investor attention to a return shock is less long lasting and often dies out after 20-25 days. As for the response of realized volatility to an attention shock, an increase in investor attention causes a short series of increases in volatility that generally die out in 10-15 days.

In the next step, we explore the asymmetric effect of index return on realized volatility and investor attention using the ARDL model. In Model 1, we focus on the contemporaneous and dynamic asymmetric relationship between return and volatility as well as between return and investor attention. In the model, we use the special interaction term which allows us to separately measure and compare the impacts from positive and negative returns. The corresponding regression results for return and realized volatility are presented in Table 2.6. As we can see, the coefficients for current return are positive and highly statistically significant for all indexes except CAC40. On the other hand, the interaction term coefficients at lag zero are negative and significant at the 1% level for all the indexes. The result indicates that both positive and negative contemporaneous returns generally increase realized volatility, but negative returns have a stronger impact on volatility than do positive returns of the same absolute magnitude. In other words, the impact of positive and negative returns on realized volatility is asymmetric. Thus, we have clear evidence of volatility asymmetry for all of the stock market indexes under analysis, which is in line with the rich evidence in past literature (see., e.g., Black, 1976; Ebens et al., 1999; Andersen et al., 2001; Bollerslev and Zhou, 2006; Baur and Dimpfl, 2018; etc.). Moreover, if we observe lagged coefficients, the coefficients for lagged return are significant predominantly at the 1st or 2nd lag and have mixed signs.The coefficients for lagged interaction terms are mostly negative and statistically significant at the first two lags. This indicates that volatility asymmetry is not only contemporaneous but also a dynamic phenomenon which, however, can only be observed at short lags.

Table 2.7 presents the results of the Model 1 regression estimation for return and investor attention. Across the analyzed indexes, all the estimated coefficients for current return and the current interaction term are highly statistically significant, while the coefficients for lagged return and lagged interaction terms are predominantly significant. The return coefficients at lag zero or one are positive, while the corresponding interaction term coefficients are negative and large in their magnitude. On the other hand, the return coefficients at lags from two to four are mostly negative, while the corresponding interaction term coefficients are positive and large. This result shows that, at lag zero or one, both positive and negative returns increase investor attention with negative returns having a stronger impact. However, at lags from two to four, both positive and negative returns decrease investor attention with negative returns having a mostly stronger effect. Thus, there is evidence of both contemporaneous and dynamic asymmetric relationships between return and investor attention. We also note, for return coefficients, positive marginal effects at short lags tend to be offset by negative marginal effects at longer lags. And for interaction term coefficients, negative effects at short lags tend to be offset by positive effects at longer lags. The results indicate that index return has only a temporary effect on investor attention: as a result of return shock, the initial increase in attention at short lags would be offset by a further decrease in attention at longer lags. This finding is consistent with the impulse response analysis which shows that the impact of return on investor attention generally completely vanishes after 20-25 periods.

We use the so-called "news impact curve" to graphically illustrate the asymmetric effect of return on realized volatility and investor attention. Originally introduced by Engle and Ng (1993), news impact curve characterizes the impact of return shocks on volatility. In the present study, we adapt this approach to also show the response of investor attention to changes in index return. Figures 2.5 and 2.6 present the news impact curves for realized volatility and investor attention respectively. Based on the regressions in Model 1, the curves show how current realized volatility or investor attention (vertical axis) changes with the percentage change in current index return (horizontal axis), assuming that the other variables are fixed to zero. The news impact curves are centered around $R_t = 0$. As we can see across the indexes, the shape of the curves is generally very similar for realized volatility and investor attention. The curves have a V-shape, typical in the literature, where the part of the curve which corresponds to negative returns is steeper than the part which corresponds to positive returns. This particular shape of the curves indicates that both realized volatility and investor attention are similarly asymmetric in their response to good and bad market news.

As we can see from the Model 1 regression results, negative return has a stronger impact on investor attention than positive return. In other words, negative market news attract higher attention from retail investors than positive news. What are the potential reasons behind this asymmetric relationship? We believe that the main psychological reason might be the loss aversion effect described by Kahneman and Tversky (1979). Loss aversion is an essential concept in prospect theory and, according to Kahneman and

Tversky (1979), can be formulated as the idea that "losses loom larger than gains". In other words, people are more sensitive to losses than to gains; the pain of losing is psychologically more powerful than the pleasure of gaining. Loss aversion is closely related to the more general phenomenon of negativity bias in cognitive psychology. Negativity bias refers to the fact that, when of equal intensity, things of a more negative nature have a greater effect on people's psychological state and cognitive processes than positive things (see, e.g., Peeters, 1971; Lewicka, Czapinski, and Peeters, 1992; Rozin and Royzman, 2001; Baumeister et al., 2001; etc.). Thus, asymmetric investor attention to bad market news can be a consequence of an inherent nature of human psychology.

Another potential reason, of a non-psychological nature, might be negative news bias (Dzielinski, Rieger, and Talpsepp, 2011). Negative news bias refers to the fact that the share of negative news and the number of news items overall tend to be positively correlated. In such a situation, more bad market news obviously suggests more market news overall, which has a greater chance of attracting investor attention.

Finally, we move to the analysis of the impact of both return and investor attention on realized volatility in Model 2. As mentioned previously, in this model we allow the impact of current investor attention on volatility to be dependent on the sign of the current and past returns. The corresponding regression estimation results are presented in Table 2.8. As we can see, the coefficients for current return are negative and significant at the 1% level for all the indexes. The coefficients for lagged return are mostly negative and predominantly statistically significant for the first three lags. The negative sign of the coefficients for return is consistent with the results of the correlation analysis and in line with the mass of evidence in the volatility asymmetry literature (see, e.g., Ebens et al., 1999; Bollerslev and Zhou, 2006; etc.). The coefficients for current investor attention are positive and highly statistically significant across all the analyzed stock market indexes. The coefficients for lagged investor attention are negative with some of them statistically significant at different conventional levels. The interaction term coefficients at lag zero and one are positive and mostly statistically significant for all the indexes. The interaction term coefficients at lags from two to four have mixed signs and are mostly statistically insignificant. The results indicate that current investor attention has a positive effect on realized volatility, consistent with the previous findings in the literature (see, e.g., Vlastakis and Markellos, 2012; Vozlyublennaia, 2014; Andrei and Hasler, 2014; etc.). Moreover, the sign of the current and past index return can determine the magnitude of the impact of investor attention on volatility at present. In case of negative current or past return, the positive impact of current investor attention on realized volatility is even stronger. However, the results also show that investor attention has only a temporary effect on realized volatility: positive marginal effects at the current period tend to be offset by negative marginal effects at future periods. This finding is consistent with the analysis of the corresponding impulse response functions.

Our analysis clearly indicate that both volatility and investor attention are similarly asymmetric in their response to market news. Bad market news in the form of negative returns has a stronger impact on both volatility and investor attention than good news in the form of positive returns. This striking similarity cannot but suggest that the volatility asymmetry and attention asymmetry phenomena are related - one might cause the other. In line with the findings of Dzieliński, Rieger, and Talpsepp (2018), we propose that attention asymmetry is the factor that leads to volatility asymmetry. In this proposition, we are appealing to a theoretical framework of the relationship between asset prices and investor attention, provided by Andrei and Hasler (2014). In their theoretical model, market volatility is driven by investor attention which, in its turn, depends on the state of the economy represented by market return. As Andrei and Hasler (2014) claim, when investors pay little attention to news, information about the state of the economy is only gradually incorporated into prices because learning is slow; on the other hand, attentive investors immediately incorporate new information into prices. Hence, low attention results in low volatility and, respectively, high attention leads to high volatility. Indeed, in our analysis, we provide evidence of this positive relationship between investor attention and realized volatility. Consequently, asymmetrically higher attention induced by negative returns would naturally give rise to asymmetrically higher volatility. Moreover, according to our results, in the case of negative returns the magnitude of the impact of investor attention on volatility would be higher, thus even further exaggerating the asymmetry. However, our results also suggest that the effect of investor attention on volatility does not last long-term as the initial positive effect of investor attention is followed by subsequent reversal. Hence, retail investor attention can create temporary asymmetric volatility fluctuations but is unlikely to be responsible for permanent shifts in market volatility.

Table 2.6: The effect of return on realized volatility

	FTSE100	CAC40	DAX	DJIA	NIKKEI225	S&P500	SSE
γ	-1.247***	-1.072***	-1.177***	-1.454***	-1.375***	-1.289***	-1.289***
	(0.083)	(0.074)	(0.076)	(0.088)	(0.081)	(0.082)	(0.073)
α_1	0.270***	0.323***	0.321***	0.279***	0.334***	0.335***	0.343***
	(0.016)	(0.016)	(0.016)	(0.016)	(0.016)	(0.016)	(0.017)
α_2	0.186***	0.163***	0.171***	0.200***	0.172***	0.189***	0.189***
	(0.016)	(0.017)	(0.017)	(0.017)	(0.017)	(0.017)	(0.017)
α_3	0.141***	0.161***	0.156***	0.120***	0.134***	0.117***	0.135***
	(0.016)	(0.017)	(0.017)	(0.017)	(0.017)	(0.017)	(0.017)
α_4	0.168***	0.149***	0.126***	0.135***	0.103***	0.123***	0.088***
	(0.016)	(0.016)	(0.016)	(0.016)	(0.016)	(0.016)	(0.015)
β_0	10.233***	-0.122	1.656***	10.820***	3.806***	6.194***	4.942***
	(0.769)	(0.557)	(0.557)	(0.841)	(0.547)	(0.763)	(0.476)
β_1	-5.122***	-0.974*	-1.990***	-6.059***	0.779	-5.128***	3.786***
	(0.788)	(0.558)	(0.560)	(0.858)	(0.550)	(0.771)	(0.484)
β_2	-2.385***	-0.223	-0.204	-3.347***	-0.011	-1.849**	2.978***
	(0.785)	(0.553)	(0.555)	(0.858)	(0.544)	(0.771)	(0.489)
β_3	-2.887***	-1.693***	-0.802	0.592	-0.882	0.678	1.147**
	(0.778)	(0.547)	(0.550)	(0.852)	(0.543)	(0.761)	(0.488)
β_4	1.091	1.142**	1.584***	-0.060	-0.803	-0.182	1.167**
	(0.776)	(0.536)	(0.542)	(0.847)	(0.538)	(0.754)	(0.490)
δ_0	-29.66***	-12.50***	-16.19***	-32.27***	-17.34***	-23.99***	-15.38***
	(1.254)	(0.912)	(0.917)	(1.360)	(0.865)	(1.217)	(0.746)
δ_1	-1.242	-5.644***	-3.366***	-1.282	-7.193***	-2.677**	-11.48***
	(1.339)	(0.931)	(0.952)	(1.448)	(0.909)	(1.270)	(0.790)
δ_2	0.261	-2.813***	-2.467***	-1.356	-1.483	-2.919**	-2.972***
	(1.334)	(0.932)	(0.949)	(1.455)	(0.915)	(1.275)	(0.811)
δ_3	2.456*	1.208	0.269	-2.416*	1.330	-1.996	0.293
	(1.335)	(0.932)	(0.951)	(1.453)	(0.918)	(1.273)	(0.805)
δ_4	-1.724	-0.854	-1.562	0.846	1.994**	1.186	-0.281
	(1.339)	(0.931)	(0.948)	(1.457)	(0.917)	(1.276)	(0.799)
LM(1)	78.79***	116.66***	93.06***	37.42***	43.93***	36.61***	33.23***
R^2	0.731	0.767	0.751	0.750	0.718	0.779	0.787
N of obs.	3816	3853	3837	3795	3700	3798	3579

The table reports the results of the OLS regression between realized volatility and return in Model 1 for each of the stock market indexes. γ is the constant, α_1,...,α_4 are the coefficients for lagged realized volatility (RV_{t-1},...,RV_{t-4}), β_0,...,β_4 are the coefficients for current and lagged return (R_t,...,R_{t-4}), δ_0,...,δ_4 are the coefficients for interaction term ($R_{t-n} \times I\,(R_{t-n} < 0)$). LM(1) is the Breusch-Godfrey LM test statistics for the first order serial correlation in the residuals. The standard errors are in parentheses. ***, ** and * indicate statistical significance at the 1%, 5% and 10% levels respectively.

Table 2.7: The effect of return on investor attention

	FTSE100	CAC40	DAX	DJIA	NIKKEI225	S&P500	SSE
γ	0.181***	0.118***	0.197***	0.074***	0.084***	0.213***	0.036***
	(0.024)	(0.019)	(0.027)	(0.013)	(0.018)	(0.027)	(0.013)
α_1	0.505***	0.364***	0.477***	0.685***	0.385***	0.498***	0.398***
	(0.016)	(0.016)	(0.016)	(0.016)	(0.016)	(0.016)	(0.017)
α_2	0.203***	0.228***	0.169***	0.131***	0.310***	0.171***	0.241***
	(0.018)	(0.017)	(0.018)	(0.020)	(0.017)	(0.018)	(0.018)
α_3	0.119***	0.143***	0.138***	0.036*	0.150***	0.140***	0.176***
	(0.018)	(0.017)	(0.018)	(0.020)	(0.017)	(0.018)	(0.018)
α_4	0.103***	0.203***	0.147***	0.112***	0.121***	0.123***	0.142***
	(0.016)	(0.016)	(0.016)	(0.016)	(0.016)	(0.016)	(0.016)
β_0	4.363***	5.037***	2.792***	4.550***	4.589***	3.235***	4.245***
	(0.587)	(0.600)	(0.467)	(0.519)	(0.554)	(0.480)	(0.596)
β_1	2.204***	1.514**	1.637***	1.378***	0.621	0.148	1.639***
	(0.585)	(0.600)	(0.466)	(0.517)	(0.555)	(0.476)	(0.599)
β_2	-1.774***	-2.132***	-1.235***	-3.784***	-0.797	-1.895***	1.084*
	(0.573)	(0.589)	(0.456)	(0.509)	(0.542)	(0.470)	(0.597)
β_3	-0.799	-1.574***	-2.074***	-2.909***	-2.076***	-2.077***	-1.110*
	(0.564)	(0.577)	(0.450)	(0.500)	(0.536)	(0.458)	(0.594)
β_4	-1.458***	-1.601***	-0.876*	-0.706	-2.455***	-1.409***	-1.624***
	(0.561)	(0.574)	(0.449)	(0.499)	(0.530)	(0.455)	(0.594)
δ_0	-10.84***	-11.58***	-9.025***	-14.17***	-14.46***	-9.041***	-11.81***
	(0.951)	(0.974)	(0.765)	(0.831)	(0.871)	(0.758)	(0.927)
δ_1	-5.917***	-5.398***	-4.150***	-6.036***	-3.313***	-2.983***	-5.418***
	(0.954)	(0.977)	(0.768)	(0.845)	(0.895)	(0.754)	(0.945)
δ_2	3.971***	3.035***	2.055***	7.696***	3.222***	3.365***	-1.097
	(0.947)	(0.971)	(0.756)	(0.849)	(0.885)	(0.758)	(0.945)
δ_3	3.733***	3.510***	4.835***	5.751***	6.281***	4.455***	3.427***
	(0.946)	(0.964)	(0.755)	(0.841)	(0.880)	(0.746)	(0.940)
δ_4	3.445***	3.380***	2.550***	2.031**	5.401***	3.516***	4.002***
	(0.952)	(0.019)	(0.761)	(0.848)	(0.884)	(0.757)	(0.942)
LM(1)	76.58***	7.55***	62.89***	37.57***	51.13***	54.90***	42.26***
R^2	0.784	0.800	0.767	0.906	0.8733	0.774	0.911
N of obs.	3816	3853	3837	3795	3700	3798	3579

The table reports the results of the OLS regression between investor attention and return in Model 1 for each of the stock market indexes. γ is the constant, α_1,...,α_4 are the coefficients for lagged investor attention (RV_{t-1},...,RV_{t-4}), β_0,...,β_4 are the coefficients for current and lagged return (R_t,...,R_{t-4}), δ_0,...,δ_4 are the coefficients for interaction term ($R_{t-n} \times I\left(R_{t-n} < 0\right)$). LM(1) is the Breusch-Godfrey LM test statistics for the first order serial correlation in the residuals. The standard errors are in parentheses. ***, ** and * indicate statistical significance at the 1%, 5% and 10% levels respectively.

Table 2.8: The effect of return and investor attention on realized volatility

	FTSE100	CAC40	DAX	DJIA	NIKKEI225	S&P500	SSE
γ	-0.552***	-0.582***	-0.519***	-0.600***	-0.646***	-0.399***	-0.617***
	(0.062)	(0.057)	(0.057)	(0.058)	(0.056)	(0.058)	(0.061)
α_1	0.283***	0.354***	0.353***	0.295***	0.400***	0.346***	0.427***
	(0.016)	(0.016)	(0.016)	(0.016)	(0.016)	(0.016)	(0.017)
α_2	0.217***	0.186***	0.198***	0.248***	0.192***	0.235***	0.203***
	(0.016)	(0.017)	(0.017)	(0.017)	(0.017)	(0.017)	(0.018)
α_3	0.168***	0.180***	0.179***	0.179***	0.150***	0.158***	0.150***
	(0.016)	(0.017)	(0.017)	(0.016)	(0.017)	(0.017)	(0.018)
α_4	0.215***	0.168***	0.158***	0.161***	0.124***	0.156***	0.100***
	(0.016)	(0.016)	(0.016)	(0.016)	(0.016)	(0.016)	(0.016)
β_0	-3.126***	-5.436***	-4.773***	-1.652***	-4.093***	-2.292***	-2.350***
	(0.573)	(0.414)	(0.422)	(0.608)	(0.404)	(0.517)	(0.375)
β_1	-5.260***	-3.049***	-3.522***	-5.077***	-3.006***	-4.828***	-2.028***
	(0.578)	(0.423)	(0.429)	(0.616)	(0.407)	(0.524)	(0.376)
β_2	-2.734***	-2.061***	-1.759***	-4.462***	-1.091***	-3.506***	1.203***
	(0.579)	(0.421)	(0.429)	(0.618)	(0.408)	(0.530)	(0.376)
β_3	-2.651***	-1.829***	-1.088**	-0.994	-0.848**	-1.196**	0.472
	(0.578)	(0.419)	(0.426)	(0.613)	(0.403)	(0.525)	(0.374)
β_4	-0.307	0.247	0.057	-1.764***	-0.483	-1.029**	0.211
	(0.570)	(0.410)	(0.416)	(0.599)	(0.392)	(0.516)	(0.370)
λ_0	0.263***	0.117***	0.154***	0.459***	0.163***	0.290***	0.166***
	(0.022)	(0.015)	(0.019)	(0.026)	(0.017)	(0.025)	(0.014)
λ_1	-0.149***	-0.007	-0.072***	-0.303***	-0.016	-0.121***	-0.023
	(0.024)	(0.015)	(0.021)	(0.032)	(0.018)	(0.028)	(0.015)
λ_2	-0.050**	-0.046***	-0.020	-0.060*	-0.063***	-0.078***	-0.031**
	(0.025)	(0.016)	(0.021)	(0.032)	(0.018)	(0.006)	(0.015)
λ_3	-0.047*	-0.019	-0.017	-0.079**	-0.071***	-0.071**	-0.036**
	(0.024)	(0.015)	(0.021)	(0.032)	(0.018)	(0.028)	(0.015)
λ_4	-0.040*	-0.039***	-0.060***	-0.031	-0.025	-0.085***	-0.047***
	(0.022)	(0.015)	(0.019)	(0.026)	(0.016)	(0.026)	(0.014)
δ_0	0.020***	0.017***	0.020***	0.039***	0.013***	0.043***	0.009*
	(0.004)	(0.004)	(0.004)	(0.005)	(0.004)	(0.004)	(0.005)
δ_1	0.017***	0.016***	0.008**	0.023***	0.002	0.024***	0.001
	(0.004)	(0.004)	(0.004)	(0.005)	(0.004)	(0.004)	(0.005)
δ_2	0.006	-0.000	0.001	0.001	0.004	0.002	0.002
	(0.004)	(0.004)	(0.003)	(0.005)	(0.004)	(0.004)	(0.005)
δ_3	-0.001	-0.002	-0.000	-0.002	0.002	-0.005	-0.005
	(0.004)	(0.004)	(0.003)	(0.005)	(0.004)	(0.004)	(0.005)
δ_4	-0.001	-0.002	-0.004	-0.016***	-0.004	-0.008**	-0.005
	(0.004)	(0.004)	(0.003)	(0.005)	(0.004)	(0.004)	(0.005)
LM(1)	105.23***	122.44***	132.37***	43.24***	50.70***	50.57***	35.37***
R^2	0.707	0.759	0.737	0.740	0.692	0.774	0.761
N of obs.	3816	3853	3837	3795	3700	3798	3579

The table reports the results of the OLS regression between realized volatility, investor attention and return in Model 2 for each of the stock market indexes. γ is the constant, α_1,...,α_4 are the coefficients for lagged realized volatility (RV_{t-1},...,RV_{t-4}), β_0,...,β_4 are the coefficients for current and lagged return (R_t,...,R_{t-4}), λ_0,...,λ_4 are the coefficients for for current and lagged investor attention, δ_0,...,δ_4 are the coefficients for interaction term ($SVI_t \times I\,(R_{t-n} < 0)$). LM(1) is the Breusch-Godfrey LM test statistics for the first order serial correlation in the residuals. The standard errors are in parentheses. ***, ** and * indicate statistical significance at the 1%, 5% and 10% levels respectively.

Figure 2.2: Impulse response of realized volatility to return shock

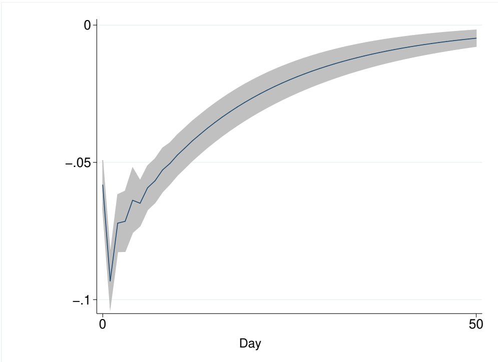

(a) FTSE100

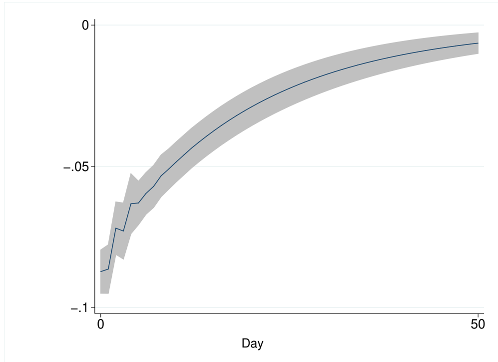

(b) CAC40

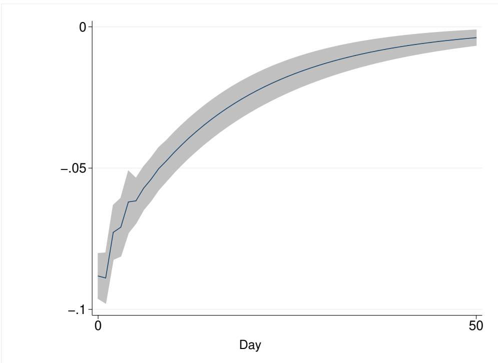

(c) DAX

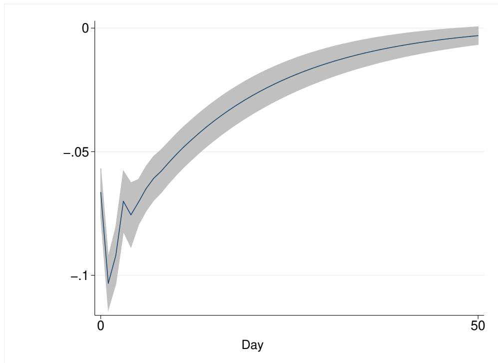

(d) DJIA

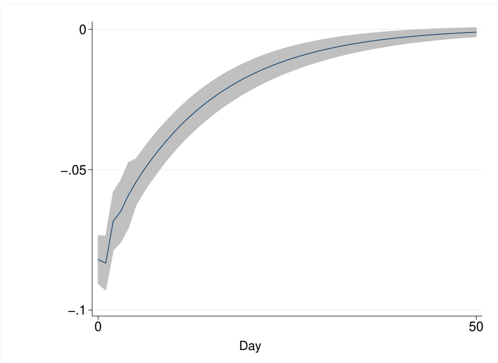

(e) NIKKEI225

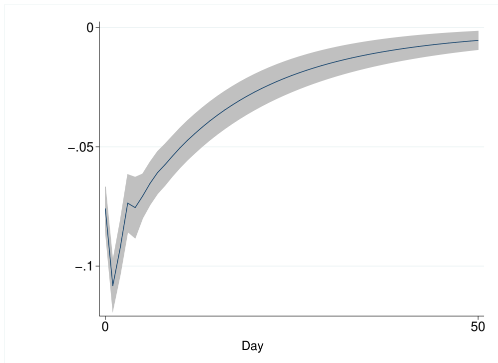

(f) S&P500

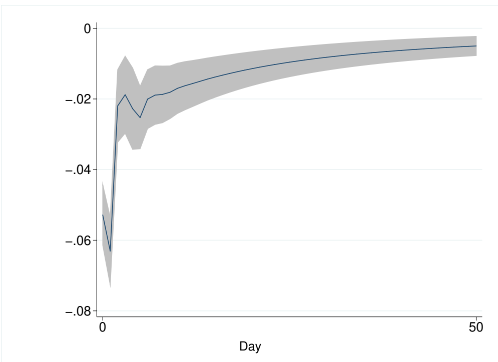

(g) SSE

Figure 2.3: Impulse response of investor attention to return shock

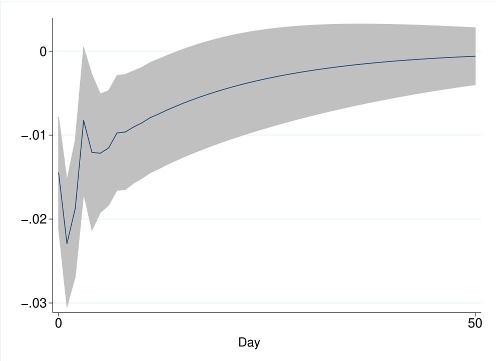

(a) FTSE100

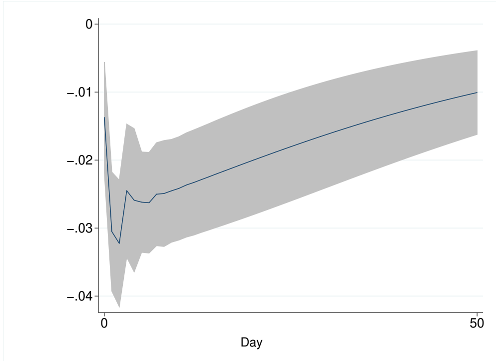

(b) CAC40

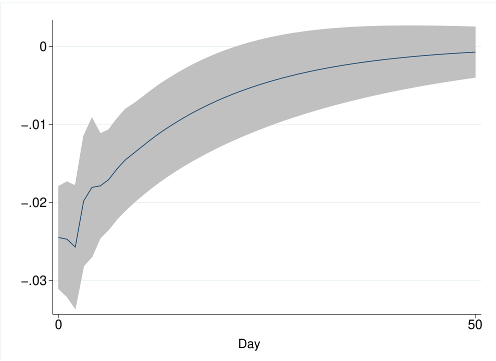

(c) DAX

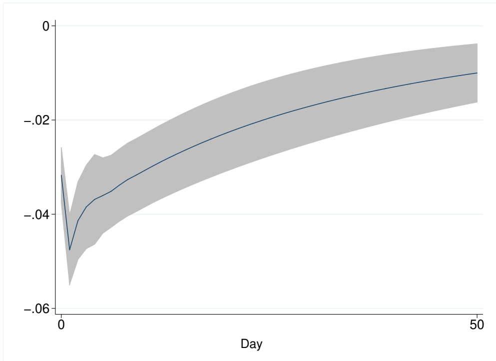

(d) DJIA

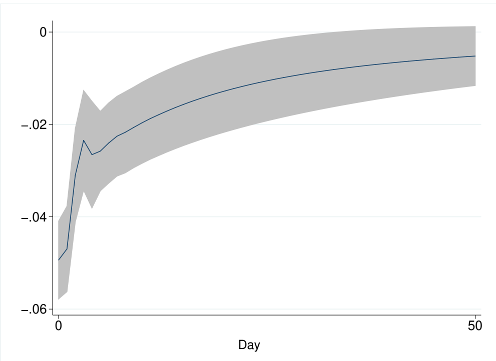

(e) NIKKEI225

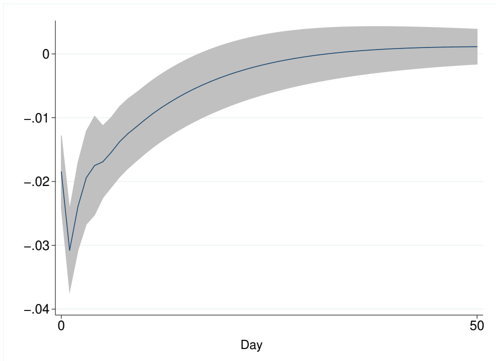

(f) S&P500

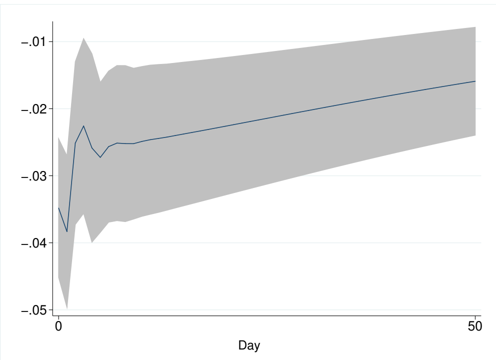

(g) SSE

Figure 2.4: Impulse response of realized volatility to investor attention shock

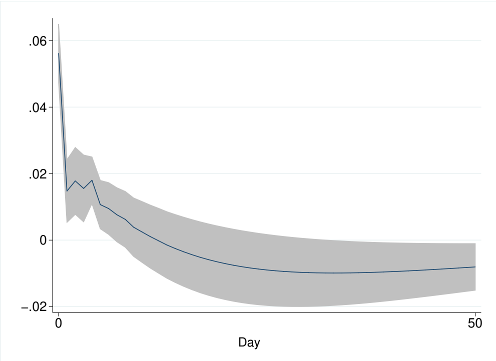

(a) FTSE100

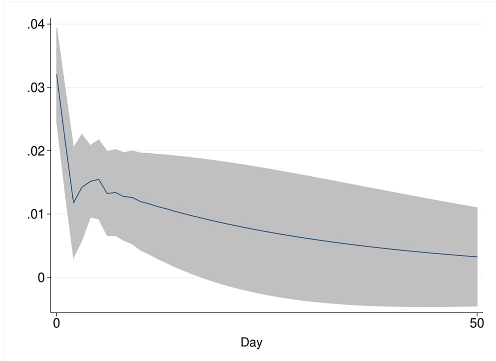

(b) CAC40

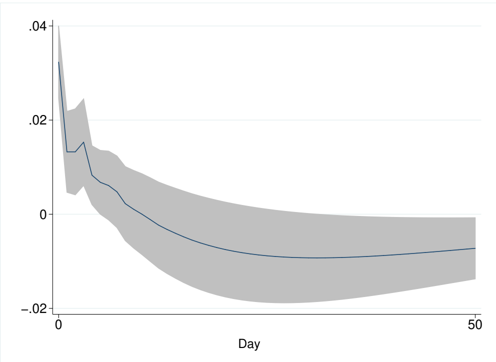

(c) DAX

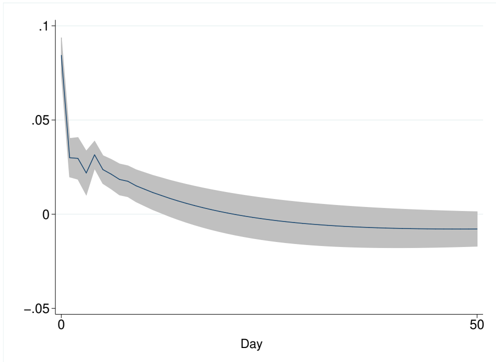

(d) DJIA

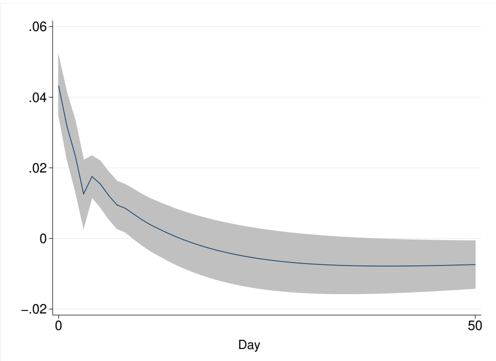

(e) NIKKEI225

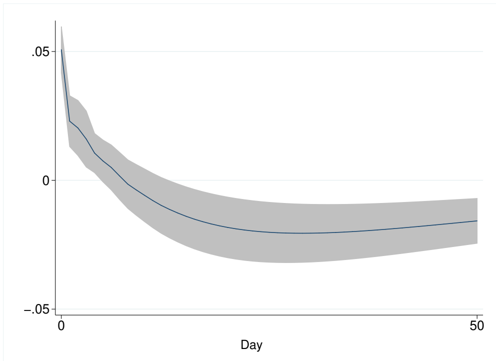

(f) S&P500

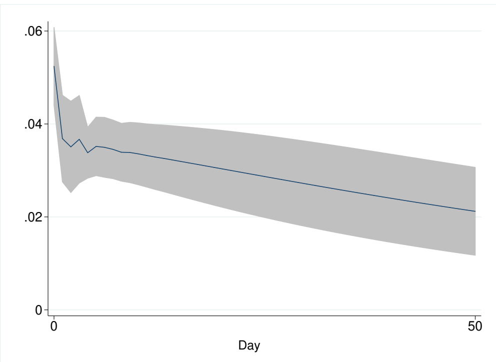

(g) SSE

Figure 2.5: News impact curve for realized volatility

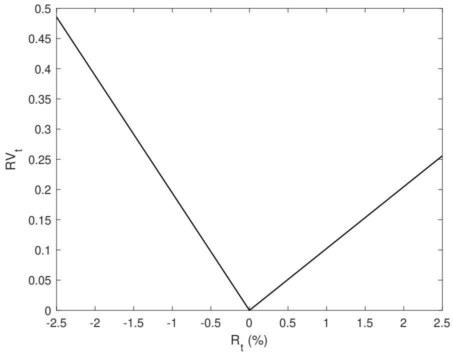

(a) FTSE100

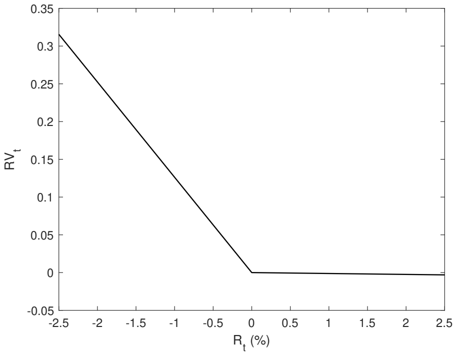

(b) CAC40

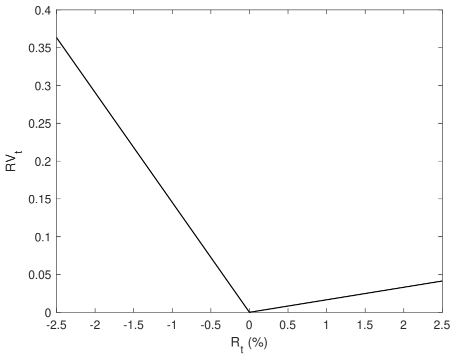

(c) DAX

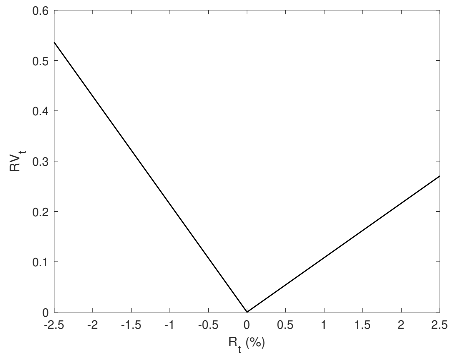

(d) DJIA

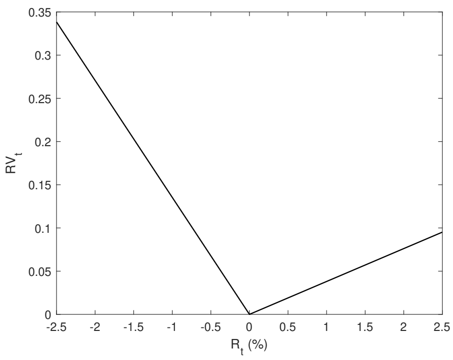

(e) NIKKEI225

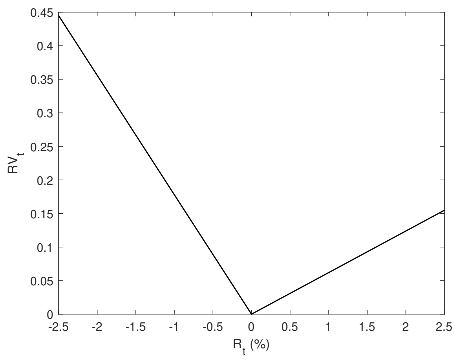

(f) S&P500

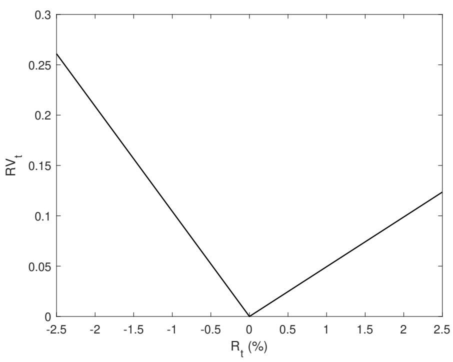

(g) SSE

Figure 2.6: News impact curve for investor attention

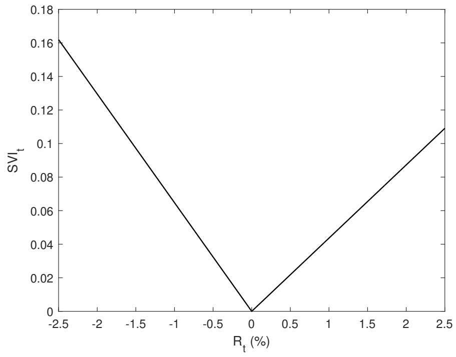

(a) FTSE100

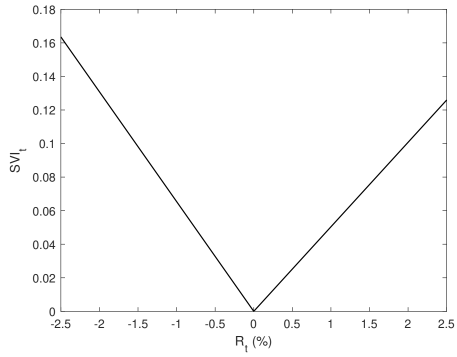

(b) CAC40

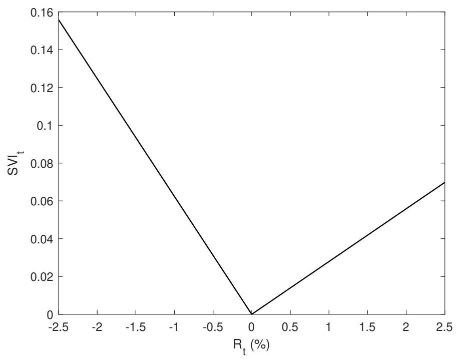

(c) DAX

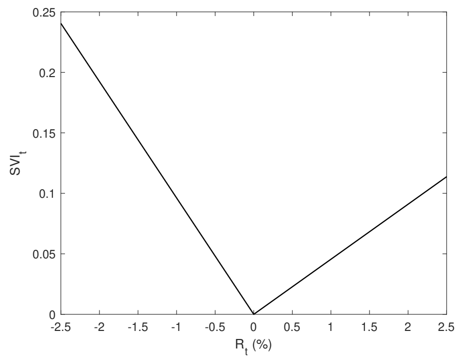

(d) DJIA

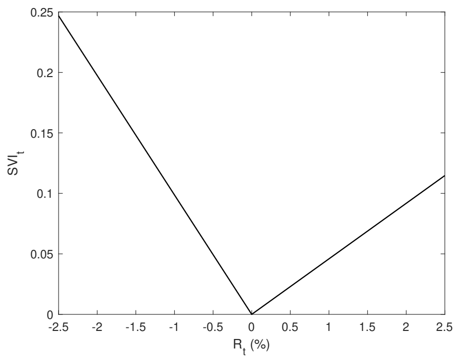

(e) NIKKEI225

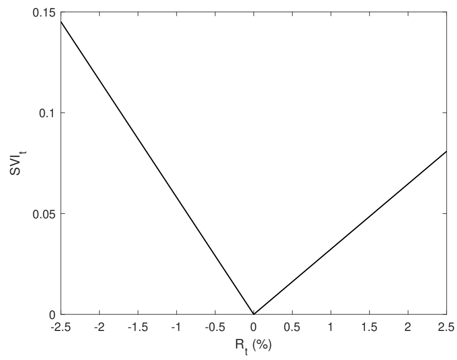

(f) S&P500

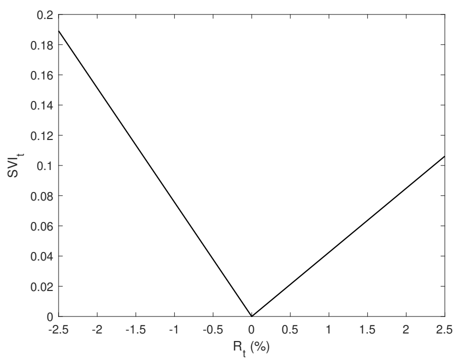

(g) SSE

2.4 Conclusion

In this chapter, we have investigated the relationship between return, investor attention and volatility for the main international stock market indexes, such as FTSE100, CAC40, DAX, Dow Jones Industrial Average (DJIA), NIKKEI225, S&P500 and Shanghai Composite (SSE). In particular, we explored the connection between the phenomenon of volatility asymmetry and the asymmetry of investor attention to good and bad news. As a measure of investor attention, we utilized the Search Volume Index (SVI) provided by the Google Trends service.

In the first step, we used the Structural Vector Autoregressive (SVAR) model and impulse response analysis to explore the short-term and long-term relationship between the analyzed variables. Our findings indicate that the effect of return on realized volatility is generally persistent and long lasting while the effects of return on investor attention and of investor attention on volatility are only temporary. Using the Granger Causality framework, we identified statistical causality from return to both volatility and investor attention and bidirectional causality between attention and volatility. In the second step, we utilized a set of Autoregressive Distributed Lag (ARDL) models to investigate the contemporaneous and dynamic asymmetry in volatility and investor attention. We demonstrated that both volatility and investor attention are similarly asymmetric in their response to market news represented by index return: negative return has a stronger impact on both volatility and investor attention than does positive return of the same absolute magnitude. We also illustrated our findings with news impact curves for both volatility and investor attention. We proposed that the main potential reason behind the asymmetric attention might be well-known psychological anomalies, such as negativity bias and loss aversion.

We provided new evidence of the existence of a positive relationship between volatility and investor attention. Moreover, our results also indicate that the magnitude of the impact of investor attention on volatility is stronger during periods of negative returns. We demonstrated that, in the theoretical setting where market volatility is driven by investor attention which, in its turn, depends on market return, asymmetrically higher attention caused by negative returns would lead to asymmetrically higher volatility. However, we found that the effect of retail investor attention on volatility is only temporary.

The work presented in this chapter can be extended in the following ways. First, an interesting line of further investigation would be to study in greater detail the transition mechanism between investor attention and volatility. What kind of trading behaviour of investors, affected by negative or positive returns, leads, respectively, to higher or lower market volatility? Moreover, as the measure of investor attention in the present work represents only the attention of retail investors, an important direction for future research would be to investigate the attention of professional or institutional investors. What is the appropriate way to measure the attention of professional investors and does it exhibit the same kind of asymmetry to good and bad market news? Also, as we can notice from the empirical results, the estimated SVAR and ARDL models are not free of the residual autocorrelation. This fact can be explained by the highly persistent nature of realized volatility and investor attention. Hence, exploring the possibility of a cointegrative dynamics between volatility and investor attention, such as potential fractional cointegration, is an interesting direction of further research. Finally, we claim that behavioural phenomena, such as asymmetric attention, are most certainly not the only explanation of such a complex phenomenon as volatility asymmetry. The other factors, which contribute to volatility asymmetry, are also worth further investigations.

2.5 Appendix

2.5.1 The SVAR model estimation results

Table 2.9: The estimated SVAR model results

	FTSE100	CAC40	DAX	DJI	NIKKEI225	SP500	SSE
a_{11}	1	1	1	1	1	1	1
a_{21}	1.342***	1.054***	1.872***	2.996***	3.341***	1.628***	2.117***
	(0.313)	(0.319)	(0.255)	(0.282)	(0.288)	(0.253)	(0.320)
a_{31}	5.032***	6.574***	6.444***	4.901***	4.994***	6.231***	2.859***
	(0.413)	(0.289)	(0.301)	(0.449)	(0.289)	(0.401)	(0.259)
a_{12}	0	0	0	0	0	0	0
a_{22}	1	1	1	1	1	1	1
a_{32}	-0.269***	-0.124***	-0.156***	-0.460***	-0.167***	-0.287***	-0.166***
	(0.021)	(0.014)	(0.019)	(0.026)	(0.016)	(0.025)	(0.013)
a_{13}	0	0	0	0	0	0	0
a_{23}	0	0	0	0	0	0	0
a_{33}	1	1	1	1	1	1	1
b_{11}	0.011***	0.013***	0.013***	0.011***	0.014***	0.011***	0.016***
	(0.000)	(0.000)	(0.000)	(0.000)	(0.000)	(0.000)	(0.000)
b_{21}	0	0	0	0	0	0	0
b_{31}	0	0	0	0	0	0	0
b_{12}	0	0	0	0	0	0	0
b_{22}	0.208***	0.258***	0.207***	0.184***	0.259***	0.177***	0.315***
	(0.002)	(0.003)	(0.002)	(0.002)	(0.003)	(0.002)	(0.004)
b_{32}	0	0	0	0	0	0	0
b_{13}	0	0	0	0	0	0	0
b_{23}	0	0	0	0	0	0	0
b_{33}	0.275***	0.233***	0.243***	0.288***	0.255***	0.279***	0.253***
	(0.000)	(0.003)	(0.003)	(0.003)	(0.003)	(0.003)	(0.003)
LM(1)	189.77***	159.63***	195.44***	101.29***	118.73***	107.59***	92.06***
LM(5)	31.82***	62.01***	48.83***	17.86**	9.83	16.10*	10.94
LM(10)	12.86	34.48***	30.64***	18.83**	9.21	16.77*	23.59***
N of obs.	3816	3853	3837	3795	3700	3798	3579

The table reports the results of the estimated three-dimensional SVAR model for return, investor attention and realized volatility for each of the stock market indexes. a_{ij} and b_{ij} refer to the elements of the matrices A and B respectively. 1 and 0 mean the restricted elements of the matrices A and B. LM(1), LM(5) and LM(10) refer to the LM test statistics for the first, fifths and tens order serial correlation in the residuals respectively. The standard errors are in parentheses. ***, ** and * indicate statistical significance at the 1%, 5% and 10% levels respectively.

Table 2.10: The estimated reduced-form VAR model results

Panel A: Equation for returns

	FTSE100	CAC40	DAX	DJI	NIKKEI225	SP500	SSE
R							
R_{t-1}	-0.029*	-0.018	0.001	-0.092***	-0.041**	-0.100***	0.026
	(0.017)	(0.017)	(0.017)	(0.017)	(0.017)	(0.017)	(0.017)
R_{t-2}	-0.049***	-0.052***	-0.031*	-0.060***	-0.004	-0.069***	-0.013
	(0.017)	(0.017)	(0.017)	(0.017)	(0.018)	(0.018)	(0.017)
R_{t-3}	-0.023	-0.040**	-0.026	0.030*	-0.022	0.022	0.023
	(0.017)	(0.017)	(0.017)	(0.017)	(0.018)	(0.017)	(0.017)
R_{t-4}	0.028*	0.016	0.011	-0.033**	-0.019	-0.025	0.054***
	(0.016)	(0.016)	(0.016)	(0.017)	(0.017)	(0.017)	(0.017)
SVI_{t-1}	0.000	-0.000	0.000	0.001	-0.001	-0.000	0.000
	(0.001)	(0.001)	(0.001)	(0.001)	(0.001)	(0.001)	(0.001)
SVI_{t-2}	-0.001	0.001	-0.000	0.001	0.000	-0.000	0.000
	(0.001)	(0.001)	(0.001)	(0.001)	(0.001)	(0.001)	(0.001)
SVI_{t-3}	0.001	0.000	0.001	-0.002*	0.002*	0.002	-0.001
	(0.001)	(0.001)	(0.001)	(0.001)	(0.001)	(0.001)	(0.001)
SVI_{t-4}	0.001	-0.001	0.001	0.001	-0.001	-0.000	0.001
	(0.001)	(0.001)	(0.001)	(0.001)	(0.001)	(0.001)	(0.001)
RV_{t-1}	-0.000	0.000	-0.000	-0.002***	0.001	-0.002**	0.002**
	(0.001)	(0.001)	(0.001)	(0.001)	(0.001)	(0.001)	(0.001)
RV_{t-2}	0.001	-0.001	0.000	0.001	-0.001	0.002**	-0.001
	(0.001)	(0.001)	(0.001)	(0.001)	(0.001)	(0.001)	(0.001)
RV_{t-3}	0.000	-0.000	-0.001	-0.000	-0.001	-0.001	-0.000
	(0.001)	(0.001)	(0.001)	(0.001)	(0.001)	(0.001)	(0.001)
RV_{t-4}	-0.000	0.001	0.001	0.000	0.001	0.000	-0.000
	(0.001)	(0.001)	(0.001)	(0.001)	(0.001)	(0.001)	(0.001)
$Cons$	-0.000	-0.001	-0.002	-0.004*	-0.001	-0.003	0.003
	(0.002)	(0.003)	(0.003)	(0.002)	(0.003)	(0.002)	(0.004)
R^2	0.006	0.006	0.004	0.017	0.005	0.016	0.007
N of obs.	3816	3853	3837	3795	3700	3798	3579

The table reports the results of the reduced-form VAR model for return, investor attention and realized volatility for each of the stock market indexes. $R_{t-1}, ..., R_{t-4}$ indicate the coefficients on lagged return, $SVI_{t-1}, ..., SVI_{t-4}$ indicate the coefficients on lagged investor attention, $RV_{t-1}, ..., RV_{t-4}$ indicate the coefficients on lagged realized volatility. $Cons$ indicates the coefficient on the constant. The standard errors are in parentheses. ***, ** and * indicate statistical significance at the 1%, 5% and 10% levels respectively.

Table 2.10: The estimated reduced-form VAR model results

Panel B: Equation for investor attention

	FTSE100	CAC40	DAX	DJI	NIKKEI225	SP500	SSE
SVI							
R_{t-1}	-1.199***	-1.536***	-0.876***	-2.174***	-1.525***	-1.759***	-1.209***
	(0.320)	(0.340)	(0.273)	(0.294)	(0.310)	(0.264)	(0.328)
R_{t-2}	-0.075	-0.982***	-0.583**	-0.526*	0.226	-0.583**	0.280
	(0.329)	(0.346)	(0.278)	(0.306)	(0.315)	(0.275)	(0.332)
R_{t-3}	0.847***	-0.250	-0.083	-0.559*	0.548*	-0.275	0.136
	(0.327)	(0.343)	(0.274)	(0.305)	(0.313)	(0.273)	(0.332)
R_{t-4}	0.028	-0.244	0.058	-0.102	0.164	0.035	-0.008
	(0.319)	(0.325)	(0.261)	(0.293)	(0.299)	(0.261)	(0.326)
SVI_{t-1}	0.511***	0.373***	0.494***	0.701***	0.408***	0.505***	0.409***
	(0.016)	(0.016)	(0.016)	(0.017)	(0.017)	(0.016)	(0.017)
SVI_{t-2}	0.190***	0.216***	0.159***	0.101***	0.293***	0.160***	0.237***
	(0.018)	(0.017)	(0.018)	(0.021)	(0.018)	(0.018)	(0.018)
SVI_{t-3}	0.115***	0.145***	0.127***	0.039*	0.127***	0.131***	0.178***
	(0.018)	(0.017)	(0.018)	(0.021)	(0.018)	(0.018)	(0.018)
SVI_{t-4}	0.114***	0.206***	0.147***	0.125***	0.133***	0.126***	0.141***
	(0.016)	(0.016)	(0.016)	(0.017)	(0.017)	(0.016)	(0.017)
RV_{t-1}	0.044***	0.062***	0.013	0.035***	0.052***	0.020*	0.079***
	(0.012)	(0.018)	(0.014)	(0.010)	(0.017)	(0.010)	(0.021)
RV_{t-2}	-0.006	0.002	0.009	-0.036***	-0.032*	-0.021*	0.008
	(0.012)	(0.018)	(0.014)	(0.011)	(0.018)	(0.011)	(0.022)
RV_{t-3}	-0.003	-0.032*	-0.027*	-0.006	-0.026	-0.014	-0.048**
	(0.012)	(0.018)	(0.014)	(0.011)	(0.018)	(0.011)	(0.022)
RV_{t-4}	-0.035***	-0.014	-0.005	0.001	-0.013	-0.002	-0.008
	(0.012)	(0.017)	(0.013)	(0.010)	(0.017)	(0.010)	(0.021)
$Cons$	0.203***	0.236***	0.179***	0.060	0.016	0.158***	0.222***
	(0.047)	(0.062)	(0.049)	(0.037)	(0.058)	(0.038)	(0.076)
R^2	0.773	0.791	0.753	0.894	0.858	0.761	0.905
N of obs.	3816	3853	3837	3795	3700	3798	3579

The table reports the results of the reduced-form VAR model for return, investor attention and realized volatility for each of the stock market indexes. $R_{t-1}, ..., R_{t-4}$ indicate the coefficients on lagged return, $SVI_{t-1}, ..., SVI_{t-4}$ indicate the coefficients on lagged investor attention, $RV_{t-1}, ..., RV_{t-4}$ indicate the coefficients on lagged realized volatility. $Cons$ indicates the coefficient on the constant. The standard errors are in parentheses. ***, ** and * indicate statistical significance at the 1%, 5% and 10% levels respectively.

Table 2.10: The estimated reduced-form VAR model results

Panel C: Equation for realized volatility

	FTSE100	CAC40	DAX	DJI	NIKKEI225	SP500	SSE
RV							
R_{t-1}	-7.013***	-4.165***	-4.358***	-7.669***	-3.216***	-6.987***	-2.345***
	(0.439)	(0.330)	(0.341)	(0.485)	(0.319)	(0.435)	(0.274)
R_{t-2}	-3.125***	-1.860***	-1.771***	-4.702***	-1.301***	-3.706***	1.162***
	(0.452)	(0.336)	(0.347)	(0.505)	(0.324)	(0.454)	(0.276)
R_{t-3}	-2.325***	-1.347***	-0.997***	-1.377***	-0.793**	-1.118**	0.714***
	(0.449)	(0.333)	(0.343)	(0.504)	(0.322)	(0.451)	(0.277)
R_{t-4}	-0.381	0.226	0.342	-0.451	-0.068	-0.226	0.345
	(0.437)	(0.316)	(0.326)	(0.483)	(0.308)	(0.431)	(0.272)
SVI_{t-1}	-0.011	0.039**	0.008	0.014	0.056***	0.022	0.045***
	(0.023)	(0.015)	(0.020)	(0.028)	(0.017)	(0.027)	(0.014)
SVI_{t-2}	0.012	-0.024	0.007	-0.006	-0.016	-0.010	0.008
	(0.025)	(0.016)	(0.022)	(0.034)	(0.018)	(0.030)	(0.015)
SVI_{t-3}	-0.016	-0.001	0.004	-0.041	-0.056***	-0.032	-0.002
	(0.025)	(0.016)	(0.022)	(0.034)	(0.018)	(0.030)	(0.015)
SVI_{t-4}	-0.011	-0.005	-0.041**	0.020	0.003	-0.043	-0.025*
	(0.022)	(0.015)	(0.020)	(0.028)	(0.017)	(0.027)	(0.014)
RV_{t-1}	0.303***	0.362***	0.359***	0.326***	0.402***	0.377***	0.434***
	(0.016)	(0.017)	(0.017)	(0.017)	(0.017)	(0.017)	(0.017)
RV_{t-2}	0.211***	0.191***	0.195***	0.224***	0.193***	0.211***	0.208***
	(0.017)	(0.018)	(0.018)	(0.018)	(0.019)	(0.018)	(0.019)
RV_{t-3}	0.164***	0.176***	0.179***	0.173***	0.149***	0.154***	0.143***
	(0.017)	(0.018)	(0.018)	(0.018)	(0.018)	(0.018)	(0.019)
RV_{t-4}	0.208***	0.161***	0.154***	0.160***	0.119***	0.149***	0.099***
	(0.016)	(0.017)	(0.017)	(0.017)	(0.017)	(0.017)	(0.017)
$Cons$	-0.484***	-0.546***	-0.475***	-0.547***	-0.633***	-0.344***	-0.589***
	(0.064)	(0.061)	(0.061)	(0.062)	(0.059)	(0.062)	(0.063)
R^2	0.678	0.719	0.694	0.697	0.651	0.738	0.741
N of obs.	3816	3853	3837	3795	3700	3798	3579

The table reports the results of the reduced-form VAR model for return, investor attention and realized volatility for each of the stock market indexes. $R_{t-1}, ..., R_{t-4}$ indicate the coefficients on lagged return, $SVI_{t-1}, ..., SVI_{t-4}$ indicate the coefficients on lagged investor attention, $RV_{t-1}, ..., RV_{t-4}$ indicate the coefficients on lagged realized volatility. *Cons* indicates the coefficient on the constant. The standard errors are in parentheses. ***, ** and * indicate statistical significance at the 1%, 5% and 10% levels respectively.

Chapter 3

Combining econometrics and machine learning to forecast realized volatility of exchange rates

3.1 Introduction

Volatility is a key concept in finance and has important applications in risk management, portfolio analysis, asset pricing and derivative valuation. The high predictability of volatility was extensively documented in the literature (see, e.g., Poon and Granger, 2003) and led to the development of massive research area devoted to volatility modeling and forecasting. According to Brandt and Jones (2006), there are two main factors that determine the efficiency and accuracy of a volatility model. First of all, as true volatility is not observable directly, its modeling inevitably depends on the adequacy of the proxy (measure) of the true unobserved volatility that is used in the model. Traditional and commonly used volatility proxies are based on absolute or squared returns. These measures are known to be unbiased but relatively noisy estimators of the latent integrated volatility as they include no information about the intra-period price fluctuations.

Given the growing availability of high frequency financial data in recent decades, attention of researchers have moved to alternative volatility estimators. Andersen et al. (2001) proposed a new volatility measure based on intra-period high frequency returns which is called realized volatility. Realized volatility has proven to be much less noisy volatility estimator than traditional proxies. Moreover, under realized volatility approach, financial volatility is treated as observable variable and can be modeled directly.

Another volatility estimator that exploits information about the intra-period price movements is called range-based volatility. This estimator, proposed in earlier works of Parkinson (1980) and Garman and Klass (1980), is defined as the scaled difference between the intra-period highest and lowest prices. As noted by Molnár (2012), range-based volatility is also less noisy volatility proxy than squared returns.

Precise specification of the process that drives volatility dynamics is the second factor determining the accuracy and efficiency of a volatility model. For many years, autoregressive conditional heteroscedasticity (ARCH) and generalized autoregressive conditional heteroscedasticity (GARCH) models developed by Engle (1982) and Bollerslev (1986) respectively remained the most popular financial volatility models. Under ARCH and GARCH approach, volatility measured by squared returns follows a linear autoregressive dynamics. ARCH and GARCH framework gave rise to dozens of its advanced modifications developed to capture different stylized facts of financial returns and volatility, such as clustering, long memory, leptokurtosis and leverage effects. An alternative approach of volatility modeling is to model the series of realized volatility directly, rather than applying GARCH-type models to the series of returns. Autoregressive fractionally integrated moving average (ARFIMA) of Granger and Joyeux (1980) and Hosking (1981) is a widely used modeling approach to capture both long memory and clustering in realized volatility.

Qualitatively similar to ARFIMA but easier to estimate model of realized volatility is the heterogeneous autoregressive (HAR) model of Corsi (2009). The model is based on the Heterogeneous Market Hypothesis and the asymmetric propagation of volatility between long and short horizons. It includes an additive cascade of different volatility components generated by the actions of various types of financial market participants. This additive cascade implies an autoregressive-based model of volatility with the feature of considering volatilities realized over different time horizons. Similar to ARFIMA, the HAR model can successfully imitate the long memory volatility dynamics.

Recently, multi-component volatility models have attracted growing attention of researchers and practitioners. One of the most famous component GARCH models was introduced by Engle and Lee (1999). In the model, the dynamics of volatility is decomposed into two additive components: a highly persistent long-run component and a strongly stationary transitory short-run component. Many empirical studies find that the two-component GARCH models outperform the one-component specifications in explaining the dynamics of financial volatility (see, e.g., Engle and Rosenberg, 2000;

Adrian and Rosenberg, 2008; Christoffersen et al., 2008; Engle, Ghysels, and Sohn, 2013). In a number of works, two-component models are applied to range-based volatility measures. For example, Brandt and Jones (2006) use one-component and two-component EGARCH model for the range-based volatility of the S&P500 index and show that the two-component model provides better fit to the data. Harris, Stoja, and Yilmaz (2011) use the two-component cyclical volatility model in the spirit of Engle and Lee (1999) to forecast exchange rates range-based volatility. In the first step, they apply the low-pass filter of Hodrick and Prescott (1997) to decompose the exchange rates range-based volatility into the long-run trend and the short-run cyclical components. In the second step, the two components are forecasted separately using the simple random walk model for the trend component and AR(1) model for the cyclical component. The final forecast of the volatility series is the sum of the individual forecasts of the trend and the cyclical components. According to Harris, Stoja, and Yilmaz (2011), the cyclical volatility model using the Hodrick-Prescott filter provides an improvement in forecast performance over the two-component EGARCH and FIEGARCH models, in terms of both accuracy and informational content. Engle and Sokalska (2012) propose multiplicative decomposition of volatility and apply the multiplicative component GARCH model to forecast intraday volatility in the US equity market. Hansen, Huang, and Shek (2012) propose an interesting modification of the GARCH approach which is called Realized GARCH. The Realized GARCH model includes both the latent and the observed (realized) volatility components and assumes both linear and log-linear volatility dynamics. An empirical application of the Realized GARCH model leads to improvements in volatility modeling over the standard GARCH model.

Alternative to the traditional econometric models, the development of artificial intelligence methods has led to the widespread use of machine learning algorithms in the field of financial modeling and forecasting. For example, Kimoto et al. (1990) propose artificial neural network (ANN) system for stock market prediction. Nikolopoulos and Fellrath (1994) use genetic algorithms and neural networks to develop an expert system for investment advising. Pai and Lin (2005) apply ARIMA model and support vector machines for stock price prediction. Fischer and Krauss (2018) compare the performance of different machine learning algorithms in forecasting returns of the S&P500 index.

A number of studies adapted machine learning methods to volatility forecasting. Rosa et al. (2014) suggest an evolving fuzzy neural network modelling approach for forecasting realized volatility of several equity market indices. Barunık and Křehlık (2016) apply artificial neural networks to forecast energy market realized volatility. They document the superior forecasting performance of the machine learning algorithms compared to the traditional econometric models such as ARFIMA and HAR. Vortelinos (2017) compares volatility forecasting accuracy of machine learning algorithms (such as principal components analysis and artificial neural networks) against econometric models (such as GARCH and HAR). His findings indicate the similar performance of the principal components and HAR models. Fičura et al. (2017) apply echo state neural networks to forecast realized volatility of major stock market indices.

Some studies proposed a hybrid approach of volatility forecasting that is based on combination of GARCH-type models with artificial neural networks. The idea of the hybrid approach is that the input variables for neural networks are initially extracted by applying GARCH-type models to the data. There is growing empirical evidence that the hybrid GARCH-ANN approach is more efficient in terms of volatility forecasting accuracy than just basic GARCH-type models (see, e.g., Roh, 2007; Wang, 2009; Hajizadeh et al., 2012; Kristjanpoller, Fadic, and Minutolo, 2014; Monfared and Enke, 2014; Kristjanpoller and Minutolo, 2016; Kim and Won, 2018; etc).

Yao et al. (2017) suggested a neural network modification of the cyclical volatility model of Engle and Lee (1999) and Harris, Stoja, and Yilmaz (2011). According to the modified approach, the time series of realized volatility is decomposed by the low-pass Hodrick-Prescott filter into the long-run and short-run components which are then modelled by the autoregressive neural network and AR(1) model respectively. Yao et al. (2017) show that using the autoregressive neural network instead of the random walk model to forecast the long-run component of volatility made it possible to improve the forecast accuracy in comparison with the basic model of Harris, Stoja, and Yilmaz (2011). Cao, Liu, and Zhai (2018) proposed a further improvement of the model by using ARMA model to forecast the short-run volatility component instead of the simple AR(1) specification.

Inspired by the previous research in the field of multi-component and hybrid econometrics-machine learning volatility models, we propose a new two-component volatility model that is based on methodological combination of long memory econometrics with artificial neural networks. In contrast to the described above approach of combining machine learning with GARCH-type models, we work directly with time series of realized volatility as it is much less noisy and generally more adequate volatility proxy than squared returns. Our approach is based on the widely known proposition that the dynamics of financial volatility includes not only linear but also complex nonlinear dependencies (see, e.g., Diebold and Lopez, 1995; Hsieh, 1995; Robinson and Zaffaroni, 1998; Christoffersen and Diebold, 2006; Raggi and Bordignon, 2012; etc). Moreover, volatility dynamics may be nonlinear in ways missed by standard volatility models. For example, Dıaz, Grau-Carles, and Mangas (2002) show that standard ARFIMA model, though effective in describing long memory, is not able to capture the nonlinearities in the time series of financial volatility. To model a time series that is generated by a complex composition of linear and nonlinear underlying processes, Zhang (2003) suggested a hybrid methodology combining ARIMA framework with artificial neural networks. Under the approach, the time series under study is decomposed into the linear and nonlinear components, then ARIMA is used to model the linear part and neural network is used to model the nonlinear part of the time series. Thus, the method of Zhang (2003) exploits both the strength of ARIMA in linear modeling and the flexible nonlinear modeling capability of artificial neural networks. We adapt the approach of Zhang (2003) to the task of modeling realized volatility. Our proposed hybrid methodology consists of two steps. In the first step, ARFIMA is used to model the linear long memory component of realized volatility. In the second step, the nonlinear autoregressive neural network (NAR) is used to analyze the nonlinear component of realized volatility in the form of the residuals from the ARFIMA model. Thus, the suggested hybrid ARFIMA-ANN model is intended to capture both the phenomena of long memory and nonlinearity in the dynamics of realized volatility. To the best of our knowledge, our research is the first work where the stated hybrid approach of time series modeling is applied in the context of financial volatility.

We implement the hybrid ARFIMA-ANN model using the time series of daily realized volatility of the GBP/USD and the EUR/GBP foreign exchange rates over the period from January 4, 2010 to December 30, 2016. We use the model to generate a series of one-step-ahead out-of-sample forecasts of the realized volatility of the exchange rates. As a benchmark, we compare the forecasting accuracy of the hybrid ARFIMA-ANN model with those of the standard random walk model, ARFIMA model and the nonlinear autoregressive neural network applied directly to the series of realized volatility. We also compare the forecasting accuracy of the proposed model with those of the two-component cyclical volatility model of Harris, Stoja, and Yilmaz (2011), Yao et al. (2017) and Cao, Liu, and Zhai (2018). Moreover, we propose a modification of the cyclical volatility model where we use artificial neural networks to forecast both trend and cyclical components of the realized volatility. We show that the hybrid ARFIMA-ANN model and the proposed modification of the cyclical volatility model provide an improvement in forecast performance over the competing approaches, in terms of both accuracy and informational content. We make a conclusion about the benefits and perspectives of using multi-component models and combination of econometrics and machine learning in predictive modeling of financial volatility.

The remainder of the chapter is organized as follows. In Section 3.2, we present the basic theoretical framework of the models under consideration. Section 3.3 describes the data used in the empirical analysis and the forecast evaluation criteria. Section 3.4 presents the empirical results. In Section 3.5, we provide a summary and suggest potential directions of further research.

3.2 Theoretical framework

3.2.1 Realized volatility

Here we formally introduce the concept of realized volatility. Assume that the logarithmic price $p(t)$ of a liquid asset follows the standard continuous time process

$$\mathrm{d}p(t) = \mu(t)\ \mathrm{d}t + \sigma(t)\ \mathrm{d}W(t), \tag{3.1}$$

where $W(t)$ is a standard Brownian motion, $\mu(t)$ is an instantaneous conditional mean and $\sigma(t)$ is an instantaneous conditional volatility of the process. The integrated volatility associated with day t, for this diffusion process, is the integral of the instantaneous volatility over the one day interval $(t-1d; t)$, where a full trading day is represented by the time interval $1d$,

$$\sigma_t^{(d)} = \left(\int_{t-1d}^{t} \sigma^2(\omega)\mathrm{d}\omega \right)^{1/2}. \tag{3.2}$$

As firstly proposed by Merton (1980) and then by Andersen et al. (2001), the sum of intraday squared returns can be used to approximate the integrated volatility $\sigma_t^{(d)}$ to an arbitrary precision. The nonparametric estimator of the integrated (actual) volatility based on the sum of intraday squared returns is called realized volatility. Following Andersen et al. (2001) and Corsi (2009), the realized volatility over a time interval of one day can be defined as

$$RV_t^{(d)} = \sqrt{\sum_{j=0}^{M-1} r_{t-j\Delta}^2}, \tag{3.3}$$

where $\Delta = \frac{1d}{M}$ ($1d$ indicates one trading day; M indicates the number of intraday periods) and $r_{t-j\Delta} = p(t-j\Delta) - p(t-(j+1)\Delta)$ defines continuously compounded Δ-frequency returns, that is, intraday returns sampled at time interval Δ (the subscript t indexes the day, while j indexes the time within the day t).

In other words, realized volatility over a time interval of one day is the square root of the sum of squared high frequency intraday returns. Under certain assumptions, realized volatility is an unbiased estimator of the true integrated volatility. Moreover, Andersen et al. (2003) show that, in terms of out-of-sample forecasting accuracy, direct time series modeling of realized volatility strongly outperforms the models of GARCH family.

3.2.2 ARFIMA model

Autoregressive fractionally integrated moving average (ARFIMA), proposed by Granger and Joyeux (1980) and Hosking (1981), is the popular approach to model long memory in the dynamics of a time series. ARFIMA model is a generalization of autoregressive integrated moving average (ARIMA) - the famous linear univariate time series model of Box and Jenkins (1976).

Formally, an ARFIMA(p, d, q) process y_t can be defined as

$$\phi(L)(1-L)^d y_t = \theta(L)\epsilon_t, \tag{3.4}$$

where L is the backshift (lag) operator, $\phi(L) = 1 - \sum_{j=1}^{p} \phi_j L^j$ and $\theta(L) = 1 + \sum_{j=1}^{q} \theta_j L^j$ are autoregressive and moving average polynomials of orders p and q respectively, ϵ_t is a white noise process and $-0.5 < d < 0.5$.

The fractional differencing operator $(1-L)^d$ can be represented in the following form using the binomial series expansion:

$$(1-L)^d = \sum_{j=0}^{\infty} \frac{\Gamma(j-d)}{\Gamma(j+1)\Gamma(-d)} L^j, \tag{3.5}$$

where $\Gamma(\cdot)$ is the gamma function.

ARFIMA model offers a parsimonious way to model a long memory - the phenomenon of a slowly decaying autocorrelation function of a time series. The characteristics of an ARFIMA(p, d, q) series depend on the value of the fractional differencing parameter d. For $-0.5 < d < 0.5$ the process is stationary and for $0 < d < 0.5$ the process exhibit long memory properties. In an ARFIMA(p, d, q) model, parameter d describes the long run behavior of the underlying process y_t (it describes the autocorrelation structure of distant observations of the process), whereas autoregressive and moving average polynomials $\phi(L) = 1 - \sum_{j=1}^{p} \phi_j L^j$ and $\theta(L) = 1 + \sum_{j=1}^{q} \theta_j L^j$ describes the behavior of the series in the short run (and, respectively, capture the process's autocorrelation structure for low lags).

3.2.3 Nonlinear autoregressive neural networks for time series modeling

Modeling complex nonlinear dependencies of a time series is a nontrivial task that, often, cannot be successfully solved within the framework of traditional econometric models. The rapid development of statistical and machine learning methods in recent decades has led to the emergence of artificial neural networks which are now widely used in time series analysis for modeling nonlinearities in the data.

As stated by Zhang (2003), ANNs are flexible computing frameworks for modeling a broad range of nonlinear problems. Artificial neural networks are universal approximators which are able to approximate a large class of functions with a high degree of accuracy. The power of ANNs comes from the parallel processing of the information from the data. ANNs provide a substantial advantage over other classes of nonlinear models as they do not require any prior assumption of the model specification in the process of model building. Instead, the model specification is directly determined by the characteristics of the time series data.

Nowadays, the most popular neural network model form for time series modeling and forecasting is a single hidden layer feedforward neural network. Feedforward neural network model analyzes the relationship between the output y_t and the inputs $(y_{t-1}, y_{t-2}, ..., y_{t-p})$ and can be formally written as

$$y_t = \alpha_0 + \sum_{j=1}^{q} \alpha_j g \left(\beta_{0j} + \sum_{i=1}^{p} \beta_{ij} y_{t-i} \right) + \epsilon_t, \tag{3.6}$$

where $\alpha_j (j = 0, 1, 2, ..., q)$ and $\beta_{ij} (i = 0, 1, 2, ..., p; j = 1, 2, ..., q)$ are the parameters of the model to be estimated (which are sometimes called the connection weights), p is the number of input nodes (lags), q is the number of hidden nodes (neurons) and g is the hidden layer transfer function which is usually deterministic and symmetrically nonlinear. In this study, the hyperbolic tangent sigmoid function is used as the transfer function.[1]

In fact, the artificial neural network defined above performs as a univariate nonlinear autoregression. In other words, as stated in Zhang (2003), nonlinear autoregressive neural network performs a nonlinear functional mapping from the past observations $(y_{t-1}, y_{t-2}, ..., y_{t-p})$ to the future value y_t of the time series, i.e.,

$$y_t = f\left(y_{t-1}, y_{t-2}, ..., y_{t-p}, w\right) + \epsilon_t, \tag{3.7}$$

where f is a nonlinear function determined by network structure and connection weights, w is a vector of all parameters of the model.

The single hidden layer feedforward neural network given in Equation 3.6 is able to arbitrary well approximate any nonlinear function as the number of hidden nodes q is sufficiently large (Hornik, Stinchcombe, and White, 1989, Siegelmann, Horne, and Giles, 1997).

One of the most important tasks of ANN modeling is to determine the appropriate architecture of a network, that is, the number of hidden nodes q and the number of lagged observations p. The number of hidden nodes

[1] The hyperbolic tangent sigmoid function is defined as: $tanh(x) = \frac{2}{1+e^{-2x}} + 1$.

determines the capacity of a model, its ability to capture complicated patterns. The number of lagged observations (that is also the dimension of the input vector) describes the nonlinear autocorrelation structure of the time series. In practice, however, there is no systematic rule that can be used to choose the best architecture of the neural network, the choice of the p and q is always data dependent. Generally, a number of experiments with different values of the parameters p and q is conducted in order to select the appropriate architecture.

Practically, relatively simple ANN models with a small number of hidden nodes often show good performance in terms of out-of-sample forecasting. Apparently, the simply structured models are less prone to the overfitting effect. Overfitting is a modeling error which occurs when a model excellently fits in-sample data but has poor generalization ability for data out of the sample (Zhang, 2003). Overfitting is a typical problem of machine learning algorithms.

After selecting the values of p and q, the next step in the process of ANN modeling is to estimate the set of parameters w. The process of estimating the unknown set of parameters for a given sample of data is known as training of the neural network. In the process of training, the set of parameters is estimated in a way to minimize a certain accuracy criterion, such as the mean squared error. This is done using one of the complicated algorithms of nonlinear optimization. In this study, the training process of the neural networks is performed with the Levenberg-Marquardt algorithm. In order to prevent overfitting, a special validation sample is used. Unlike training sample, validation sample is used not to estimate the set of parameters w but to measure network generalization. In the process of training, when the error over the training sample decreases but the error over the validation sample increases or stays the same, the training is stopped. The estimated neural network model is usually evaluated using a separate hold-out sample that was not involved in the process of training and validation. In practice, a neural network is usually retrained several times to ensure that a model of good accuracy has been found.

3.2.4 The hybrid ARFIMA-ANN model of realized volatility

Financial volatility is a complicated stochastic process which includes number of sophisticated patterns. Motivated by the previous findings that the complex nature of volatility can be well described by multi-component structures, we propose a new model where volatility is a function of linear and nonlinear factors. In line with the works of Andersen et al. (2001), Corsi (2009), Yao et al. (2017), etc., we use realized volatility as an advanced proxy of the true unobserved volatility.

Following the hybrid time series modeling methodology of Zhang (2003), we assume that realized volatility σ_t (as defined in Equation 3.3) follows a two-component process given by

$$\sigma_t = L_t + N_t, \tag{3.8}$$

where L_t is the linear component and N_t is the nonlinear component.

In other words, we assume that realized volatility can be decomposed into the linear and the nonlinear components and that there is an additive relationship between the two components. The linear and the nonlinear components of the time series of realized volatility are modeled separately by different methods. Hence, the proposed hybrid methodology involves essentially two steps. In the first step, ARFIMA is used to model the linear component and also to capture the long-range dependence in volatility. The residuals from the fitted linear ARFIMA model will contain the nonlinear relationships. The series of residuals at time t from the linear model, denoted as e_t, can be generated as

$$e_t = \sigma_t - \hat{L}_t, \tag{3.9}$$

where $\hat{L}_t$ is the predicted value at time t from the estimated linear ARFIMA model and σ_t is the actual value of realized volatility at time t.

In the second step, the residual series e_t is modelled independently using the nonlinear autoregressive artificial neural network to discover the nonlinear relationships in volatility. The ANN model for the residuals can be represented as

$$e_t = f\left(e_{t-1}, e_{t-2}, ..., e_{t-n}, w\right) + \epsilon_t, \tag{3.10}$$

where f is a nonlinear function determined by the neural network, w is a vector of parameters and n is a number of input nodes (lags). Denote $\hat{N}_t$ as the forecast of e_t, the combined forecast is:

$$\hat{\sigma_t} = \hat{L}_t + \hat{N}_t. \tag{3.11}$$

To sum up briefly, the proposed hybrid ARFIMA-ANN methodology of realized volatility modeling and forecasting consists of two steps. In the first step, ARFIMA is used to model the linear long memory component of realized volatility. In the second step, the nonlinear autoregressive neural network (NAR) is used to analyze the nonlinear component of realized volatility in the form of the residuals from the ARFIMA model. Finally, the predictions obtained on each step are summed. We propose that it could be advantageous to model linear and nonlinear patterns separately by using different models and then combine the forecasts to improve the overall modeling and forecasting performance. The suggested hybrid method, that exploits the strength of both ARFIMA and ANN approaches and has both linear and nonlinear modeling capabilities, can be a powerful strategy for the practical purposes of realized volatility modeling.

3.2.5 The cyclical model of realized volatility

The cyclical volatility model, developed by Harris, Stoja, and Yilmaz (2011) and modified by Yao et al. (2017) and Cao, Liu, and Zhai (2018), is based on the additive decomposition of volatility into the long-run and the short-run components. Formally, let us assume that realized volatility σ_t (as defined in Equation 3.3) follows a two-component process given by

$$\sigma_t = L_t + S_t, \tag{3.12}$$

where L_t is the long-run trend component and S_t is the short-run cyclical component.

Decomposition of the realized volatility series into the two components is done nonparametrically using the special filtering method. Firstly, the low-pass filter of Hodrick and Prescott (1997) is applied to extract the long-run trend component from the time series. The Hodrick-Prescott filter is well known for its application in macroeconomics. The objective function for the Hodrick-Prescott filter filter has the following form:

$$\min_L \sum_{t=1}^{T} (\sigma_t - L_t)^2 + \lambda \sum_{t=2}^{T-1} \left((L_{t+1} - L_t) - (L_t - L_{t-1})\right)^2, \tag{3.13}$$

where σ_t is a raw time series of realized volatility, L_t is the long-run component, λ is a smoothing parameter and $t = 1, ..., T$. After extracting the long-term component L_t, the short-term cyclical component S_t can be obtained simply by $S_t = \sigma_t - L_t$.

The extracted long-run and short-run components L_t and S_t are then modeled and forecasted separately using different approaches. In the basic version of the cyclical volatility model of Harris, Stoja, and Yilmaz (2011), the long-run component of the volatility is assumed to be following a random walk over the forecast horizon, so that $\hat{L}_t = L_{t-1}$. The short-run component is assumed to follow an AR(1) process, so that $\hat{S}_t = \alpha S_{t-1} + \epsilon_t$, where the parameter α measures the speed of reversion of the cyclical component of volatility to the long-run trend. In the modified version of the cyclical volatility model of Yao et al. (2017) and Cao, Liu, and Zhai (2018), the long-run trend component of the volatility follows the nonlinear autoregressive process as given in Equation 3.7 and is modeled by ANN. The short-run cyclical component is assumed to follow an AR(1) or ARMA processes.

In the present chapter, we also propose a new modification of the cyclical volatility model. We assume that both the long-run and the short-run components follow the nonlinear autoregressive process and use the neural network approach to separately model and forecast both components. Here we are motivated by the question whether the ANN approach is more effective in forecasting the short-term cyclical component of the realized volatility than the simple linear ARMA framework.

The forecast of the time series of realized volatility at time t, denoted as $\hat{\sigma_t}$ is the additive combination of the individual forecasts of the long-run trend component $\hat{L}_t$ and the short-run cyclical component $\hat{S}_t$ at time t. Formally,

$$\hat{\sigma_t} = \hat{L}_t + \hat{S}_t. \tag{3.14}$$

3.3 Data and forecast evaluation

3.3.1 Data

We use the two-component volatility models defined in Section 3.2 to forecast the daily realized volatility of the GBP/USD and the EUR/GBP foreign exchange rates. Our dataset consists of the high frequency tick-by-tick spot exchange rates quotation data for the GBP/USD and the EUR/GBP currency pairs over a sample period from January 4, 2010 to December 30, 2016. Logarithmic middle prices are computed as averages of the logarithmic bid and ask quotes. In order to avoid complicating the inference by the slower trading activity on weekends and holiday periods, we exclude from the data sample all the price quotations from Saturday 00:00:00 GMT to Sunday 23:59:59 GMT and some other inactive days.

The realized volatility estimator is constructed using the foreign exchange rates intraday logarithmic returns sampled at 5 minutes frequency. There is a massive empirical literature claiming that, for the purposes of calculating realized volatility, 5 minutes is an appropriate time scale of returns sampling as it provides an optimal trade off between the precision of the volatility estimator and bias induced by the market microstructure noise (see, e.g., Barndorff-Nielsen and Shephard, 2002, Andersen et al., 2003, etc). The obtained time series of daily realized volatility consists of 1800 observations over the full sample period for each currency pair. The first 1621 observations are used for the initial in-sample estimation of the models, while the remained data of 179 observations is used for out-of-sample evaluation (in other words, approximately 90% of the data is used for in-sample estimation and 10% of the data is used for out-of-sample testing). For the purposes of ANN modeling, the in-sample data is again divided into training sample (75% of the original series) and validation sample (15% of the original series).

Table 3.1 reports descriptive statistics for the time series of realized volatility of the GBP/USD and the EUR/GBP exchange rates for the full sample of 1800 observations. The table shows the mean, standard deviation, minimum, maximum, skewness, kurtosis and the Ljung-Box (Ljung and Box, 1978) portmanteau test Q-statistics for up to 50-lags, 100-lags and 200-lags serial correlation in the realized volatility. The two series of realized volatility are clearly non-normal and highly autocorrelated.

Plots (a) and (b) of Figure 3.1 show the time series of the GBP/USD and the EUR/GBP realized volatility over the full sample period of 1800 observations. Plots (c) and (d) of Figure 3.1 show the correlograms of the the GBP/USD and the EUR/GBP realized volatility for up to 200 lags while plots (e) and (f) present the corresponding periodograms. Notably, the autocorrelation functions decay very slowly and the spectral density functions have a spike at zero frequency indicating the presence of long memory dynamics in the both time series of realized volatility. Table 3.2 reports the values of the long memory parameter estimated by the semiparametric methodology of Geweke and Porter-Hudak (1983). The values of the parameter are between 0 and 0.5 and highly statistically significant, that is another evidence of the long-range dependence in the data. As we can see, the behaviour of the realized volatility of both currency pairs is consistent with the widely documented styled facts of volatility clustering and long memory.

Table 3.1: Descriptive statistics

	GBP/USD	EUR/GBP
Observations	1800	1800
Mean	0.0054	0.0053
Std Dev	0.0030	0.0024
Minimum	0.0007	0.0002
Maximum	0.0690	0.0475
Skewness	10.4635	6.4321
Kurtosis	182.3159	93.5568
$Q(50)$	4840.3164***	5436.4014***
$Q(100)$	7491.3163***	8683.9294***
$Q(200)$	8520.6530***	11947.3126***

The table reports descriptive statistics for the time series of realized volatility of the GBP/USD and the EUR/GBP exchange rates: the mean, standard deviation, minimum, maximum, skewness, kurtosis and the Ljung-Box portmanteau test Q-statistics for up to 50-lags, 100-lags and 200-lags serial correlation. The sample period is from January 4, 2010 to December 30, 2016 (1800 observations). ***, ** and * indicate statistical significance at the 1%, 5% and 10% levels respectively.

Table 3.2: GPH estimate of the long memory parameter

GBP/USD	EUR/GBP
0.358***	0.402***

The table reports the values of the long memory parameter d estimated by the semiparametric methodology of Geweke and Porter-Hudak (1983) for the time series of realized volatility for both GBP/USD and EUR/GBP currency pairs. The number of frequencies used in the GPH regression is chosen to be $N^{0.5}$, where N is the sample size. The sample is 1800 observations for each time series. ***, ** and * indicate statistical significance at the 1%, 5% and 10% levels respectively.

3.3.2 Forecast evaluation

We apply the proposed hybrid ARFIMA-ANN model to generate the iterative one-step-ahead forecasts of the realized volatility over the out-of-sample

Figure 3.1: The time series of realized volatility

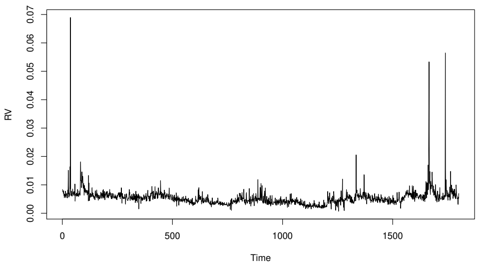

(a) GBP/USD realized volatility

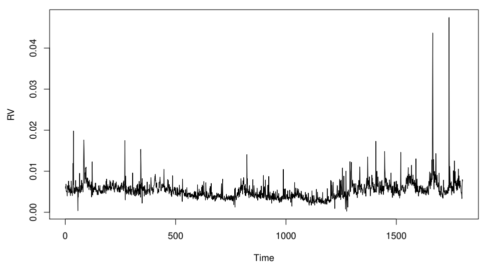

(b) EUR/GBP realized volatility

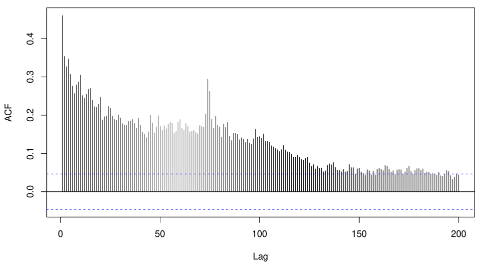

(c) Correlogram of GBP/USD realized volatility

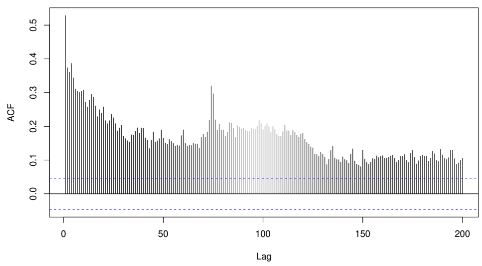

(d) Correlogram of EUR/GBP realized volatility

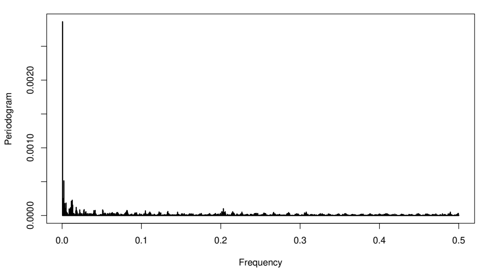

(e) Periodogram of GBP/USD realized volatility

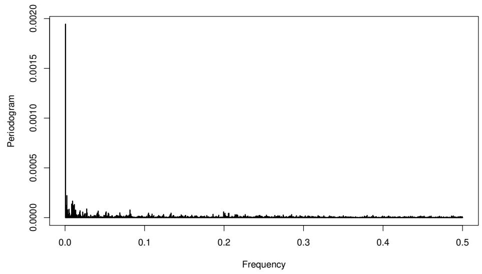

(f) Periodogram of EUR/GBP realized volatility period of 179 observations. As a benchmark, we compare the forecasting accuracy of the hybrid ARFIMA-ANN model with those of the standard random walk model, ARFIMA model and the nonlinear autoregressive neural network applied directly to the series of realized volatility. We also compare the forecasting performance of the proposed hybrid ARFIMA-ANN approach with those of the different versions of the cyclical volatility model which are described in Section 3.2. In total, we estimate 8 models for each of the two considered time series of realized volatility. Table 3.3 shows the complete list of the analyzed volatility models along with the corresponding notations.[2]

Table 3.3: Volatility models

Notation	Description
RW	The random walk model applied directly to the time series of realized volatility.
ARFIMA	ARFIMA model applied directly to the time series of realized volatility.
ANN	Nonlinear autoregressive artificial neural network applied directly to the time series of realized volatility.
ARFIMA-ANN	The proposed hybrid model. The linear component of the realized volatility is modeled using ARFIMA while the nonlinear component is modeled using the nonlinear autoregressive artificial neural network
CV(RW-AR(1))	The cyclical volatility model, version of Harris, Stoja, and Yilmaz (2011). The trend component of the realized volatility is modeled using the random walk model while the cyclical component is modeled using the AR(1) model.
CV(ANN-AR(1))	The cyclical volatility model, version of Yao et al. (2017). The trend component of the realized volatility is modeled using the nonlinear autoregressive artificial neural network while the cyclical component is modeled using the AR(1) model.
CV(ANN-ARMA)	The cyclical volatility model, version of Cao, Liu, and Zhai (2018). The trend component of the realized volatility is modeled using the nonlinear autoregressive artificial neural network while the cyclical component is modeled using the ARMA model.
CV(ANN-ANN)	The proposed modification of the cyclical volatility model. Both the trend and the cyclical components of the realized volatility is modeled separately using the nonlinear autoregressive artificial neural networks.

The table reports the complete list of the volatility models analyzed in this chapter, along with the corresponding notations. Each model is used to forecast realized volatility of the GBP/USD and the EUR/GBP foreign exchange rates. For more detailed description of the considered models, see Section 3.2.

The forecasting accuracy of the analyzed models is evaluated and compared using the following criteria: root mean squared error (RMSE), mean absolute error (MAE) and the coefficient U of Theil (Theil, 1966). A model that minimizes these criteria is considered superior. Formally, the criteria are given by

[2]In order to avoid comparing volatility models which are based on different volatility proxies, in this work we do not use as a benchmark the models of GARCH family.

$$RMSE = \sqrt{\frac{1}{T}\sum_{t=1}^{T}\left(\sigma_t - \hat{\sigma_t}\right)^2} \qquad (3.15)$$

$$MAE = \frac{1}{T}\sum_{t=1}^{T}\left|\sigma_t - \hat{\sigma_t}\right| \qquad (3.16)$$

$$U = \frac{\left(\sum_{t=1}^{T}\left(\sigma_t - \hat{\sigma_t}\right)^2\right)^{\frac{1}{2}}}{\left(\sum_{t=1}^{T}\sigma_t^2\right)^{\frac{1}{2}}}, \qquad (3.17)$$

where σ_t is the actual value of the realized volatility at time t, $\hat{\sigma_t}$ is the forecast of the realized volatility at time t and T is the size of the out-of-sample period.

As stated by Patton (2011), the use of a conditionally unbiased, but imperfect, volatility proxy can lead to distortion in standard methods for comparing volatility forecasts. Patton (2011) considers a loss function as robust if its feasible ranking of two forecasts obtained using an imperfect volatility proxy is the same as the infeasible ranking that would be obtained using the unobservable true conditional volatility. In particular, the class of MSE loss functions is found to be robust for various volatility proxies. In the present work, we use the robust MSE loss function in the form of RMSE.

Moreover, we also use the Mincer-Zarnowitz regression (Mincer and Zarnowitz, 1969) to measure the efficiency and unbiasedness of a model's forecast. Formally, the Mincer-Zarnowitz regression is given by

$$\sigma_t = \beta_0 + \beta_1\hat{\sigma_t} + u_t, \qquad (3.18)$$

where σ_t is the actual value of the realized volatility at time t, $\hat{\sigma_t}$ is the forecast of the realized volatility at time t, β_0 and β_1 are the parameters of the regression and u_t is the error term.

In other words, the Mincer-Zarnowitz regression is the simple OLS regression of the actual value of the realized volatility on the corresponding forecast. The null hypothesis of the forecast's unbiasedness and efficiency can be tested by the joint test that $\beta_0 = 0$ and $\beta_1 = 1$. Rejection of the null hypothesis indicates that the forecast is biased and inefficient. The Wald test is used to test the null hypothesis. Furthermore, the coefficient of determination R^2 of the Mincer-Zarnowitz regression is a measure of the information content of a model's forecast. Thus, the R^2-coefficient can be used to evaluate and compare the explanatory power of the considered volatility models. A model that maximizes the R^2 of the Mincer-Zarnowitz regression is considered superior.

3.4 Empirical results

In this section, we describe the process of practical implementation of the considered models to forecast the realized volatility of the GBP/USD and the EUR/GBP exchange rates and analyze the obtained results.

We begin with the proposed hybrid ARFIMA-ANN model. Firstly, we estimate an ARFIMA(p, d, q) model to forecast the linear component of the realized volatility. Akaike Information Criterion (AIC) is used to select the best in-sample ARFIMA specification across various possible specifications with $p = 0, 1, 2, 3$ and $q = 0, 1, 2, 3$.[3] The model which gives the lowest value of the AIC is selected as the best model. Table 3.4 reports the values of the AIC of the various estimated ARFIMA specifications. For the GBP/USD and the EUR/GBP realized volatility, the best models are found to be the ARFIMA($2, d, 3$) and the ARFIMA($3, d, 3$) respectively.

Table 3.4: AIC values of the estimated ARFIMA(p, d, q) specifications

ARFIMA	AIC (GBP/USD)	AIC (EUR/GBP)
$(0, d, 0)$	-15491.88	-16616.18
$(1, d, 0)$	-15521.19	-16617.43
$(1, d, 1)$	-15527.43	-16628.88
$(2, d, 1)$	-15530.53	-16628.03
$(2, d, 2)$	-15530.61	-16630.25
$(1, d, 2)$	-15529.02	-16627.68
$(0, d, 2)$	-15524.43	-16624.73
$(0, d, 1)$	-15524.66	-16618.21
$(2, d, 0)$	-15520.44	-16619.48
$(3, d, 2)$	-15538.01	-16635.62
$(3, d, 3)$	-15536.87	-16638.53*
$(2, d, 3)$	-15538.82*	-16634.14
$(3, d, 1)$	-15530.85	-16636.65
$(1, d, 3)$	-15530.95	-16633.91
$(3, d, 0)$	-15527.38	-16638.08
$(0, d, 3)$	-15532.85	-16634.43

The table reports the values of the Akaike Information Criterion (AIC) of the various estimated specifications of an ARFIMA(p, d, q) model with $p = 0, 1, 2, 3$ and $q = 0, 1, 2, 3$. The sample is 1621 observations for the both time series of the GBP/USD and the EUR/GBP realized volatility. * indicates the best fitting specification.

Table 3.5 shows the results of the in-sample estimation of the ARFIMA($2, d, 3$) and the ARFIMA($3, d, 3$) models applied to the time series of the GBP/USD and the EUR/GBP realized volatility respectively. All the estimated coefficients are highly significant. Note that the estimated values of the fractional differencing parameter d lie within a range from 0 to 0.5, indicating the long

[3] Although not reported here, the best in-sample specification is assessed up to $p = 4$ and $q = 4$.

memory dynamics of the time series. The estimated models are then used to obtain the series of out-of-sample predictions.

Table 3.5: ARFIMA estimation results

Parameter	ARFIMA$(2, d, 3)$ GBP/USD	ARFIMA$(3, d, 3)$ EUR/GBP
$\hat{\phi}_1$	0.5794***	0.9127***
	(0.0192)	(0.1012)
$\hat{\phi}_2$	-0.9736***	-1.1611***
	(0.0194)	(0.0699)
$\hat{\phi}_3$	-	0.3417***
		(0.0959)
$\hat{d}$	0.4070***	0.4720***
	(0.0337)	(0.0317)
$\hat{\theta}_1$	-0.8347***	-1.0937***
	(0.0474)	(0.1019)
$\hat{\theta}_2$	1.1002***	1.2351***
	(0.0357)	(0.0790)
$\hat{\theta}_3$	-0.2580***	-0.5178***
	(0.0441)	(0.0957)
$Cons$	0.0055***	0.0054***
	(0.0010)	(0.0019)

The table reports the values of the estimated coefficients with the corresponding standard errors (in brackets) of the ARFIMA$(2, d, 3)$ and the ARFIMA$(3, d, 3)$ models applied to the time series of the GBP/USD and the EUR/GBP realized volatility respectively. The sample is 1621 observations. ***, ** and * indicate statistical significance at the 1%, 5% and 10% levels respectively.

To explore the presence of nonlinear relationships in the realized volatility, we extract and analyze the residuals from the estimated linear ARFIMA models. Table 3.6 shows the results of the Brock, Dechert and Scheinkman (BDS) test for independence (Brock et al., 1996) applied to the series of the in-sample and out-of-sample residuals. The BDS test is a nonparametric method for testing for serial dependence and nonlinear structure in a time series.[4] The test can be considered as a nonlinear analog of the Ljung-Box (Ljung and Box, 1978) portmanteau test. The null hypothesis of the test is that a time series process is independent and identically distributed. As we can see from Table 3.6, the null hypothesis of the residuals being independent and identically distributed is overwhelmingly rejected. This indicates the presence of certain nonlinear dependencies in the series of residuals. Apparently, the dynamics of the realized volatility is driven by some nonlinear patterns which are not captured by the estimated ARFIMA models. Our finding is consistent with the empirical evidence in the previous literature that ARFIMA model is not able to capture nonlinear relationships in volatility dynamics (see., e.g., Dıaz, Grau-Carles, and Mangas, 2002).

[4]The description of the BDS test is provided in Section 3.6.1 (Appendix).

Table 3.6: BDS test results on the residuals from the estimated ARFIMA models

	ARFIMA$(2, d, 3)$ GBP/USD	ARFIMA$(3, d, 3)$ EUR/GBP
$m = 2$	10.4684***	9.9212***
$m = 3$	11.2007***	10.8257***
$m = 4$	11.6436***	10.8999***
$m = 5$	12.1008***	11.3050***

The table reports the test statistics of the Brock, Dechert and Scheinkman (BDS) test for independence on the series of the in-sample and out-of-sample residuals from the ARFIMA$(2, d, 3)$ and the ARFIMA$(3, d, 3)$ models applied to the GBP/USD and the EUR/GBP realized volatility respectively. The sample is 1800 observations (1621 of the in-sample residuals and 179 of the out-of-sample residuals). m is the correlation dimension or the number of lags upon which the dependence is tested. ***, ** and * indicate statistical significance at the 1%, 5% and 10% levels respectively.

As a next step, to model and forecast the explored nonlinear component in the dynamics of the realized volatility, we use the nonlinear autoregressive artificial neural network framework. Following the structure of the ARFIMA-ANN approach, the residuals from the estimated linear models are analyzed through the ANN. The in-sample residuals are used to train the neural network while the out-of-sample residuals are used to evaluate the network. In order to find the best neural network architecture, we experimented with different networks having $p = 1, 2, 3, ..., 10$ input nodes (lagged observations) and $q = 5, 10, 15, 20, 25$ hidden nodes. Each network was trained 100 times and used to create the out-of-sample forecasts. The optimal model is considered to be the model with the best out-of-sample performance. For the GBP/USD, the best neural network model was found to be the model with $q = 10$ hidden nodes and $p = 1$ input node. For the EUR/GBP, the best neural network model includes $q = 15$ hidden nodes and $p = 1$ input node.

Next we apply the different versions of the cyclical volatility model to forecast the realized volatility of the GBP/USD and the EUR/GBP exchange rates. The Hodrick–Prescott filter is used to decompose the raw series of the realized volatility into the long-run trend and the short-run cyclical components. Following Baxter and King (1999), Harris, Stoja, and Yilmaz (2011), Yao et al. (2017), the value of the smoothing parameter is set to the value of 100 multiplied by the squared frequency of the data, which for daily data (assuming 255 trading days per year) is 6,502,500.[5] Plots (a) and (b) of Figure 3.2 show the estimated long-run trend components of the realized volatility of the GBP/USD and the EUR/GBP respectively, plots (c) and (d) show the corresponding short-run cyclical components.

[5]However, as stated by Harris, Stoja, and Yilmaz (2011), moderate changes in the smoothing parameter value appear to have relatively little impact on forecast performance.

Figure 3.2: Realized volatility decomposition using the Hodrick–Prescott filter

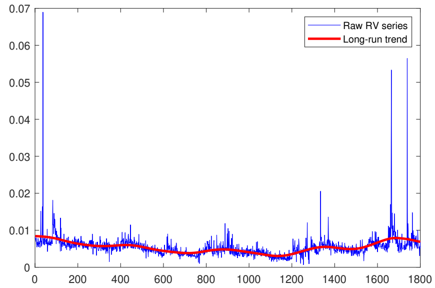

(a) GBP/USD Long-run trend component

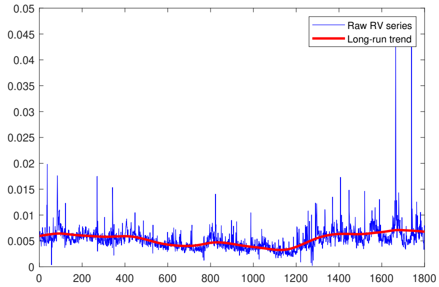

(b) EUR/GBP Long-run trend component

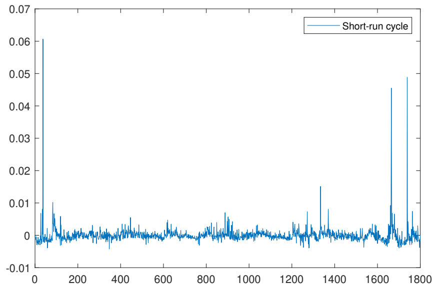

(c) GBP/USD Short-run cyclical component

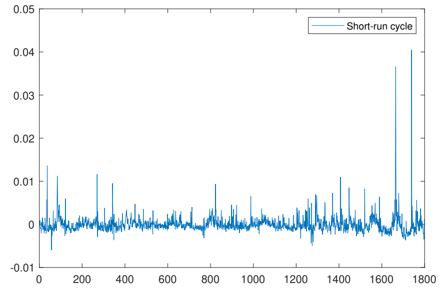

(d) EUR/GBP Short-run cyclical component

Following the idea of the cyclical volatility model, the extracted long-run and short-run components of the realized volatility are modeled and forecasted separately. For the both components, 1621 observations are used for the initial in-sample estimation of the models and 179 observations are used for out-of-sample evaluation. Selection of the best neural networks architectures is done following the procedure described above. In ARMA modeling, the optimal model specification is defined according to the AIC. For the sake of comparison, we also run the simple random walk model and the neural network model applied directly to the series of realized volatility. For the both series of the GBP/USD and the EUR/GBP realized volatility, Table 3.7 reports a complete list of the used forecasting models and describes the configuration and specification of each model.

Table 3.7: Configuration and specification of the applied forecasting models

Model	GBP/USD	EUR/GBP
RW	The simple random walk model: $\hat{RV}_t = RV_{t-1}$	The simple random walk model: $\hat{RV}_t = RV_{t-1}$
ARFIMA	ARFIMA$(2, d, 3)$	ARFIMA$(3, d, 3)$
ANN	ANN$(q = 10, p = 1)$	ANN$(q = 15, p = 2)$
ARFIMA-ANN	ARFIMA$(2, d, 3)$ for the linear component, ANN$(q = 10, p = 1)$ for the nonlinear component	ARFIMA$(3, d, 3)$ for the linear component, ANN$(q = 15, p = 1)$ for the nonlinear component
CV(RW-AR(1))	The random walk for the long-run component, AR(1) for the short-run component	The random walk for the long-run component, AR(1) for the short-run component
CV(ANN-AR(1))	ANN$(q = 15, p = 4)$ for the long-run component, AR(1) for the short-run component	ANN$(q = 5, p = 10)$ for the long-run component, AR(1) for the short-run component
CV(ANN-ARMA)	ANN$(q = 15, p = 4)$ for the long-run component, ARMA$(1, 1)$ for the short-run component	ANN$(q = 5, p = 10)$ for the long-run component, ARMA$(2, 1)$ for the short-run component
CV(ANN-ANN)	ANN$(q = 15, p = 4)$ for the long-run component, ANN$(q = 15, p = 1)$ for the short-run component	ANN$(q = 5, p = 10)$ for the long-run component, ANN$(q = 20, p = 1)$ for the short-run component

The table describes the configuration and specification of each model used in this chapter to forecast the realized volatility of the GBP/USD and the EUR/GBP exchange rates.

For each model, Figures 3.3 and 3.4 show the plots of the actual values of the realized volatility against the predictions over the out-of-sample period. Tables 3.8 and 3.9 report the corresponding values of the forecast accuracy measures for the out-of-sample predictions. As we can see for the both GBP/USD and EUR/GBP realized volatility, the proposed ARFIMA-ANN and CV(ANN-ANN) models have similar forecasting accuracy according to the RMSE and the U-coefficient and outperform all other competing models. In terms of the MAE, the ARFIMA-ANN model shows the best performance. However, the ANN model applied directly to the series of realized volatility also demonstrates the relatively good accuracy, only slightly inferior to the hybrid ARFIMA-ANN approach. The naive random walk model has the worst forecasting accuracy in terms of the RMSE, MAE and the U-coefficient.

Tables 3.10 and 3.11 report the results of the Mincer-Zarnowitz regression for the out-of-sample forecasts of the realized volatility of the GBP/USD and the EUR/GBP respectively. The tables report the estimated intercept β_0, slope β_1, R^2-coefficient and the F-statistic to test the null hypothesis of unbiasedness and efficiency of the forecasts. As we can see for the both currency pairs, the null hypothesis is rejected at the 1% level for the random walk model and at the 5% level for the ANN model. For the GBP/USD realized volatility, the null hypothesis of unbiasedness and efficiency is also rejected at the 1% level for the CV(RW-AR(1)) and CV(ANN-AR(1)) models. According to the R^2 and for both GBP/USD and EUR/GBP realized volatility predictions, the ARFIMA-ANN and CV(ANN-ANN) models have the highest explanatory power and are followed by the ANN model. Surprisingly, the ARFIMA model has the lowest explanatory power in terms of the Mincer-Zarnowitz R^2.

As we can see, the realized volatility forecast produced by the hybrid ARFIMA-ANN approach is more accurate than the individual forecasts by either ARFIMA or ANN models. This result is consistent for the both GBP/USD and EUR/GBP realized volatility and for all applied forecasting accuracy measures, including the R^2 from the Mincer-Zarnowitz regression. As shown in Figures 3.3 and 3.4, although at some data points the hybrid approach provides worse predictions than either ARFIMA or ANN forecasts, its overall forecasting performance has improved. On the other hand, the relatively good accuracy of the ANN model applied directly to the raw series of the realized volatility is also a notable fact. It indicates that the realized volatility can be quite well approximated by a nonlinear autoregression with just a small number of lags.

Interestingly, even the simple two-component model (such as, for example, CV(RW-AR(1)) approach) has very similar predictive accuracy with the ARFIMA, that is much more complicated model in terms of its estimation. It seems that a naive random walk model is a good approximation for the trend component of the realized volatility in short forecasting horizons (here our findings are in line with those of Harris, Stoja, and Yilmaz, 2011). As we can see, even using the neural network instead of the random walk approach to model the long-run trend component, almost has not improved the accuracy of the cyclical volatility model. However, introducing the ANN to model the short-run component has allowed to improve the performance of the cyclical volatility model greatly.

Table 3.8: GBP/USD Out-of-sample forecasting accuracy

Model	RMSE	MAE	U
RW	0.0063270	0.0025284	0.6467
ARFIMA	0.0056350	0.0021310	0.5759
ANN	0.0048992	0.0019295	0.5007
ARFIMA-ANN	0.0046889	0.0018338	0.4792
CV(RW-AR(1))	0.0056180	0.0023167	0.5741
CV(ANN-AR(1))	0.0056174	0.0023158	0.5741
CV(ANN-ARMA)	0.0055916	0.0021833	0.5715
CV(ANN-ANN)	0.0046760	0.0020109	0.4779

The table reports the root mean squared error (RMSE), mean absolute error (MAE) and the coefficient U of Theil for the out-of-sample forecasts of the GBP/USD realized volatility for each model. The forecast is one-step-ahead, the out-of-sample period includes 179 observations.

Table 3.9: EUR/GBP Out-of-sample forecasting accuracy

Model	RMSE	MAE	U
RW	0.0052822	0.0021772	0.6138
ARFIMA	0.0045189	0.0017959	0.5251
ANN	0.0041494	0.0016899	0.4821
ARFIMA-ANN	0.0039256	0.0016243	0.4562
CV(RW-AR(1))	0.0044727	0.0019184	0.5197
CV(ANN-AR(1))	0.0044725	0.0019186	0.5197
CV(ANN-ARMA)	0.0044779	0.0018094	0.5203
CV(ANN-ANN)	0.0039424	0.0017900	0.4581

The table reports the root mean squared error (RMSE), mean absolute error (MAE) and the coefficient U of Theil for the out-of-sample forecasts of the EUR/GBP realized volatility for each model. The forecast is one-step-ahead, the out-of-sample period includes 179 observations.

Table 3.10: GBP/USD Mincer-Zarnowitz regression results

Model	β_0	β_1	R^2	F-stat
RW	0.0043	0.4437	0.1969	34.1109***
	(0.0007)	(0.0673)		
ARFIMA	0.0012	0.8812	0.1229	0.5484
	(0.0014)	(0.1769)		
ANN	0.0015	0.9144	0.3618	4.0080**
	(0.0007)	(0.0913)		
ARFIMA-ANN	0.0012	0.8881	0.3982	1.3618
	(0.0007)	(0.0821)		
CV(RW-AR(1))	-0.0127	2.7034	0.2050	9.1447***
	(0.0031)	(0.4002)		
CV(ANN-AR(1))	-0.0127	2.7014	0.2051	9.1498***
	(0.0030)	(0.3997)		
CV(ANN-ARMA)	-0.0032	1.4378	0.1448	1.4270
	(0.0020)	(0.2626)		
CV(ANN-ANN)	0.0005	0.9277	0.3947	0.3522
	(0.0008)	(0.0863)		

The table reports the estimated intercept β_0, slope β_1 and R^2-coefficient of the Mincer-Zarnowitz regression for the out-of-sample forecasts of the GBP/USD realized volatility for each model. The standard errors for the estimated parameters are in parentheses. The table also reports the F-statistic for the null hypothesis that the intercept is equal to zero and the slope is equal to one. The forecast is one-step-ahead, the out-of-sample period includes 179 observations. ***, ** and * indicate statistical significance at the 1%, 5% and 10% levels respectively.

Table 3.11: EUR/GBP Mincer-Zarnowitz regression results

Model	β_0	β_1	R^2	F-stat
RW	0.0041	0.4234	0.1794	35.8728***
	(0.0006)	(0.0681)		
ARFIMA	0.0009	0.8923	0.1594	0.3621
	(0.0011)	(0.1540)		
ANN	0.0018	0.7978	0.3175	3.7759**
	(0.0007)	(0.0879)		
ARFIMA-ANN	0.0011	0.8470	0.3753	1.7351
	(0.0006)	(0.0821)		
CV(RW-AR(1))	-0.0019	1.2759	0.1818	0.9398
	(0.0015)	(0.2034)		
CV(ANN-AR(1))	-0.0019	1.2760	0.1819	0.9404
	(0.0015)	(0.2034)		
CV(ANN-ARMA)	-0.0007	1.1075	0.1730	0.1846
	(0.0013)	(0.1820)		
CV(ANN-ANN)	0.0009	0.8708	0.3657	1.1381
	(0.0007)	(0.0862)		

The table reports the estimated intercept β_0, slope β_1 and R^2-coefficient of the Mincer-Zarnowitz regression for the out-of-sample forecasts of the EUR/GBP realized volatility for each model. The standard errors for the estimated parameters are in parentheses. The table also reports the F-statistic for the null hypothesis that the intercept is equal to zero and the slope is equal to one. The forecast is one-step-ahead, the out-of-sample period includes 179 observations. ***, ** and * indicate statistical significance at the 1%, 5% and 10% levels respectively.

Figure 3.3: GBP/USD Out-of-sample forecast of the realized volatility

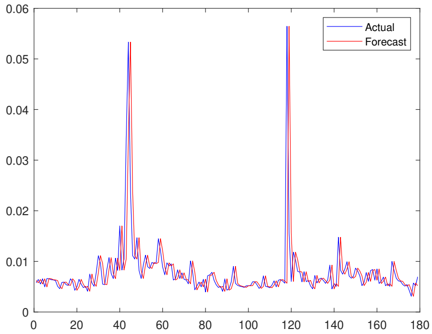

(a) RW

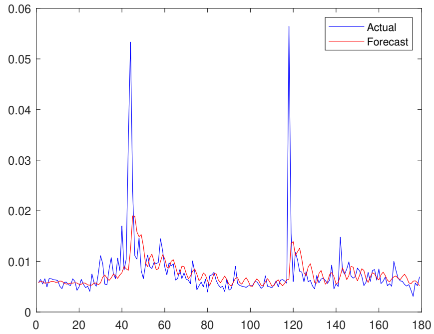

(b) ARFIMA

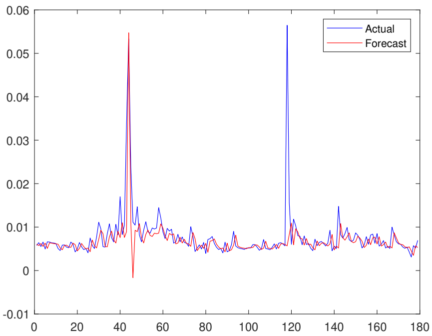

(c) ANN

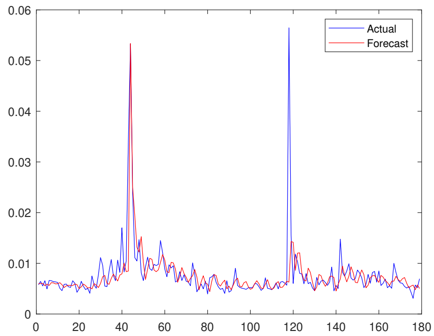

(d) ARFIMA-ANN

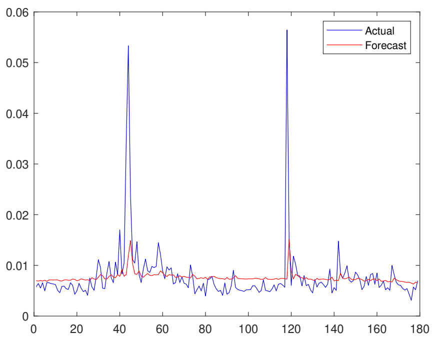

(e) CV(RW-AR(1))

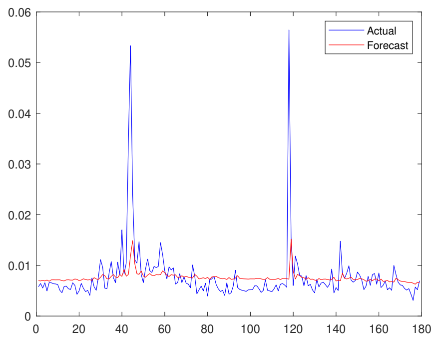

(f) CV(ANN-AR(1))

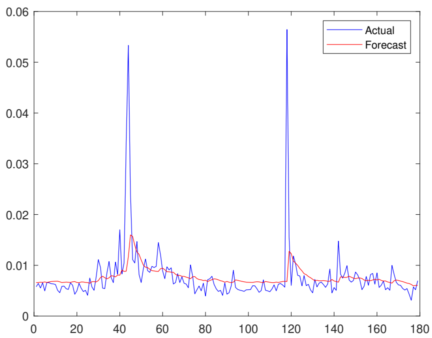

(g) CV(ANN-ARMA)

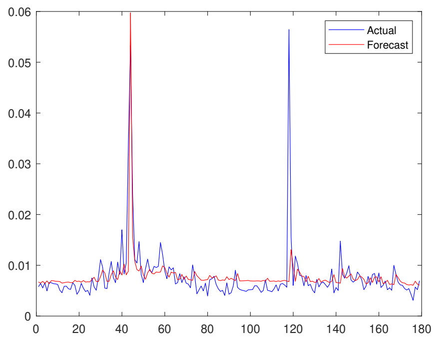

(h) CV(ANN-ANN)

Figure 3.4: EUR/GBP Out-of-sample forecast of the realized volatility

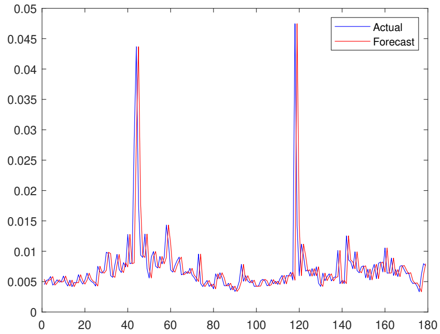

(a) RW

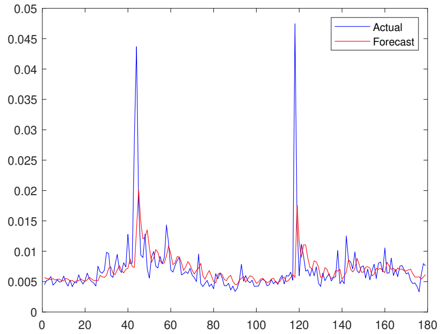

(b) ARFIMA

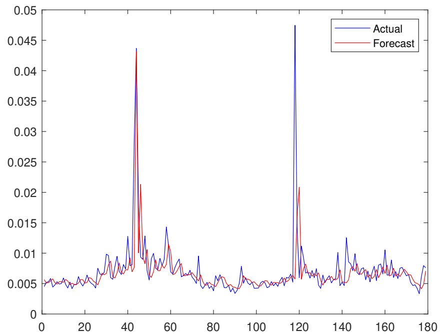

(c) ANN

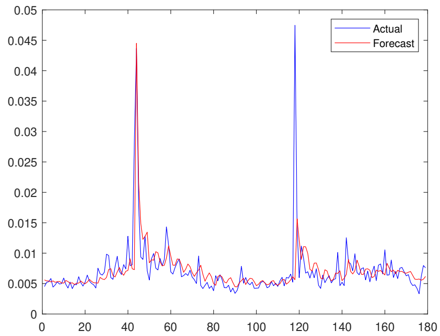

(d) ARFIMA-ANN

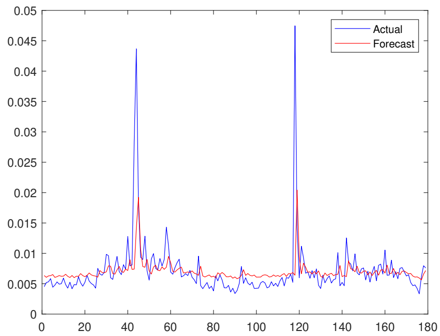

(e) CV(RW-AR(1))

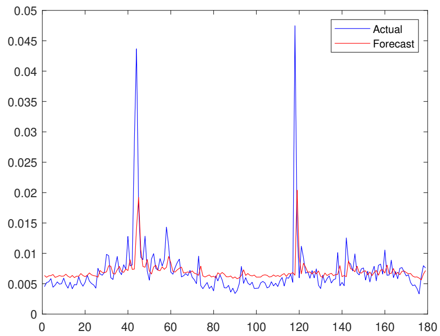

(f) CV(ANN-AR(1))

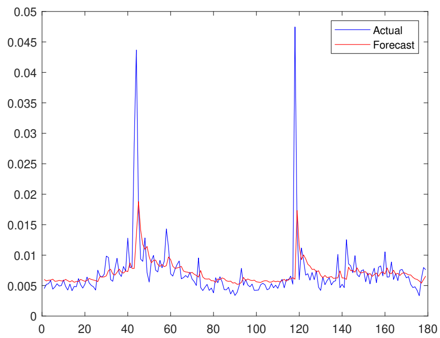

(g) CV(ANN-ARMA)

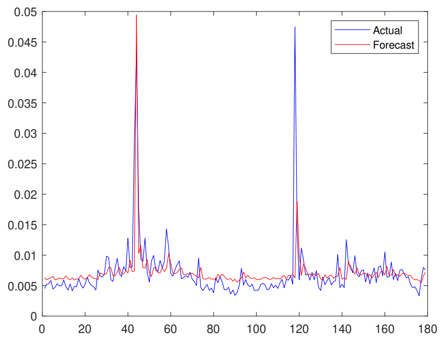

(h) CV(ANN-ANN)

3.5 Conclusion

A process of financial volatility has a complex structure which comprises various heterogeneous components. In this chapter, we introduced a new two-component realized volatility model which exploits the power of both econometrics and machine learning in linear and nonlinear time series modeling respectively. Our proposed hybrid methodology consists of two steps. In the first step, ARFIMA is used to model the linear long memory component of realized volatility. In the second step, the nonlinear autoregressive neural network (NAR) is used to analyze the nonlinear component of realized volatility in the form of the residuals from the ARFIMA model. The combined model is intended to capture both the widely documented phenomena of long memory and nonlinearity in the dynamics of realized volatility. We also proposed a modification of the cyclical volatility model which is based on decomposition of volatility into its trend and cycle components using the low-pass filter. In the suggested modification, nonlinear artificial neural networks are used to model and forecast both trend and cyclical components of realized volatility. The proposed models provide an improvement in out-of-sample forecast performance over the competing approaches, in terms of both accuracy and informational content.

Apparently, the structure of many time series processes arising in economics or finance might be too complex to be successfully described by just a single econometric model. On the example of realized volatility in this chapter, we show that, in terms of forecasting accuracy, it can be beneficial to decompose a time series into separate factors which are then modeled and predicted individually. The extracted components might contain simpler patterns than the initial raw time series and can be easier captured by appropriate models. Moreover, the multi-component approach is more flexible and robust to potential misspecification of one of the component models.

Despite the sort of a dichotomy of econometrics and machine learning existing in academia, our work emphasizes the advantages of methodological combination of econometric and machine learning techniques for predictive modeling of financial time series. The realized volatility forecast produced by the hybrid ARFIMA-ANN model in our chapter is more accurate than the individual forecasts by either ARFIMA or ANN models. Introducing neural networks to the cyclical volatility model also leads to improvements in predicting accuracy.

The work presented in this chapter can be extended in many ways. For example, an interesting natural line of further investigations would be to consider decomposition of realized volatility time series into many components, more than just two. Also, an important direction for future research would be to develop the multivariate versions of the models proposed in this chapter.

3.6 Appendix

3.6.1 BDS test for nonlinearity

The BDS test is developed by Brock et al. (1996) and is widely used for detecting non-random chaotic dynamics or nonlinear dependencies in a time series. The main concept of the BDS test is the correlation integral, which is a measure of the frequency with which temporal patterns are repeated in the data. Consider a time series x_t for $t = 1, 2, .., T$ and define its m-history as $x_t^m = (x_t, x_{t-1}, ..., x_{t-m+1})$. The correlation integral at embedding dimension m can be estimated by:

$$C_{m,\epsilon} = \frac{2}{T_m(T_m - 1)} \sum\sum_{m \leq s < t \leq T} I(x_t^m, x_s^m; \epsilon), \tag{3.19}$$

where $T_m = T - m + 1$ and $I(x_t^m, x_s^m; \epsilon)$ is an indicator function which is equal to one if $|x_{t-i} - x_{s-i}| < \epsilon$ for $i = 0, 1, ..., m - 1$ and zero otherwise. Intuitively the correlation integral estimates the probability that any two m-dimensional points are within a distance of ϵ of each other. If x_t are iid, this probability should be equal to $C_{1,\epsilon}^m = Pr(|x_t - x_s| < \epsilon)^m$ in the limiting case. Brock et al. (1996) define the BDS test statistic as follows:

$$V_{m,\epsilon} = \sqrt{T}\frac{C_{m,\epsilon} - C_{1,\epsilon}^m}{s_{m,\epsilon}}, \tag{3.20}$$

where $s_{m,\epsilon}$ is the standard deviation of $\sqrt{T}(C_{m,\epsilon} - C_{1,\epsilon}^m)$ and can be estimated consistently. Under moderate regularity conditions, the BDS test statistic converges in distribution to $N(0, 1)$. The null hypothesis is that a time series is independent and identically distributed.

Conclusion

Volatility is an essential concept in economic research and financial risk management. In this thesis, we have investigated several aspects of volatility in financial markets. We have focused on the phenomena of long memory and asymmetry in volatility. We have also considered the striking component structure of financial volatility and explored how it can be used for volatility forecasting purposes.

In Chapter 1, we investigated the long-range dependence in volatility of the foreign exchange rates returns in the context of temporal aggregation. Firstly, we generalized the up-to-date theoretical knowledge about the effect of temporal aggregation on the long memory ARFIMA processes in the time and frequency domains. The theoretical results imply the invariance of the long memory parameter to temporal aggregation. Secondly, to validate the theoretical implications about temporal aggregation in long memory processes for the particular ARFIMA estimation method, we conducted a Monte Carlo simulation and provided a regression analysis of the experiment results. The experiment results are consistent with the implications of the theory and show that the semiparametric GPH approach provides consistent estimates of the long memory parameter at different aggregation levels. Finally, we analyzed empirically the volatility of the GBP/USD exchange rate returns at various intraday and daily frequencies. After controlling for intraday periodicity, we implemented several semiparametric methods to explore the long memory in volatility of the temporally aggregated returns measured by absolute returns, squared returns and realized volatility. After implementing the Z-test with the multiple hypothesis size adjustments, we found a strong evidence that the realized volatility of the exchange rate returns is characterized by the same fractional differencing parameter across the observed time scales. Our results indicate that long memory is an intrinsic property of financial volatility.

In Chapter 2, we explored the link between the phenomenon of volatility asymmetry and the asymmetry of investor attention to good and bad news. We utilized a novel measure of investor attention - the Search Volume Index (SVI) provided by the Google Trends service. Firstly, we studied the relationship between return, investor attention and volatility in the SVAR framework. We identified statistical causality from return to both volatility and investor attention and bidirectional causality between attention and volatility. Using the impulse response analysis, we found that the effect of return on realized volatility is generally persistent and long lasting while the effects of return on investor attention and of investor attention on volatility are only temporary. Secondly, using the ARDL framework, we found that both volatility and investor attention have stronger reaction to negative returns than to positive ones. We illustrated the asymmetric effect with the news impact curves. Finally, we provided a new evidence of a positive relationship between volatility and investor attention. Hence, in the established theoretical framework, asymmetrically higher attention caused by negative returns can lead to asymmetrically higher volatility. We also demonstrated that the magnitude of the impact of investor attention on volatility is stronger during periods of negative returns. This fact can exaggerate the asymmetry even further.

In Chapter 3, we introduced a new realized volatility forecasting model which is based on the component structure of financial volatility. The proposed hybrid ARFIMA-ANN model exploits the power of both econometrics and machine learning in linear and nonlinear time series modeling respectively. The hybrid methodology consists of two steps: firstly, ARFIMA framework is used to model the linear long memory component of realized volatility; secondly, the nonlinear autoregressive neural network is used to analyze the nonlinear component of realized volatility in the form of the residuals from the ARFIMA model. We also proposed a new modification of the cyclical volatility model, where nonlinear artificial neural networks are used to model and forecast both trend and cyclical components of realized volatility. We found that the proposed models provide an improvement in out-of-sample forecast performance over the competing approaches. Overall, we found evidence that decomposing a time series into separately modeled factors can be beneficial for forecasting purposes.

The research presented in this thesis can be extended in different ways. In general, we think that implementation of artificial intelligence techniques for modeling financial and economic processes is a very promising research area. It seems surprising that machine learning methods, which have been essentially transformative for many other areas of systemic modeling, have contributed so little in the field of finance or economics. At the same time, artificial intelligence provides powerful tools for simulation exercises or predictive modeling which can be extremely effective in solving tasks practically unsolvable by standard econometric methods.

Artificial intelligence methods can be useful for behavioral research in financial markets. The behavioral foundations of the striking features of financial volatility dynamics, such as long memory and asymmetry, are of particular interest. This research direction is a difficult challenge for the rapidly growing area of behavioral finance but, at the same time, it provides an important step towards a deeper understanding of the functioning of financial markets. Specifically, the artificial intelligence framework of agent-based modeling (ABM) can be used to simulate the complex architecture of modern financial markets to see how business activities of various traders affect asset prices and volatility dynamics.

We claim that long memory and nonlinearity are important properties and should always be incorporated in volatility modeling. Aside from this, the structure of volatility is highly complicated for a number of reasons, particularly, with respect to asymmetry. The complex volatility structure calls for advanced state-of-the-art modeling strategies which exploit the rapidly growing power of machine learning methods. Specifically, it would be interesting to use the promising technology of the Long Short-Term Memory (LSTM) neural networks to model the long-range nonlinear dependence in financial volatility. Also, our proposed hybrid econometrics-machine learning approach can be enhanced by implementing the investor attention variable as an external regressor to see if it helps to improve the predicting power of the model.

On these directions we intend to focus our attention in future research.

Bibliography

Adrian, Tobias and Joshua V Rosenberg (2008). "Stock returns and volatility: Pricing the short-run and long-run components of market risk". In: *The Journal of Finance* 63.6, pp. 2997–3030.

Aloy, Marcel, Mohamed Boutahar, Karine Gente, and Anne Péguin-Feissolle (2011). "Purchasing power parity and the long memory properties of real exchange rates: Does one size fit all?" In: *Economic Modelling* 28.3, pp. 1279–1290.

Andersen, Torben G and Tim Bollerslev (1997a). "Heterogeneous Information Arrivals and Return Volatility Dynamics: Uncovering the Long-Run in High Frequency Returns". In: *The Journal of Finance* 52.3, pp. 975–1005.

— (1997b). "Intraday periodicity and volatility persistence in financial markets". In: *Journal of Empirical finance* 4.2-3, pp. 115–158.

Andersen, Torben G, Tim Bollerslev, Francis X Diebold, and Paul Labys (2001). "The distribution of realized exchange rate volatility". In: *Journal of the American Statistical Association* 96.453, pp. 42–55.

— (2003). "Modeling and forecasting realized volatility". In: *Econometrica* 71.2, pp. 579–625.

Andrei, Daniel and Michael Hasler (2014). "Investor attention and stock market volatility". In: *The Review of Financial Studies* 28.1, pp. 33–72.

Antweiler, Werner and Murray Z Frank (2004). "Is all that talk just noise? The information content of internet stock message boards". In: *The Journal of Finance* 59.3, pp. 1259–1294.

Arteche, Josu (2004). "Gaussian semiparametric estimation in long memory in stochastic volatility and signal plus noise models". In: *Journal of Econometrics* 119.1, pp. 131–154.

Avramov, Doron, Tarun Chordia, and Amit Goyal (2006). "The impact of trades on daily volatility". In: *The Review of Financial Studies* 19.4, pp. 1241–1277.

Aydemir, A Cevdet, Michael Gallmeyer, and Burton Hollifield (2007). “Financial leverage and the leverage effect: a market and firm analysis”. In: *Tepper School of Business* 3.1, pp. 1–44.

Bae, Jinho, Chang-Jin Kim, and Charles R Nelson (2007). “Why are stock returns and volatility negatively correlated?” In: *Journal of Empirical Finance* 14.1, pp. 41–58.

Baillie, Richard, Fabio Calonaci, Dooyeon Cho, and Seunghwa Rho (2018). *How Important is Modeling Long Memory in Realized Volatility?* Tech. rep. Working paper.

Baillie, Richard, Aydin A Cecen, and Young Wook Han (2015). “High frequency Deutsche mark-US dollar returns: FIGARCH representations and non linearities”. In: *Multinational Finance Journal* 4.3, pp. 247–267.

Baillie, Richard, Theo Nijman, and Rolf Tschernig (1994). *Temporal aggregation of fractionally integrated ARMA models.*

Bansal, Ravi and Amir Yaron (2004). “Risks for the long run: A potential resolution of asset pricing puzzles”. In: *The Fournal of Finance* 59.4, pp. 1481–1509.

Barber, Brad M and Terrance Odean (2001). “The internet and the investor”. In: *Journal of Economic Perspectives* 15.1, pp. 41–54.

— (2007). “All that glitters: The effect of attention and news on the buying behavior of individual and institutional investors”. In: *The Review of Financial Studies* 21.2, pp. 785–818.

Barndorff-Nielsen, Ole E and Neil Shephard (2002). “Econometric analysis of realized volatility and its use in estimating stochastic volatility models”. In: *Journal of the Royal Statistical Society: Series B (Statistical Methodology)* 64.2, pp. 253–280.

Barunık, Jozef and Tomáš Křehlık (2016). “Combining high frequency data with non-linear models for forecasting energy market volatility”. In: *Expert Systems with Applications* 55, pp. 222–242.

Baumeister, Roy F, Ellen Bratslavsky, Catrin Finkenauer, and Kathleen D Vohs (2001). “Bad is stronger than good”. In: *Review of General Psychology* 5.4, pp. 323–370.

Baur, Dirk G (2012). “Asymmetric volatility in the gold market”. In: *The Journal of Alternative Investments* 14.4, pp. 26–38.

Baur, Dirk G and Thomas Dimpfl (2016). “Googling gold and mining bad news”. In: *Resources Policy* 50, pp. 306–311.

— (2018). “Think again: volatility asymmetry and volatility persistence”. In: *Studies in Nonlinear Dynamics & Econometrics* 23.1, pp. 1–19.

Baxter, Marianne and Robert G King (1999). “Measuring business cycles: approximate band-pass filters for economic time series”. In: *Review of Economics and Statistics* 81.4, pp. 575–593.

Bekaert, Geert and Guojun Wu (2000). "Asymmetric volatility and risk in equity markets". In: *The Review of Financial Studies* 13.1, pp. 1–42.

Bhar, R (1994). "Testing for long-term memory in yen/dollar exchange rate". In: *Financial Engineering and the Japanese Markets* 1.2, pp. 101–109.

Bijl, Laurens, Glenn Kringhaug, Peter Molnár, and Eirik Sandvik (2016). "Google searches and stock returns". In: *International Review of Financial Analysis* 45, pp. 150–156.

Black, Fischer (1976). "Studies of stock market volatility changes". In: *Proceedings of the American Statistical Association Bisiness and Economic Statistics Section.*

Black, Fischer and Myron Scholes (1973). "The pricing of options and corporate liabilities". In: *Journal of Political Economy* 81.3, pp. 637–654.

Bollerslev, Tim (1986). "Generalized autoregressive conditional heteroskedasticity". In: *Journal of econometrics* 31.3, pp. 307–327.

Bollerslev, Tim and Jonathan Wright (2000). "Semiparametric estimation of long-memory volatility dependencies: The role of high-frequency data". In: *Journal of Econometrics* 98.1, pp. 81–106.

Bollerslev, Tim and Hao Zhou (2006). "Volatility puzzles: a simple framework for gauging return-volatility regressions". In: *Journal of Econometrics* 131.1-2, pp. 123–150.

Bonferroni, C (1936). "Teoria statistica delle classi e calcolo delle probabilita". In: *Pubblicazioni del R Istituto Superiore di Scienze Economiche e Commericiali di Firenze* 8, pp. 3–62.

Box, George EP and Gwilym M Jenkins (1976). "Time series analysis. Forecasting and control". In: *Holden-Day Series in Time Series Analysis, Revised ed., San Francisco: Holden-Day, 1976.*

Brandt, Michael W and Christopher S Jones (2006). "Volatility forecasting with range-based EGARCH models". In: *Journal of Business & Economic Statistics* 24.4, pp. 470–486.

Brock, William A, José Alexandre Scheinkman, W Davis Dechert, and Blake LeBaron (1996). "A test for independence based on the correlation dimension". In: *Econometric reviews* 15.3, pp. 197–235.

Campbell, John Y and Ludger Hentschel (1992). "No news is good news: An asymmetric model of changing volatility in stock returns". In: *Journal of Financial Economics* 31.3, pp. 281–318.

Cao, Yi, Xiaoquan Liu, and Jia Zhai (2018). "A neural network enhanced volatility component model". In: *Working Paper.*

Caporale, Guglielmo Maria and Luis A Gil-Alana (2013). "Long memory and fractional integration in high frequency data on the US dollar/British pound spot exchange rate". In: *International Review of Financial Analysis* 29, pp. 1–9.

Chambers, Marcus J (1998). "Long memory and aggregation in macroeconomic time series". In: *International Economic Review*, pp. 1053–1072.

Chkili, Walid, Shawkat Hammoudeh, and Duc Khuong Nguyen (2014). "Volatility forecasting and risk management for commodity markets in the presence of asymmetry and long memory". In: *Energy Economics* 41, pp. 1–18.

Choi, Kyongwook, Wei-Choun Yu, and Eric Zivot (2010). "Long memory versus structural breaks in modeling and forecasting realized volatility". In: *Journal of International Money and Finance* 29.5, pp. 857–875.

Christie, Andrew A (1982). "The stochastic behavior of common stock variances: Value, leverage and interest rate effects". In: *Journal of Financial Economics* 10.4, pp. 407–432.

Christoffersen, Peter F (2012). *Elements of financial risk management*. Academic Press.

Christoffersen, Peter F and Francis X Diebold (2006). "Financial asset returns, direction-of-change forecasting, and volatility dynamics". In: *Management Science* 52.8, pp. 1273–1287.

Christoffersen, Peter, Kris Jacobs, Chayawat Ornthanalai, and Yintian Wang (2008). "Option valuation with long-run and short-run volatility components". In: *Journal of Financial Economics* 90.3, pp. 272–297.

Chronopoulos, Dimitris K, Fotios I Papadimitriou, and Nikolaos Vlastakis (2018). "Information demand and stock return predictability". In: *Journal of International Money and Finance* 80, pp. 59–74.

Comte, Fabienne and Eric Renault (1998). "Long memory in continuous-time stochastic volatility models". In: *Mathematical finance* 8.4, pp. 291–323.

Cont, Rama (2001). "Empirical properties of asset returns: stylized facts and statistical issues". In: *Quantitative Finance* 1, pp. 223–236.

Cooley, James W and John W Tukey (1965). "An algorithm for the machine calculation of complex Fourier series". In: *Mathematics of Computation* 19.90, pp. 297–301.

Corsi, Fulvio (2009). "A simple approximate long-memory model of realized volatility". In: *Journal of Financial Econometrics* 7.2, pp. 174–196.

Cox, David R, Gudmundur Gudmundsson, Georg Lindgren, Lennart Bondesson, Erik Harsaae, Petter Laake, Katarina Juselius, and Steffen L Lauritzen (1981). "Statistical analysis of time series: Some recent developments [with discussion and reply]". In: *Scandinavian Journal of Statistics*, pp. 93–115.

Da, Zhi, Joseph Engelberg, and Pengjie Gao (2011). "In Search of Attention". In: *Journal of Finance* 66.5, pp. 1461–1499.

Dacorogna, Michael, Ulrich A Müller, Robert J Nagler, Richard B Olsen, and Olivier V Pictet (1993). "A geographical model for the daily and

weekly seasonal volatility in the foreign exchange market". In: *Journal of International Money and Finance* 12.4, pp. 413–438.
Dacorogna, Michael, Ulrich Müller, Olivier Pictet, and Richard Olsen (1998). "Modelling short-term volatility with GARCH and HARCH models". In: *SSRN Electronic Journal*, pp. 1–17.
DellaVigna, Stefano and Joshua M Pollet (2009). "Investor inattention and Friday earnings announcements". In: *The Journal of Finance* 64.2, pp. 709–749.
Dennis, Patrick, Stewart Mayhew, and Chris Stivers (2006). "Stock returns, implied volatility innovations, and the asymmetric volatility phenomenon". In: *Journal of Financial and Quantitative Analysis* 41.2, pp. 381–406.
Deo, Rohit S and Clifford M Hurvich (2001). "On the log periodogram regression estimator of the memory parameter in long memory stochastic volatility models". In: *Econometric Theory* 17.4, pp. 686–710.
Dickey, David A and Wayne A Fuller (1979). "Distribution of the estimators for autoregressive time series with a unit root". In: *Journal of the American Statistical Association* 74.366a, pp. 427–431.
Diebold, Francis X and Atsushi Inoue (2001). "Long memory and regime switching". In: *Journal of Econometrics* 105.1, pp. 131–159.
Diebold, Francis X and Jose A Lopez (1995). "Modeling volatility dynamics". In: *Macroeconometrics*. Springer, pp. 427–472.
Diebold, Francis X and Glenn D Rudebusch (1989). "Long memory and persistence in aggregate output". In: *Journal of Monetary Economics* 24.2, pp. 189–209.
Dimpfl, Thomas and Stephan Jank (2016). "Can internet search queries help to predict stock market volatility?" In: *European Financial Management* 22.2, pp. 171–192.
Ding, Zhuanxin and Clive WJ Granger (1996). "Modeling volatility persistence of speculative returns: a new approach". In: *Journal of Econometrics* 73.1, pp. 185–215.
Ding, Zhuanxin, Clive WJ Granger, and Robert F Engle (1993). "A long memory property of stock market returns and a new model". In: *Journal of Empirical Finance* 1.1, pp. 83–106.
Dıaz, Andrés Fernandéz, Pilar Grau-Carles, and Lorenzo Escot Mangas (2002). "Nonlinearities in the exchange rates returns and volatility". In: *Physica A: Statistical Mechanics and its Applications* 316.1-4, pp. 469–482.
Drechsler, Itamar and Amir Yaron (2010). "What's vol got to do with it". In: *The Review of Financial Studies* 24.1, pp. 1–45.
Dufrénot, Gilles, Sandrine Lardic, Laurent Mathieu, Valérie Mignon, and Anne Peguin-Feissolle (2008). "Explaining the European exchange rates

deviations: Long memory or non-linear adjustment?" In: *Journal of International Financial Markets, Institutions and Money* 18.3, pp. 207–215.

Dzielinski, Michal (2012). "Measuring economic uncertainty and its impact on the stock market". In: *Finance Research Letters* 9.3, pp. 167–175.

Dzielinski, Michal, Marc Oliver Rieger, and Tonn Talpsepp (2011). "Volatility asymmetry, news, and private investors". In: *The Handbook of News Analytics in Finance*, pp. 255–270.

Dzieliński, Michał, Marc Oliver Rieger, and Tonn Talpsepp (2018). "Asymmetric attention and volatility asymmetry". In: *Journal of Empirical Finance* 45, pp. 59–67.

Ebens, Heiko et al. (1999). "Realized stock volatility". In: *Department of Economics, Johns Hopkins University.*

Engle, Robert F (1982). "Autoregressive conditional heteroscedasticity with estimates of the variance of United Kingdom inflation". In: *Econometrica: Journal of the Econometric Society*, pp. 987–1007.

Engle, Robert F, Eric Ghysels, and Bumjean Sohn (2013). "Stock market volatility and macroeconomic fundamentals". In: *Review of Economics and Statistics* 95.3, pp. 776–797.

Engle, Robert F and Gary Lee (1999). "A long-run and short-run component model of stock return volatility". In: *Cointegration, Causality, and Forecasting: A Festschrift in Honour of Clive WJ Granger*, pp. 475–497.

Engle, Robert F, David M Lilien, and Russell P Robins (1987). "Estimating time varying risk premia in the term structure: The ARCH-M model". In: *Econometrica: Journal of the Econometric Society*, pp. 391–407.

Engle, Robert F and Victor K Ng (1993). "Measuring and testing the impact of news on volatility". In: *The Journal of Finance* 48.5, pp. 1749–1778.

Engle, Robert F and Joshua V Rosenberg (2000). "Testing the Volatility Term Structure Using Option Hedging Criteria." In: *Journal of Derivatives* 8.1, pp. 10–28.

Engle, Robert F and Magdalena E Sokalska (2012). "Forecasting intraday volatility in the us equity market. multiplicative component garch". In: *Journal of Financial Econometrics* 10.1, pp. 54–83.

Fama, Eugene F (1970). "Efficient capital markets: A review of theory and empirical work". In: *The Journal of Finance* 25.2, pp. 383–417.

Fičura, Milan et al. (2017). "Forecasting Stock Market Realized Variance with Echo State Neural Networks". In: *European Financial and Accounting Journal* 2017.3, pp. 145–156.

Figlewski, Stephen and Xiaozu Wang (2000). "Is the'Leverage Effect'a leverage effect?" In: *SSRN Electronic Journal*, pp. 1–40.

Fischer, Thomas and Christopher Krauss (2018). "Deep learning with long short-term memory networks for financial market predictions". In: *European Journal of Operational Research* 270.2, pp. 654–669.

Fox, Robert and Murad S Taqqu (1986). "Large-sample properties of parameter estimates for strongly dependent stationary Gaussian time series". In: *The Annals of Statistics*, pp. 517–532.

French, Kenneth R, G William Schwert, and Robert F Stambaugh (1987). "Expected stock returns and volatility". In: *Journal of Financial Economics* 19.1, pp. 3–29.

Garman, Mark B and Michael J Klass (1980). "On the estimation of security price volatilities from historical data". In: *Journal of Business*, pp. 67–78.

Geweke, John and Susan Porter-Hudak (1983). "The estimation and application of long memory time series models". In: *Journal of Time Series Analysis* 4.4, pp. 221–238.

Gradshteyn, Izrail Solomonovich and Iosif Moiseevich Ryzhik (2014). *Table of integrals, series, and products*. Academic press.

Granger, Clive WJ (1969). "Investigating causal relations by econometric models and cross-spectral methods". In: *Econometrica: journal of the Econometric Society*, pp. 424–438.

— (1980). "Long memory relationships and the aggregation of dynamic models". In: *Journal of Econometrics* 14.2, pp. 227–238.

Granger, Clive WJ and Namwon Hyung (2004). "Occasional structural breaks and long memory with an application to the S&P 500 absolute stock returns". In: *Journal of Empirical Fieinance* 11.3, pp. 399–421.

Granger, Clive WJ and Roselyne Joyeux (1980). "An introduction to long-memory time series models and fractional differencing". In: *Journal of Time Series Analysis* 1.1, pp. 15–29.

Grossman, Sanford J and Joseph Stiglitz (1980). "On the impossibility of informationally efficient markets". In: *The American Economic Review* 70.3, pp. 393–408.

Gurgul, Henryk, Tomasz Wójtowicz, et al. (2006). "Long memory on the German stock exchange". In: *Czech Journal of Economics and Finance* 56.09-10, pp. 447–468.

Hajizadeh, Ehsan, Abbas Seifi, MH Fazel Zarandi, and IB Turksen (2012). "A hybrid modeling approach for forecasting the volatility of S&P 500 index return". In: *Expert Systems with Applications* 39.1, pp. 431–436.

Hamid, Alain and Moritz Heiden (2015). "Forecasting volatility with empirical similarity and Google Trends". In: *Journal of Economic Behavior & Organization* 117, pp. 62–81.

Hansen, Peter Reinhard, Zhuo Huang, and Howard Howan Shek (2012). "Realized GARCH: a joint model for returns and realized measures of volatility". In: *Journal of Applied Econometrics* 27.6, pp. 877–906.

Harris, Richard DF, Evarist Stoja, and Fatih Yilmaz (2011). "A cyclical model of exchange rate volatility". In: *Journal of Banking & Finance* 35.11, pp. 3055–3064.

Hasanhodzic, Jasmina and Andrew W Lo (2011). "Black's leverage effect is not due to leverage". In: *SSRN Electronic Journal*, pp. 1–34.

Haslett, John and Adrian E Raftery (1989). "Space-time modelling with long-memory dependence: Assessing Ireland's wind power resource". In: *Applied Statistics*, pp. 1–50.

Hens, Thorsten and Sven C Steude (2009). "The leverage effect without leverage". In: *Finance Research Letters* 6.2, pp. 83–94.

Hochberg, Yosef (1988). "A sharper Bonferroni procedure for multiple tests of significance". In: *Biometrika* 75.4, pp. 800–802.

Hodrick, Robert J and Edward C Prescott (1997). "Postwar US business cycles: an empirical investigation". In: *Journal of Money, credit, and Banking*, pp. 1–16.

Holm, Sture (1979). "A simple sequentially rejective multiple test procedure". In: *Scandinavian journal of statistics*, pp. 65–70.

Hommel, Gerhard (1988). "A stagewise rejective multiple test procedure based on a modified Bonferroni test". In: *Biometrika* 75.2, pp. 383–386.

Hornik, Kurt, Maxwell Stinchcombe, and Halbert White (1989). "Multilayer feedforward networks are universal approximators". In: *Neural Networks* 2.5, pp. 359–366.

Hosking, Jonathan RM (1981). "Fractional differencing". In: *Biometrika* 68.1, pp. 165–176.

Hsieh, David A (1995). "Nonlinear dynamics in financial markets: evidence and implications". In: *Financial Analysts Journal* 51.4, pp. 55–62.

Huberman, Gur and Tomer Regev (2001). "Contagious speculation and a cure for cancer: A nonevent that made stock prices soar". In: *The Journal of Finance* 56.1, pp. 387–396.

Hurst, Harold Edwin (1951). "Long term storage capacity of reservoirs". In: *ASCE Transactions* 116.776, pp. 770–808.

— (1957). "A suggested statistical model of some time series which occur in nature". In: *Nature* 180.4584, p. 494.

Hwang, Soosung (2000). "The effects of systematic sampling and temporal aggregation on discrete time long memory processes and their finite sample properties". In: *Econometric Theory* 16.3, pp. 347–372.

Ji, Qiang and Ying Fan (2012). "How does oil price volatility affect non-energy commodity markets?" In: *Applied Energy* 89.1, pp. 273–280.

Joseph, Kissan, M Babajide Wintoki, and Zelin Zhang (2011). “Forecasting abnormal stock returns and trading volume using investor sentiment: Evidence from online search”. In: *International Journal of Forecasting* 27.4, pp. 1116–1127.

Kahneman, Daniel and Amos Tversky (1979). “Prospect theory: An analysis of decision under risk”. In: *Econometrica* 47.2, pp. 363–391.

Kang, Sang Hoon, Chongcheul Cheong, and Seong-Min Yoon (2010). “Long memory volatility in Chinese stock markets”. In: *Physica A: Statistical Mechanics and its Applications* 389.7, pp. 1425–1433.

Kim, Ha Young and Chang Hyun Won (2018). “Forecasting the volatility of stock price index: A hybrid model integrating LSTM with multiple GARCH-type models”. In: *Expert Systems with Applications* 103, pp. 25–37.

Kimoto, Takashi, Kazuo Asakawa, Morio Yoda, and Masakazu Takeoka (1990). “Stock market prediction system with modular neural networks”. In: *Neural Networks, 1990., 1990 IJCNN International Joint Conference on.* IEEE, pp. 1–6.

Kristjanpoller, Werner, Anton Fadic, and Marcel C Minutolo (2014). “Volatility forecast using hybrid neural network models”. In: *Expert Systems with Applications* 41.5, pp. 2437–2442.

Kristjanpoller, Werner and Marcel C Minutolo (2016). “Forecasting volatility of oil price using an artificial neural network-GARCH model”. In: *Expert Systems with Applications* 65, pp. 233–241.

Laopodis, Nikiforus-Themistocles (1998). “Asymmetric volatility spillovers in deutsche mark exchange rates”. In: *Journal of Multinational Financial Management* 8.4, pp. 413–430.

Lewicka, Maria, Janusz Czapinski, and Guido Peeters (1992). “Positive-negative asymmetry or ‘When the heart needs a reason’”. In: *European Journal of Social Psychology* 22.5, pp. 425–434.

Li, Qi, Jian Yang, Cheng Hsiao, and Young-Jae Chang (2005). “The relationship between stock returns and volatility in international stock markets”. In: *Journal of Empirical Finance* 12.5, pp. 650–665.

Ljung, Greta M and George EP Box (1978). “On a measure of lack of fit in time series models”. In: *Biometrika* 65.2, pp. 297–303.

Lo, Andrew W (1991). “Long-Term Memory in Stock Market Prices”. In: *Econometrica* 59.5, pp. 1279–1313.

Lobato, Ignacio N and Nathan E Savin (1998). “Real and spurious long-memory properties of stock-market data”. In: *Journal of Business & Economic Statistics* 16.3, pp. 261–268.

Man, KS and GC Tiao (2006). “Aggregation effect and forecasting temporal aggregates of long memory processes”. In: *International Journal of Forecasting* 22.2, pp. 267–281.

Mandelbrot, Benoit B (1971). “When can price be arbitraged efficiently? A limit to the validity of the random walk and martingale models”. In: *The Review of Economics and Statistics*, pp. 225–236.

Mandelbrot, Benoit B and John W Van Ness (1968). “Fractional Brownian motions, fractional noises and applications”. In: *Society for Industrial and Applied Mathematics Review* 10.4, pp. 422–437.

Markowitz, Harry (1952). “Portfolio Selection”. In: *The Journal of Finance* 7.1, pp. 77–91.

McKenzie, Michael (2002). “The economics of exchange rate volatility asymmetry”. In: *International Journal of Finance & Economics* 7.3, pp. 247–260.

McMillan, David G and Alan EH Speight (2004). “Intra-day periodicity, temporal aggregation and time-to-maturity in FTSE-100 index futures volatility”. In: *Applied Financial Economics* 14.4, pp. 253–263.

Mcmillan, David G and Alan EH Speight (2008). “Long-memory in high-frequency exchange rate volatility under temporal aggregation”. In: *Quantitative Finance* 8.3, pp. 251–261.

McQueen, Grant and Keith Vorkink (2004). “Whence GARCH? A preference-based explanation for conditional volatility”. In: *Review of Financial Studies* 17.4, pp. 915–949.

Merton, Robert C (1980). “On estimating the expected return on the market: An exploratory investigation”. In: *Journal of Financial Economics* 8.4, pp. 323–361.

— (1987). “A simple model of capital market equilibrium with incomplete information”. In: *The Journal of Finance* 42.3, pp. 483–510.

Mincer, Jacob A and Victor Zarnowitz (1969). “The evaluation of economic forecasts”. In: *Economic forecasts and expectations: analysis of forecasting behavior and performance*. NBER, pp. 3–46.

Molnár, Peter (2012). “Properties of range-based volatility estimators”. In: *International Review of Financial Analysis* 23, pp. 20–29.

Monfared, Soheil Almasi and David Enke (2014). “Volatility forecasting using a hybrid GJR-GARCH neural network model”. In: *Procedia Computer Science* 36, pp. 246–253.

Nikolopoulos, Chris and Paul Fellrath (1994). “A hybrid expert system for investment advising”. In: *Expert Systems* 11.4, pp. 245–250.

Ohanissian, Arek, Jeffrey R Russell, and Ruey S Tsay (2008). “True or spurious long memory? A new test”. In: *Journal of Business & Economic Statistics* 26.2, pp. 161–175.

Pai, Ping-Feng and Chih-Sheng Lin (2005). "A hybrid ARIMA and support vector machines model in stock price forecasting". In: *Omega* 33.6, pp. 497–505.

Parkinson, Michael (1980). "The extreme value method for estimating the variance of the rate of return". In: *Journal of Business*, pp. 61–65.

Parzen, Emanuel (1980). *Time Series Model Identification and Prediction Variance Horizon*. Tech. rep.

Patton, Andrew J (2011). "Volatility forecast comparison using imperfect volatility proxies". In: *Journal of Econometrics* 160.1, pp. 246–256.

Peeters, Guido (1971). "The positive-negative asymmetry: On cognitive consistency and positivity bias". In: *European Journal of Social Psychology* 1.4, pp. 455–474.

Peng, Lin and Wei Xiong (2006). "Investor attention, overconfidence and category learning". In: *Journal of Financial Economics* 80.3, pp. 563–602.

Pesaran, M Hashem and Yongcheol Shin (1998). "An autoregressive distributed-lag modelling approach to cointegration analysis". In: *Econometric Society Monographs* 31, pp. 371–413.

Pindyck, Robert S (1984). "Risk, Inflation, and the Stock Market". In: *The American Economic Review* 74.3, pp. 335–351.

Poon, Ser-Huang and Clive WJ Granger (2003). "Forecasting volatility in financial markets: A review". In: *Journal of Economic Literature* 41.2, pp. 478–539.

Priestley, Maurice Bertram (1981). *Spectral analysis and time series: probability and mathematical statistics*. 04; QA280, P7.

Radner, Roy and Joseph Stiglitz (1984). "A Nonconcavity in the Value of Information". In: *Bayesian models in Economic Theory* 5, pp. 33–52.

Raggi, Davide and Silvano Bordignon (2012). "Long memory and nonlinearities in realized volatility: a Markov switching approach". In: *Computational Statistics & Data Analysis* 56.11, pp. 3730–3742.

Robinson, Peter M and Paolo Zaffaroni (1998). "Nonlinear time series with long memory: a model for stochastic volatility". In: *Journal of Statistical Planning and Inference* 68.2, pp. 359–371.

Rodrigues, Paulo MM, Matei Demetrescu, and Antonio Rubia (2018). *Testing the fractionally integrated hypothesis using M estimation: With an application to stock market volatility*. Tech. rep.

Roh, Tae Hyup (2007). "Forecasting the volatility of stock price index". In: *Expert Systems with Applications* 33.4, pp. 916–922.

Rosa, Raul, Leandro Maciel, Fernando Gomide, and Rosangela Ballini (2014). "Evolving hybrid neural fuzzy network for realized volatility forecasting with jumps". In: *Computational Intelligence for Financial Engineering & Economics (CIFEr), 2104 IEEE Conference on*. IEEE, pp. 481–488.

Rossi, Eduardo and Paolo Santucci De Magistris (2013). "Long memory and tail dependence in trading volume and volatility". In: *Journal of Empirical Finance* 22, pp. 94–112.

— (2014). "Estimation of long memory in integrated variance". In: *Econometric Reviews* 33.7, pp. 785–814.

Rozin, Paul and Edward B Royzman (2001). "Negativity bias, negativity dominance, and contagion". In: *Personality and Social Psychology Review* 5.4, pp. 296–320.

Rubin, Amir and Eran Rubin (2010). "Informed investors and the internet". In: *Journal of Business Finance & Accounting* 37.7-8, pp. 841–865.

Schwert, G William (1989). "Why does stock market volatility change over time?" In: *The Journal of Finance* 44.5, pp. 1115–1153.

Sentana, Enrique and Sushil Wadhwani (1992). "Feedback traders and stock return autocorrelations: evidence from a century of daily data". In: *The Economic Journal* 102.411, pp. 415–425.

Shefrin, Hersh (2008). *A behavioral approach to asset pricing*. Elsevier.

Shiller, Robert J. (1981). "Do Stock Prices Move Too Much to be Justified by Subsequent Changes in Dividends?" In: *The American Economic Review* 71.3, pp. 421–436.

Siegelmann, Hava T, Bill G Horne, and C Lee Giles (1997). "Computational capabilities of recurrent NARX neural networks". In: *IEEE Transactions on Systems, Man, and Cybernetics, Part B (Cybernetics)* 27.2, pp. 208–215.

Simes, R John (1986). "An improved Bonferroni procedure for multiple tests of significance". In: *Biometrika* 73.3, pp. 751–754.

Sims, Christopher A (1980). "Macroeconomics and reality". In: *Econometrica: Journal of the Econometric Society*, pp. 1–48.

— (2003). "Implications of rational inattention". In: *Journal of Monetary Economics* 50.3, pp. 665–690.

Souza, Leonardo Rocha (2005). "A NOTE ON CHAMBERS'S "LONG MEMORY AND AGGREGATION IN MACROECONOMIC TIME SERIES"". In: *International Economic Review* 46.3, pp. 1059–1062.

Sowell, Fallaw (1992). "Maximum likelihood estimation of stationary univariate fractionally integrated time series models". In: *Journal of Econometrics* 53.1-3, pp. 165–188.

Talpsepp, Tonn and Marc Oliver Rieger (2010). "Explaining asymmetric volatility around the world". In: *Journal of Empirical Finance* 17.5, pp. 938–956.

Tan, S, M Khan, et al. (2010). "Long memory features in return and volatility of the Malaysian stock market". In: *Economics Bulletin* 30.4, pp. 3267–3281.

Tauchen, George, Harold Zhang, and Ming Liu (1996). "Volume, volatility, and leverage: A dynamic analysis". In: *Journal of Econometrics* 74.1, pp. 177–208.

Teles, P, WWS Wei, and N Crato (1999). "The use of aggregate series in testing for long memory". In: *Bulletin of the International Statistical Institute* 52, pp. 341–342.

Theil, Henri (1966). *Applied economic forecasting.* Amsterdam: North-Holland Pub. Co.

Tschernig, Rolf et al. (1995). "Long memory in foreign exchange rates revisited". In: *Journal of International Financial Markets, Institutions and Money* 5, pp. 53–78.

Vlastakis, Nikolaos and Raphael N Markellos (2012). "Information demand and stock market volatility". In: *Journal of Banking & Finance* 36.6, pp. 1808–1821.

Vortelinos, Dimitrios I (2017). "Forecasting realized volatility: HAR against Principal Components Combining, neural networks and GARCH". In: *Research in International Business and Finance* 39, pp. 824–839.

Vozlyublennaia, Nadia (2014). "Investor attention, index performance, and return predictability". In: *Journal of Banking & Finance* 41, pp. 17–35.

Wang, Changyun (2004). "Futures trading activity and predictable foreign exchange market movements". In: *Journal of Banking & Finance* 28.5, pp. 1023–1041.

Wang, Yi-Hsien (2009). "Nonlinear neural network forecasting model for stock index option price: Hybrid GJR–GARCH approach". In: *Expert Systems with Applications* 36.1, pp. 564–570.

Wang, Jianxin and Minxian Yang (2009). "Asymmetric volatility in the foreign exchange markets". In: *Journal of International Financial Markets, Institutions and Money* 19.4, pp. 597–615.

Wasserfallen, Walter and Heinz Zimmermann (1985). "The behavior of intradaily exchange rates". In: *Journal of Banking & Finance* 9.1, pp. 55–72.

Wenger, Kai, Christian Leschinski, and Philipp Sibbertsen (2017). *The memory of volatility.* Tech. rep. Hannover Economic Papers (HEP).

Yao, Yuan, Jia Zhai, Yi Cao, Xuemei Ding, Junxiu Liu, and Yuling Luo (2017). "Data analytics enhanced component volatility model". In: *Expert Systems with Applications* 84, pp. 232–241.

Zhang, G Peter (2003). "Time series forecasting using a hybrid ARIMA and neural network model". In: *Neurocomputing* 50, pp. 159–175.